Axon Development and Synapse Formation in Olfactory Sensory Neurons

by Florencia Marcucci

Submitted in partial fulfillment of the requirements for the degree of Doctor of Philosophy in the Graduate School of Arts and Sciences

Columbia University

2011

ABSTRACT

Axonal development and synapse formation in olfactory sensory neurons

By Florencia Marcucci

The olfactory epithelium (OE) possesses the rare capacity among neuronal tissues to regenerate throughout life. As a result, progenitor cells continuously proliferate and differentiate into olfactory sensory neurons (OSNs) that project their axons to the olfactory bulb (OB) where they establish connections to the central nervous system. The olfactory epithelium is therefore an attractive model for the study of axonal growth and synapse formation.

The present set of studies attempts to provide insights into synapse formation and axonal development of olfactory sensory neurons. First, I sought to understand the regulation of expression of pre-synaptic molecules in the olfactory epithelium. I established by *in situ* hybridization that as OSNs mature, they express sequentially groups of pre-synaptic genes. Genes encoding for proteins that play a structural role at the active zone showed an early onset of expression, whereas genes encoding for proteins associated with synaptic vesicles showed a later onset of expression. In particular, the signature molecule for glutamatergic neurons VGLUT2 shows the latest onset of expression. The sequential onset of expression suggests the existence of discrete steps in pre-synaptic development. In addition, contact with the targets in the olfactory bulb is not controlling pre-synaptic protein gene expression, suggesting that olfactory sensory neurons follow an intrinsic program of development.

Second, in order to visualize simultaneously OSN axonal arborizations and their pre-synaptic specializations *in vivo,* I developed a method based on post-natal electroporation of the mouse nasal cavity. This technique allowed me to perform a temporal study where I followed the elaboration of axons and synapses in olfactory sensory neurons at different post-natal ages. The results show that olfactory sensory axons develop with exuberant growth and synapse formation. Exuberant branches and synapses are eliminated to achieve the mature pattern of connectivity in a process likely to be regulated by neural activity.

Finally I investigated the consequences of suppressing neural activity in olfactory sensory neuron axonal morphology and synaptic composition. To this end I utilized two anosmic mouse models: cyclic nucleotide gated (CNG) channel and adenylyl cyclase 3 (AC3) knock-out mice. I observed that in the CNG knock-out mice, where OSNs do not generate action potentials after odor stimulation, the morphology of terminal arborizations and the synaptic composition were indistinguishable from wild-type littermates. In sharp contrast, AC3 knock-out mice, where there is no induction of cAMP production after odor stimulation, both the morphology and synaptic composition of OSN axons are severely altered. These results provide evidence that, unlike odor-induced membrane depolarization, odor-induced cAMP signaling events are critical for axonal growth and synapse formation in OSNs.

TABLE OF CONTENTS

LIST OF FIGURES AND TABLES

Chapter I

Chapter II

Chapter III

Chapter IV

ACKNOWLEDGMENTS

I would like to thank Dr. Stuart Firestein for giving me the opportunity of pursuing my questions of interest with entire freedom. I would like to thank members of the Firestein Lab who provided help and support through the ups and downs of graduate school: Jesse Brann and Shari Saideman for their advice and friendship and Cen Zhang for her skilled technical help and support. DongJing Zou was instrumental for my graduate research; he pointed me to the direction of synapse formation and he provided invaluable guidance.

I would also like to thank my family, in special my husband Christoph. He has been a constant source of inspiration and an example; our mutual interest for science fuelled his patience and unconditional support throughout these years. I thank my parents, sister, and daughter Anna for their patience and love.

CHAPTER I

INTRODUCTION

A. Organization of the olfactory system

Most mammals use the sense of smell to identify food sources, predators, mates and conspecifics. The olfactory epithelium (OE) is the first site where detection and coding of sensory information from thousands of odor stimuli begin. The process of odorant detection begins with the binding of odorant compounds to olfactory receptors (ORs) located in the membrane of the cilia of olfactory sensory neurons (OSNs). Odorant receptors are seven trans-membrane receptors that, once activated by an odorant molecule, initiate a transduction cascade involving a G protein and adenylyl cyclase 3 (AC3). AC3 induces the production of cAMP which in turn activates a cyclic nucleotide gated (CNG) channel resulting in an influx of calcium and in the depolarization of the neuron. As a result of the influx of calcium, calcium-gated chloride channels open causing a chloride efflux and further depolarization of the cell that propagates in the form of an action potential down the axon of the sensory neuron to the olfactory bulb in the brain. OR-mediated depolarization is quickly dampened by the phosphorylation of the receptor, but cAMP can accumulate and activate PKA and MAPK pathways to induce CREB phosphorylation, facilitating long lasting changes in gene expression(Moon & Baker 2002) (Figure I.1).

The olfactory epithelium is a pseudo stratified neuroepithelium composed by three major cell types: progenitor cells, olfactory sensory neurons and sustentacular cells. Progenitor cells are located immediately adjacent to the basal membrane of the OE and are responsible for maintenance of cell density within the OE. There are two sub-classes of progenitor cells, horizontal and globose basal cells, each sub-class differing in morphology and rate of proliferation.

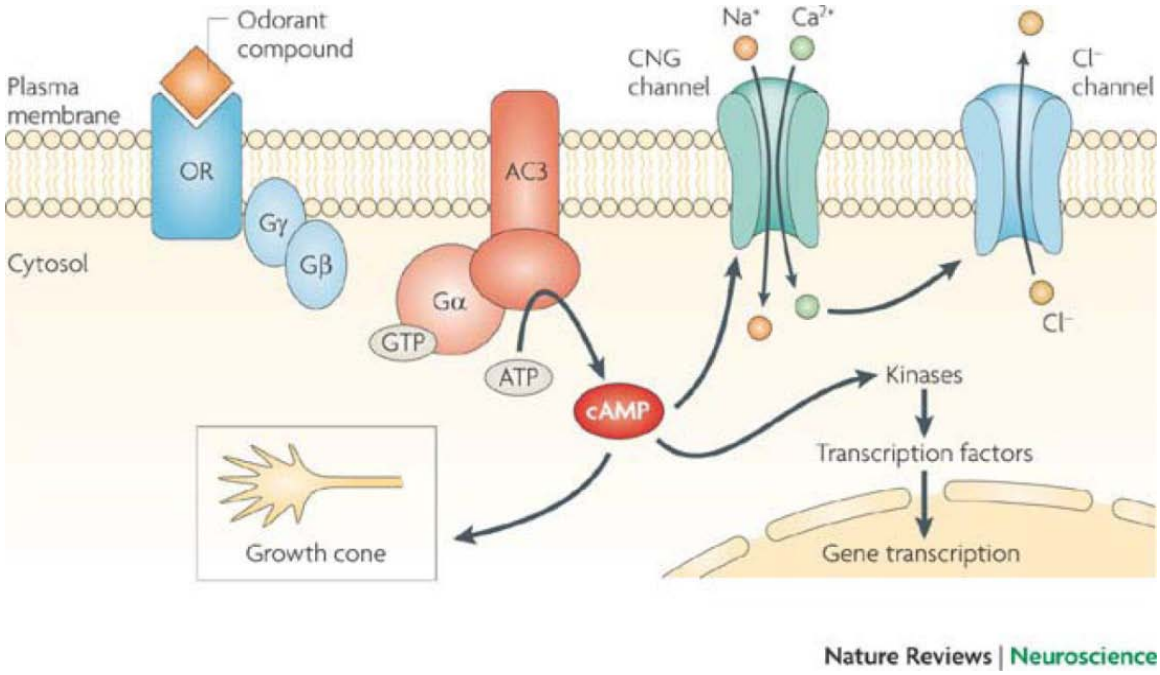

Figure I.1: *The odorant transduction pathway.*

Binding of odorant compounds to an olfactory receptor (OR) initiates a transduction cascade that involves a G protein and the activation of adenylate cyclase 3 (AC3). AC3 produces the second messenger cyclic AMP, which in turn binds to a cyclic nucleotide-gated (CNG) channel and results in the influx of Na^+ and Ca^{2+}. The influx of cations depolarizes the cell membrane and Ca^{2+} activates a Ca^{2+}-dependent Cl^- channel resulting in a further depolarization of the cell membrane. Notably, the elevated levels of cAMP in the soma have a crucial role in regulating the phosphorylation of proteins and the transcription of genes important for growth and survival of the axons of OSNs (adapted from (Zou et al 2009)).

Horizontal basal cells are in direct contact with the basal lamina whereas globose basal cells are mainly situated superficial to the horizontal basal cells. Globose basal cells are the predominant type of proliferating cell and account for the vast majority of actively dividing cells in the basal compartment of the normal epithelium (Huard & Schwob 1995). Due to the proliferative capacities of these progenitor cells, the olfactory epithelium is one of the few neuronal systems where neurogenesis occurs even in adulthood. Directly above the basal cell layer reside the immature olfactory sensory neurons, characterized by the expression of the cellular marker GAP43. Mature olfactory sensory neurons are located more apically and are identified by the expression of Olfactory Marker Protein (OMP). Mature OSNs extend their dendritic knobs to the surface of the epithelium where they elaborate cilia extending over the epithelial surface. Each olfactory sensory neuron expresses one among more than 1200 possible olfactory receptors, in a mutually exclusive and monoallelic manner, giving rise to the "one cell, one receptor" rule (Malnic et al 1999) (Chess et al 1994) (Figure I.2). Moreover, OSNs expressing the same OR converge their axons into a specific target into the olfactory bulb (Mombaerts 1996).

OSNs also extend a single unmyelinated axon to the olfactory bulb. Axons target spatially restricted structures referred as glomeruli. Within each glomerulus, axons from OSNs elaborate into complex processes and form synapses with dendrites from mitral and tufted cells, relaying the odor information to higher brain areas. Due to the regenerative capacities of olfactory sensory neurons, newly born OSNs project their axons to the olfactory bulb throughout the lifespan of the animal and connections to the central nervous system must be reestablished continuously.

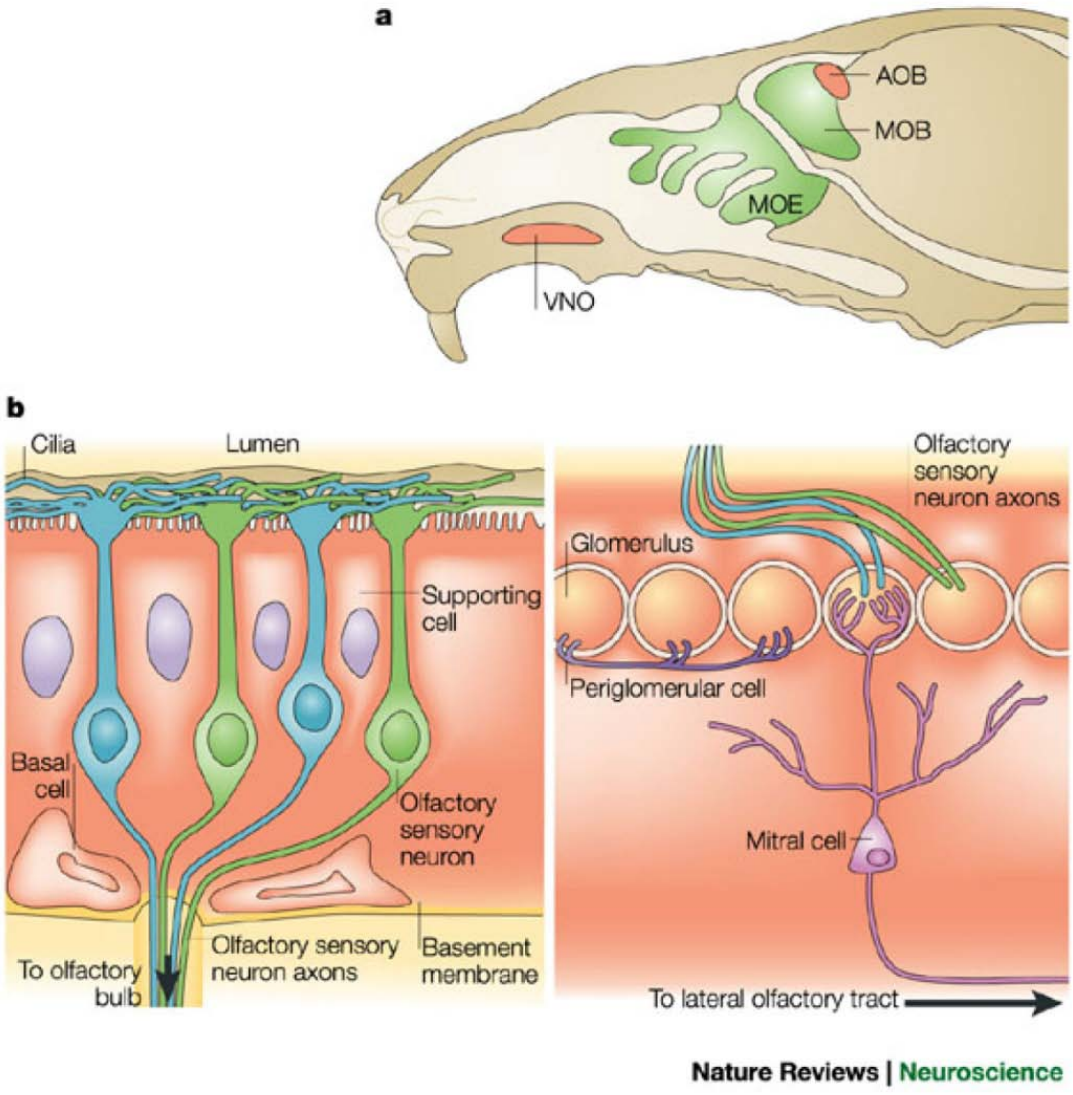

Figure I.2: *Basic organization of the olfactory system*

a) Schematic view of a bisected mouse head. MOE: main olfactory epithelium, MOB: main olfactory bulb, VNO, vomeronasal organ, AOB: accessory olfactory bulb.
b) Cross section of the mouse olfactory epithelium (left) showing the three main cell types: basal cells, olfactory sensory neurons and supporting cells. Cross section of the superficial layer of the mouse olfactory bulb (right). Axons from olfactory sensory neurons expressing different olfactory receptors (represented in blue and green) project to distinct glomeruli. Within the glomerulus, processes from olfactory sensory neurons establish excitatory synapses with mitral cells and tufted cells (not shown).

Therefore, the olfactory system emerges as a suitable model to study different aspects of synapse formation and axonal growth.

B. Building a synapse

Neurotransmission depends on the structural and functional integrity of synaptic connections. The formation of synapses requires the stabilization of contacts between axons and dendrites and formation of synaptic subcellular structures. Where and when synapses form, how components of the nascent pre-synaptic terminal accumulate at the site of synapse formation and how assembly occurs are central aspects of the process of synaptogenesis. In particular, the dissection of synapse assembly has proven difficult due to genetic redundancies that likely reflect the highly regulated nature of neurotransmitter release. For example, one explanation for the very mild synaptic phenotype of RIM1 knockout mice is that other proteins can perform a similar function to that of RIM (Schoch et al 2002).

At the pre-synaptic site, the active zone provides scaffold for the rapid fusion of synaptic vesicles filled with neurotransmitter after calcium influx. A dense network of specialized proteins that organize and interact with the synaptic vesicle release machinery composes the active zone (Figure I.3). To date, five protein families whose members are highly enriched at active zones (Munc13s, RIMs, ELKS proteins, Piccolo and Bassoon and the α-liprins) have been characterized (Schoch & Gundelfinger 2006). characterized (Schoch & Gundelfinger 2006).

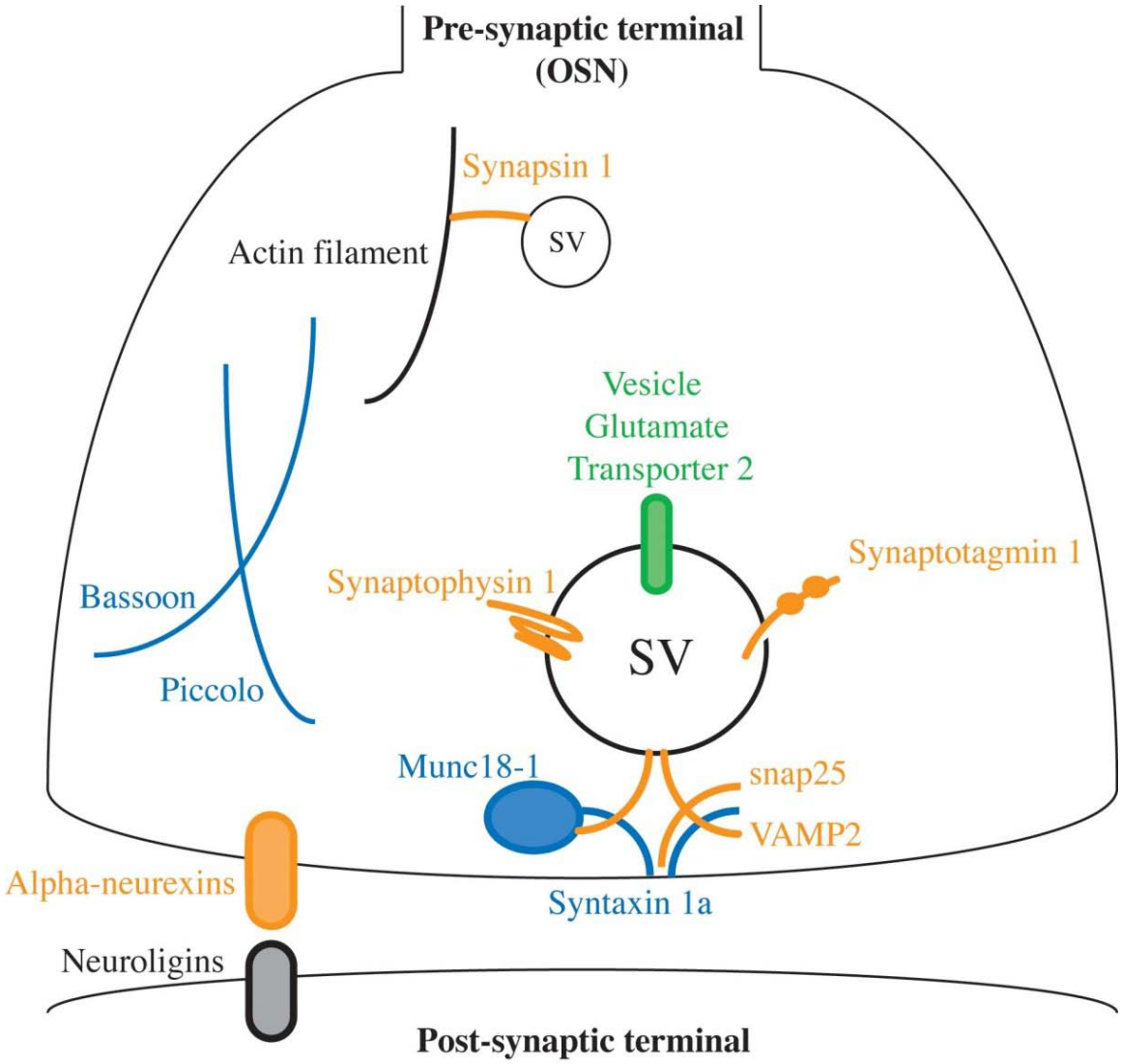

Figure I.3: Summary illustrating components of the pre-synaptic vesicle release machinery

Bassoon and piccolo interact with each other providing scaffold at the pre-synaptic active zone. Pre-synaptic vesicle associated proteins present diverse functions: synapsin 1 interacts with the vesicle membrane as well as with actin; VGLUT2 is involved in loading the vesicles with glutamate; vesicla associated proteins (synaptophysin and synaptotagmin) are believed to modulate neurotransmitter release; SNARE proteins (syntaxin 1, VAMP2 and SNAP25) together with a SNARE associated protein (Munc18-1) participate in the formation of the SNARE complex and release of neurotransmitter into the synaptic cleft; neurexins are believed to have synaptogenic properties**. Adapted from (Marcucci et al 2009).**

They form an interconnected network linked to synaptic vesicles, cytoskeletal proteins and calcium channels.

The entire cytomatrix active zone proteins are composed of multiple protein interaction domains that are the subject of intense investigation. The active zone proteins are instrumental for the integration and organization of specific steps of the synaptic vesicle cycle: Munc13 is involved in the priming of synaptic vesicles (Varoqueaux et al 2002) and piccolo might play a role in coordinating exocytic and endocytic steps (Fenster et al 2003; Leal-Ortiz et al 2008). Furthermore, RIMs and Munc13 seem to mediate changes in release during short-term and long-term synaptic plasticity (Kaeser & Sudhof 2005; Rodriguez-Castaneda et al 2010).

Synaptic vesicles contain two classes of components: transport proteins involved in neurotransmitter uptake and trafficking proteins that participate in synaptic vesicle exocytosis, endocytosis and recycling. Transport proteins are composed of a vacuolar-type proton pump that generates an electrochemical gradient that fuels neurotransmitter uptake and transporters that mediate the actual uptake. Three vesicular glutamate transporters have been identified and characterized. VGLUT1 and VGLUT2 are expressed by glutamatergic neurons, while VGLUT3 is expressed by neurons classically defined by their use of another neurotransmitter, such as acetylcholine or serotonin. Glutamate is the most abundant neurotransmitter in the nervous system and the discovery of the VGLUTs made possible to identify and specifically target glutamatergic neurons. Trafficking proteins are a diverse group composed by intrinsic membrane proteins (for example synaptotagmins, synaptophysins and synaptobrevins or VAMPs), proteins associated via post-translational modifications and peripherally bound proteins (for

example synapsins). Many but not all of the synaptic vesicle proteins interact with non-vesicular proteins and are linked to specific functions. Synaptotagmins interact with the SNARE complex in response to Ca^{2+} binding; VAMPs interact with syntaxins and SNAP25 to form the SNARE complex and synaptophysins are believed to regulated the SNARE complex by interacting with VAMPs (Figure I.3) (Sudhof 2004).

Synaptic vesicle exocytosis is mediated by three SNARE proteins: VAMPs on synaptic vesicles and syntaxin 1 ans SNAP25 on the cytosolic side of the pre-synaptic plasma membrane (Figure I.3). The model proposes that by bringing the synaptic vesicle and plasma membranes close together, the SNARE complex creates as unstable intermediates that can progress to the full fusion of the two membranes and opening of the pore that allows neurotranmitter release into the synaptic cleft (Sudhof 2004). The SNARE complex formation at the synapse seems to be controlled by a class of fusion proteins called Sec1/Munc18-1-like proteins. Munc18-1 binds to syntaxin 1 controlling synaptic vesicle priming (Deak et al 2009); and deletion of munc18-1 causes a complete loss of neurotransmitter secretion (Verhage et al 2000).

How the multiple components arrive and accumulate to the site of pre-synaptic differentiation has been the subject of intense investigation. Are these synaptic molecules independent units of assembly or synaptic assembly occurs in “modules”. Recent evidence supports the model that pre-synaptic specializations are constructed from pre-assembled “packets” composed of vesicles and associated proteins (Li & Chin 2003). These large precursor complexes are mobile along the axons from immature neurons prior to synapse formation and rapidly immobilized at sites of nascent synapses for

synapse construction. It is believed that these mobile complexes function as large packets that deliver the many components of the pre-synaptic components to the synapse.

Synapse formation in the olfactory system has remained largely un-investigated. In the olfactory bulb, numerous synapses must form between the axons of olfactory sensory neurons and the dendrites of mitral and tufted cells. The distribution of axo-axoninc and axo-dendritic synapses is highly restricted to different compartments within the glomerulus (Kasowski et al 1999). Ultrastructural analysis showed that in the mouse glomerular layer, the first synapse appears at embryonic day 14 (Hinds 1968). Moreover, synaptogenesis in the glomerular layer is coincident with the entrance of axons from the olfactory sensory neurons to the bulb (Blanchart et al 2006; Blanchart et al 2008). However, the repertoire of pre-synaptic molecules expressed by olfactory sensory neurons and whether their expression changes as neurons undergo maturation are two questions that remain unknown.

C. Axonal branching

In order to form the complex wiring pattern of the mature nervous system, primary axon projections need to elaborate their multiple ramifications during the period of axonal growth. The process of arborization is essential for neurons to innervate multiple targets allowing the distribution and integration of information. The coordination of signaling mechanisms mediating axonal branching with those regulating axonal growth and guidance is required to establish specific topographic relationships in the brain. The arborization of axonal processes substantially adds to the complexity of neuronal circuits.

Later, the retraction and pruning of inappropriate branches result in the mature pattern of connectivity. The processes of axonal arborization and pruning have been extensively studied in the visual system.

Instead of growing directly to their target, retinal ganglion cell axons initially overshoot their future termination zones in the superior colliculus. Branch elaboration is then coordinated by interplay between BDNF/TrkB and ephrinA/Eph signaling. BDNF is uniformly distributed along the tectum and promotes branching of retinal axons through the activation of TrkB (Marler et al 2008). Opposing gradients of ephrinA and EphA are required for the proper innervation of retinal axons to the superior colliculus (Rashid et al 2005). Further modifications occur mediated by neural correlated activity that induces the elimination of ectopic branches and the subsequent generation of eye-specific layers in the lateral geniculate nucleus and ocular dominance in the primary visual cortex.

Axonal branching can occur either at the growth cone or at the axon shaft (known as interstitial branching), both involve the cooperation of and remodeling of the neuronal cytoskeleton. Therefore, a major focus of interest is the question of how various signaling pathways interact and eventually converge onto the axonal cytoskeleton. Recent studies emphasized the important role of microtubules in the formation of axonal branches. Their regulation at multiple levels (polymerization, depolymerization, severing and stability) is critical for the generation of axonal branches (Schmidt & Rathjen 2010). Electron microscopy in hyppocampal neurons indicated that during the formation of interstitial branches microtubules become unbundled and undergo local fragmentation at sites where novel branches are generated (Yu et al 1994). The authors concluded that the microtubules within the new collateral branch were assembled in the parental axon and

then translocated into the new branch. Branch point protrusions at the axon shaft could be initiated by focal actin polymerization through regulators of actin dynamics, such as GTPases (Schmidt & Rathjen 2010).

In the olfactory system, few studies address olfactory sensory neuron axonal branching. Golgi impregnations revealed that olfactory sensory neurons innervated preferentially restricted sub-compartments within the glomerulus and that axons developed to the adult pattern of arborization without any sign of exuberant growth (Halasz & Greer 1993; Klenoff & Greer 1998). However, as pointed by the authors, this last result might be bias due to the heterogeneous age composition of the neurons analyzed. Therefore, the question of whether olfactory sensory neurons develop with exuberant axonal growth remains open.

D. Role of activity in synapse formation and axonal development

The formation of functional neuronal networks requires precise regulation of the growth and branching of the terminal axonal arbors. Both processes are known to be influenced by neuronal activity. Previous work has firmly established the requirement of neural activity in the development of retinal ganglion cells (RGC) projections and some of the molecular pathways involved. In zebrafish, mosaic expression of the inward rectifying potassium channel Kir2.1 or a dominant negative form of VAMP2 was used to suppress electrical or neurosecretory activity in a subset of RGCs. These forms of activity suppression strongly inhibit both the net growth and the generation of new branches in individually transfected axonal arbors (Hua et al 2005). Conversely, treatment with

BDNF significantly increased both axonal arborization and synapse number in RGCs from *Xenopus laevis* (Alsina et al 2001). Also, as mentioned in the previous section, neuronal activity plays an important role in pruning RGC projections into the lateral geniculate nucleus (LGN). Indeed, layers in the LGN emerge as RGC axons gradually remodel their branches by retracting side branches from inappropriate regions and elaborating extensive terminal arbors into the appropriate regions corresponding to the eye of origin (Shatz 1996). Elimination of side branches and their synapses is a competitive process governed by correlated activity (Ruthazer et al 2003).

Examples of activity-based competition in the olfactory system indicate that olfactory sensory neuron axons that are more active in releasing neurotransmitter persist whereas less active axons are not maintained (Yu et al 2004; Zhao & Reed 2001). However, it is still unknown whether activity is modulating synapse formation in olfactory sensory neurons. Also, when we refer to activity, this activity is not necessarily electrical. Indeed, mounting evidence suggests that cAMP levels, as a product of the activity of the odorant receptor mediated signaling cascade, have a crucial role in olfactory sensory neuron axonal growth and identity (Chesler et al 2007; Imai et al 2006; Sakano 2010; Zou et al 2009; Zou et al 2007). Although experiments addressing axonal growth and convergence of specific populations of olfactory sensory neurons have been performed, studies aimed to understand the role of activity in the development of single axons are virtually non-existents.

E. Summary

The olfactory epithelium possesses the rare characteristic among neural tissues that neurogenesis persists even in adulthood. Since connections to the central nervous system have to be reestablished continuously, the olfactory system emerges as a suitable model to study questions of synaptogenesis and axonal development. The goal of the studies presented in the next chapters is to provide insights on how olfactory sensory neuron axons develop and arborize in the olfactory bulb and how they form synapses with mitral and tufted cells. Our results show that as olfactory sensory neurons mature, they sequentially express specific pre-synaptic molecules; molecules participating in the regulation of neurotransmitter release start to be expressed later in OSN lineage (Marcucci et al 2009). We also show that olfactory sensory neurons axonal arborizations develop with signs of exuberant growth and synapse formation. The exuberant branches and synapses are eliminated to achieve the mature pattern in a process likely to be regulated by neuronal activity (manuscript in preparation, see Chapter 2). Last, we provide evidence suggesting that odorant receptor mediated signaling activity is more important than electrical activity for olfactory sensory neuron axonal development and synapse formation.

CHAPTER II

SEQUENTIAL ONSET OF PRE-SYNAPTIC MOLECULES DURING OLFACTORY SENSORY NEURON MATURATION

ABSTRACT

Differentiated olfactory sensory neurons express specific pre-synaptic proteins, including enzymes involved in neurotransmitter transport and proteins involved in the trafficking and release of synaptic vesicles. Studying the regulation of these pre-synaptic proteins will help to elucidate the pre-synaptic differentiation process that ultimately leads to synapse formation. It has been postulated that the formation of a synapse between the axons of the sensory neurons and the dendrites of second order neurons in the olfactory bulb is a critical step in the processes of sensory neuron maturation. One approach to study the relationship between synaptogenesis and sensory neuron maturation is to examine the expression patterns of synaptic molecules as olfactpry sensory neurons mature. To this end we designed specific *in situ* hybridization probes to target messengers for proteins involved in pre-synaptic vesicle release.

Our findings show that, as they mature, mouse olfactory neurons sequentially express specific pre-synaptic genes. Furthermore, the different patterns of expression of these pre-synaptic genes suggest the existence of discrete steps in pre-synaptic development: genes encoding proteins involved in scaffolding show an early onset of expression whereas expression of genes encoding proteins involved in the regulation of vesicle release starts later. In particular, the signature molecule for glutamatergic neurons Vesicle Glutamate Transporter 2 shows the latest onset of expression. In addition, contact with the targets in the olfactory bulb is not controlling pre-synaptic protein gene expression, suggesting that olfactory sensory neurons follow an intrinsic program of development.

INTRODUCTION

Synapse formation involves the recognition of target cells by pre-synaptic neurons followed by the concerted differentiation of pre- and post-synaptic partners to form mature synapses. From a molecular perspective, this process involves the recruitment of numerous molecules to sites of physical contact between axons and dendrites and their precisely timed assimilation into functional assemblies leading to the final structure of the synapse. In particular, excitatory pre-synaptic differentiation includes the clustering of synaptic vesicles (SVs) and the formation of active zones, specialized regions within the pre-synaptic plasma membrane where SVs dock, fuse and release neurotransmitter. The active zone is tightly associated with an electron-dense cytoskeletal matrix referred as the cytomatrix of the active zone (CAZ). Not surprisingly, many types of molecules are highly concentrated at glutamatergic pre-synaptic terminals: active zone components (including the CAZ components bassoon and piccolo), proteins involved in neurotransmitter transport, molecules involved in the trafficking and release of SVs, and trans-synaptic adhesion molecules (for review on synaptogenesis (McAllister 2007; Ziv 2001). The study of the regulation of these pre-synaptic proteins should help to elucidate the still poorly understood process of pre-synaptic differentiation.

The mammalian olfactory epithelium (OE) possesses the rare capacity of continuous neurogenesis during adulthood: precursor cells continuously divide and differentiate into mature olfactory sensory neurons (OSNs) under physiological conditions and throughout the organism's life. Newly generated sensory neurons project their axons into the olfactory bulb (OB) to establish functional synapses with tufted, mitral and periglomerular cells within specialized structures known as glomeruli. Ultrastructural

aspects of synapse formation in the glomerular layer have been characterized during development (Blanchart et al 2008; Hinds & Hinds 1976). Electron microscopy studies have shown that in mice OSN axons first enter the bulb at embryonic day 11 (E11), the first synapses are observed at E13 and OMP immunoreactivity (a mature cellular marker for olfactory sensory neurons, see below) is first observed at E14 (Farbman & Margolis 1980). However the intrinsic and/or extrinsic signals leading to sensory neuron maturation, and how this later relates to pre-synaptic differentiation, remain to be explored.

Identifying synapse-associated molecules expressed by sensory neurons and changes in their expression patterns along the OE neuronal lineage is a first step toward understanding the relation between synapse formation and sensory neuron maturation. A proposed model for the neuronal lineage in the olfactory epithelium includes MASH1-expressing progenitors located basally in the neuroepithelium that give rise, after rounds of division, to receptor neurons. Within this population of postmitotic neurons, mature olfactory sensory neurons, expressing OMP, are located above immature olfactory sensory neurons, expressing growth associated protein 43 (GAP43) (Calof et al 2002). The pseudo-stratified organization of the olfactory epithelium makes it an ideal model to study the differentiation and maturation of neurons, since the entire lineage of OSNs, from progenitors to immature to mature cells, can be readily seen in a single OE tissue section.

By using a panel of specific *in situ* hybridization probes, we assessed the expression patterns of mRNA for proteins involved in the pre-synaptic vesicle release machinery in the mouse olfactory epithelium. We choose *in situ* hybridization in OE tissue instead of

immunostaining in OB sections as the method used to perform our study because we were interested in evaluating the synaptic inputs from OSNs specifically. Our results indicated a sequential onset of expression for the pre-synaptic molecules as sensory neurons mature. Genes encoding for proteins that play a structural role at the active zone showed an early onset of expression, whereas genes encoding for proteins associated with synaptic vesicles showed a later onset of expression. In particular, a signature molecule for glutamatergic neurons, the Vesicle Glutamate Transporter 2 (VGluT2) was expressed by fully mature olfactory sensory neurons only, showing the latest onset of expression. Also, the expression of all pre-synaptic molecules so far tested was restored after recovery from surgical ablation of the olfactory bulb, suggesting that olfactory sensory neurons would mature as pre-synaptic cells independently of their target. Our data set the stage for understanding the molecular events underlying the differentiation and pre-synaptic maturation of olfactory sensory neurons.

MATERIALS AND METHODS

Animals

SVE129 wild-type animals were obtained from Taconic, Farms, Inc. (Germantown, NY). All animals were housed at Columbia University in accordance with institutional requirements for animal care.

Surgical ablation of the olfactory bulb

Unilateral bulbectomies were performed on 8-week old male mice. Mice were anaesthetized by injection with Ketamine/Xylazine (18 mg/ml and 2 mg/ml, respectively) and a midline incision was made to expose the cranial bone. A small opening just above the right olfactory bulb was made with a drill, and using gentle suction the right olfactory bulb was removed. The cavity vacated by the bulb was then packed with sterile Gel Foam (UpJohn, Kalamazoo, MI). Finally, the incision in the skin over the snout was closed with Vetbond (3M Animal Care Products, St. Paul, MN). Animals were allowed to recover for 30 days after surgery. The degree of the lesion was verified visually and microscopically. We only used animals where the degree of lesion would be complete.

In situ Hybridization

In situ hybridizations were performed on 5-day, 20-day and ~3 month old mouse

olfactory epithelium (OE) tissue. In brief, mice were transcardially perfused with 4% paraformaldehyde (PFA) in phosphate-buffered saline (PBS) pH 8.00. Olfactory epithelial tissue was dissected out and postfixed overnight. The epithelial tissue was then decalcified for two days in 0.5 M EDTA pH 8.00 treated with 0.1% of diethyl pyrocarbonate (DEPC) if the animals were 20 days old and for four days if the animals were older, followed by an overnight immersion in 30% sucrose-PBS as a preparation for cryoprotection, all at 4°C. Then 10 μm thick coronal cryosections were cut and warmed to 55°C. Slides were fixed in 4% PFA, washed in DEPC-PBS, treated with 0.3% H_2O_2 in PBS for 30 minutes at room temperature in order to block endogenous peroxidases if the slides were processed for two color *in situ* hybridization, treated with 10 μg/ml proteinase K at 37°C, fixed once more in 4% PFA, washed with PBS, incubated in 0.1 M triethanolamine with 0.03% acetic anhydride and washed again. Slides were dehydrated in 60%, 80%, 95%, and twice in 100% ethanol and then each slide was hybridized overnight at 63^0C with 0.5-1 μl of biotin and/or 0.5-1 μl of digoxigenin (DIG)-labeled probes in 200 μl of hybridization solution (50% formamide, 10 mM Tris-Cl pH 8.0, 200 μg/ml yeast tRNA, 10% dextran sulfate, 1X Denhardt's solution, 600 mM NaCl, 0.25% sodium dodecyl sulfate, 1 mM EDTA pH 8.0). After hybridization, slides were washed in 2X SSC, 50% formamide, treated with 20 μg/ml RNase A at 37°C to remove any un-hybridized probe and finally washed in a series of 2X, 0.2X and 0.1X SSC. The slides were blocked in 0.5% NEN buffer (Perkin-Elmer, Boston, MA) for 1 hour and then incubated for 48 hours at 4°C in alkaline phosphatase-conjugated anti-DIG diluted 1:200 in 0.5% NEN buffer (Roche, Indianapolis, IN). Probes targeting olfactory neurons cellular markers were labeled with biotin and probes targeting pre-synaptic molecules

were labeled with DIG. For two color fluorescent in situ hybridization biotin and DIG labeled probes were detected sequentially as described in Ishii et al (Ishii et al 2004). First, biotin labeled probes were detected using the TSA biotin system (Perkin Elmer, Boston, MA) followed by an incubation with the Streptavidin Alexa Fluor 488 conjugate (Molecular probes, Eugene, OR) diluted 1:300 in the blocking buffer provided by the manufacturer. Second, DIG labeled probes were detected using the HNPP fluorescent detection set (Roche, Mannheim, Germany) incubating with the HNPP/Fast Red solution for 3x30 minutes due to the low transcript level. Although we quenched endogenous peroxidases as suggested by the manufacturer, we observed high background in the probes detected with the TSA biotin system. This non-specific label is localized above the most apical cell layer of the olfactory epithelium, in the mucus and cilia, and in the lamina propia. For chromogenic *in situ* hybridization slides were washed in 150 mM NaCl, 100 mM Tris-Cl pH 7.5, 0.05% Tween 20 and then incubated with 66 µl NBT and 33µl BCIP (NBT/BCIP, Promega, Madison, WI) in 10 ml of 100 mM NaCl, 100 mM Tris-Cl pH 9.5, 50 mM $MgCl_2$ until color develops.

In situ probes

Probes for bassoon, gap43, Munc18-1, omp, piccolo, SNAP25, synaptophysin, synaptotagmin 1, syntaxin 1A and VAMP2 were designed to target the mRNA regions described on Table II.1 and templates were cloned from olfactory epithelium or brain cDNA into pCRII-TOPO (Invitrogen, Carlsbad, CA). Probes for synapsin 1, Vesicle Glutamate Transporter 2 (VGluT2) and MASH1 were generated from cDNA clones

(IMAGE ID#s 5368098, 5357143 and 6415061, respectively) obtained from Open Biosystems (Huntsville, AL). Probes for synapsin 1 and VGluT2 were generated from cDNA clones digested with BglII and HpaI respectively (see Table 1). Probe for MASH1 was generated from full-length cDNA clone. The pan-α-neurexin probe template was generously provided by Dr. Peter Scheiffele (University of Basel, Switzerland). The sequence from pan-α-neurexin probe aligns with nucleotides 1,924-2,611 from neurexin 1 with 100% identity, nucleotides 901-1,595 from neurexin 2 with 70% identity and nucleotides 337-1,013 from neurexin 3 with 74% identity (see Table 1) (alignments were performed by using the Align Tool from NCBI http://blast.ncbi.nlm.nih.gov/Blast.cgi).

Probes preparation was done according to Ishii et al, 2004. In brief template DNA, RNA labeling mixture (Roche, Mannheim, Germany), 10x transcription buffer (Roche, Mannheim, Germany), RNasin (Roche, Mannheim, Germany) and RNA polymerase (Roche, Mannheim, Germany) were incubated at 37^0 for 2 hours. Probes were precipitated and pellets were dissolved in 25 μl DEPC treated water. Probes specificity was determined by testing sense and anti-sense probes simultaneously (Supplementary Figure II.1 and Figure II.2).

Probe Name	mRNA accession number	ISH probe nucleotides
bassoon	NM_007567	11,381-12,037
gap43	NM_008083	531-1,146
munc18-1	NM_009295	2,654-3,181
omp	NM_011010	1,373-2,012
pan-α-neurexin	NM_020252 (neurexin 1) NM_020253 (neurexin 2) NM_172544 (neurexin 3)	1,924-2,611 901-1,595 337-1,1013
piccolo	NM_011995	15,204-16,029
snap25	NM_011428	36-574
synapsin 1	BC022954	2,367-3,143
synaptophysin	NM_009305	697-1,602
synaptotagmin1	NM_009306	2,999-3,503
syntaxin1a	NM_016801	1,046-1,586
vamp2	NM_009497	1,438-2,110
VGluT2	BC038375	3,353-3,728

Table II.1: mRNAs assessed by *in situ* hybridization. Abbreviation: ISH: *In Situ* Hybridization.

Immunohistochemistry

Mice were transcardially perfused with 4% PFA in PBS. Olfactory epithelial tissue was dissected out and postfixed for 2 hours, followed by decalcification in 0.5 M EDTA pH 8.00 performed over two days for 20 days old mice and over four days for older animals and by overnight immersion in 30% sucrose-PBS, all at 4°C. Immunohistochemistry was performed on 16 μm cryosections on slides (Superfrost, Fischer, Fair Lawn, NJ). Slides were warmed to 55°C for 10 minutes followed by steaming in 0.01 M sodium citrate pH 6.0 for 10 minutes. The slides were cooled then rinsed in PBSTx (0.1% Triton X in PBS). The sections were blocked in 10% Normal Donkey Serum (NDS) in PBSTx for 2 hours and then incubated in primary antibody mixtures in 2.5% normal donkey serum in PBSTx overnight at 4°C. Sections were washed in PBSTx (4x10 minutes) and then incubated in secondary antibody in 2.5% NDS-PBSTx at room temperature for 1-2 hours. The secondary antibodies were AlexaFluor-conjugated 488 or 594-donkey anti-rabbit or anti-goat diluted 1:750 in blocking buffer (Molecular Probes, Eugene, OR). Slides were washed 2x10 minutes in PBSTx and 2x10 minutes in PBS before counterstaining with TOTO-3 diluted 1:10,000 in PBS (Molecular probes, Eugene, OR). Mounting of the sections was performed using Vectashield (Vector, Burlingame, CA).

Primary antibodies

Goat anti-OMP (Wako, Dallas, TX, #544-10001) was used in immunohistochemistry at 1:2,000. This polyclonal serum was obtained from a goat through multiple immunizations with rodent olfactory marker protein (OMP). It stains a single band of 19 kDa in Western

blot, and its specificity in immunohistochemistry has been verified by pre-adsorption of the antiserum with high-performance liquid chromatrography (HPLC)-purified OMP, which abolishes all staining (Baker et al 1989).

Rabbit anti-VGluT2 (Synaptic Systems, Goettingen, Germany, #135-403) was used at 1:1,000. This polyclonal serum was obtained from a rabbit upon immunization with a synthetic antigen containing the amino acid residues 510-582 of rat VGluT2. VGluT2 antibody recognizes a single band of 65 kDa on immunoblot. This immunoreactive band is abolished after incubation of the antiserum with the antigen used for immunization (Takamori et al 2001).

Microscopy

Tissue sections were imaged on an Olympus confocal microscope (Olympus FluoView 600) and analyzed by using Fluoview, ImageJ, and Adobe Photoshop. Images were not modified other than to balance brightness and contrast. All of the genes tested in the present study are expressed in all four zones of mouse olfactory epithelium. Images were taken from septum of mouse OE.

RESULTS

Expression of mRNAs for pre-synaptic molecules in the Olfactory Epithelium

Mouse olfactory epithelium (OE) tissue was processed for fluorescent *in situ* hybridization. To establish the temporal onset of pre-synaptic differentiation during olfactory sensory neuron lineage, we combined specific probes targeting genes encoding cellular markers expressed along the sensory neuron lineage and specific probes targeting genes encoding molecules enriched in pre-synaptic terminals. In our study we sought to examine pre-synaptic molecules with diverse functions. We therefore targeted genes that would code for active zone components (piccolo and bassoon), SNARE proteins (syntaxin 1A, VAMP2 and SNAP25), a SNARE associated protein (Munc18-1), vesicle associated proteins (synapsin 1, synaptotagmin 1 and synaptophysin), a neurotransmitter transporter protein (Vesicle Glutamate Transporter 2 or VGluT2) and trans-synaptic adhesion proteins (α-neurexins, Note: pan-α-neurexin probe recognizes the three α-neurexins gene transcripts) (Bennett et al 1992; Cases-Langhoff et al 1996; Chin et al 1995; Edelmann et al 1995; Geppert et al 1994; Lise & El-Husseini 2006; Sollner et al 1993; Takamori et al 2001; tom Dieck et al 1998; Toonen & Verhage 2007). We observed three distinct patterns of expression of pre-synaptic molecules that depended upon when during OSN lineage the onset of expression took place. We observed that the expression of mRNAs for some synaptic molecules coincided with that of MASH1, a progenitor cell marker for olfactory sensory neurons (Figure II.1) (Calof et al 2002). Examples included bassoon, piccolo, Munc18-1 and syntaxin 1A. This result suggests

that the onset of expression for these genes occurs very early in the olfactory sensory neuron lineage, when progenitor cells are at the earliest transit amplifying stage. Importantly, the expression of these mRNAs persisted through later stages in sensory neuron lineage. Sammeta et al., 2007 reported expression of piccolo only in basal and immature OSNs by using a different *in situ* hybridization probe (Sammeta et al 2007). To resolve this apparent contradiction, we tested simultaneously both probes (Figure II.2). We observed that qualitatively both probes are similar but that the positive signal obtained with our probe for piccolo was stronger, thereby explaining the apparent discrepancy. Since both probes recognize different regions from the same piccolo splice variant, different affinities might have determined different signal levels. We also obtained a weak positive signal in sustentacular cells, a non-neuronal secretory cell type located in the most apical layer of the OE (see Figure II.1D). Since piccolo is expressed by other types of secretory cells, such as the pancreatic beta cells where it is involved in secretion of insulin upon stimuli (Fujimoto et al 2002), we speculate that piccolo expression by sustentacular cells has a different role than that of piccolo expression by OSNs. Other mRNAs were not detected in MASH1+ neuronal progenitors (Figure II.3) and their expression came on later in the olfactory sensory neuron lineage, when cells differentiated into GAP43- expressing immature receptor neurons and begun to project their axons outside the epithelium (Figure II.4) (Verhaagen et al 1989).

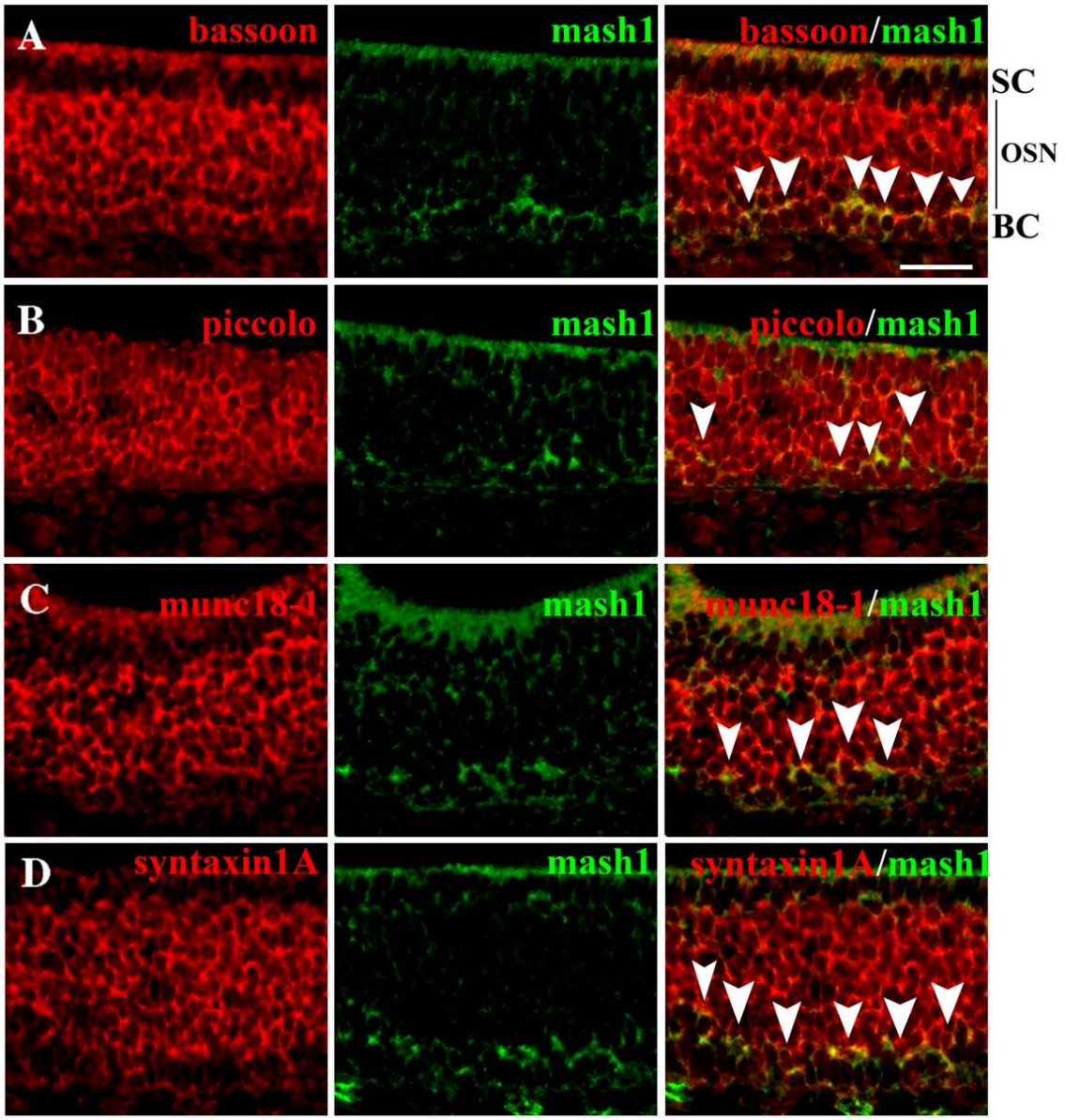

Figure II.1: Bassoon, piccolo, Munc18-1 and syntaxin 1A mRNA were expressed early in olfactory sensory neuron lineage.

Fluorescent double *in situ* hybridization was performed on coronal sections of post-natal day 5 mouse olfactory epithelium. RNA probes targeted against bassoon (A), piccolo (B), Munc18-1 (C) and syntaxin 1A (D) gene transcripts (in red) were combined individually with a probe directed against MASH1 mRNA (in green), a neuronal progenitor marker expressed by a subset of basal cells. Arrows point to OSNs that co-express the mRNA of these four genes and MASH1 mRNA (overlay red plus green). Note that the expression of the four genes was not limited to MASH1+ cells only, but they continued to be expressed throughout the sensory neuron lineage. Scale bar: 30 μm. Abbreviations: SC: Sustentacular Cells; OSNs: Olfactory Sensory Neurons; BC: Basal Cells.

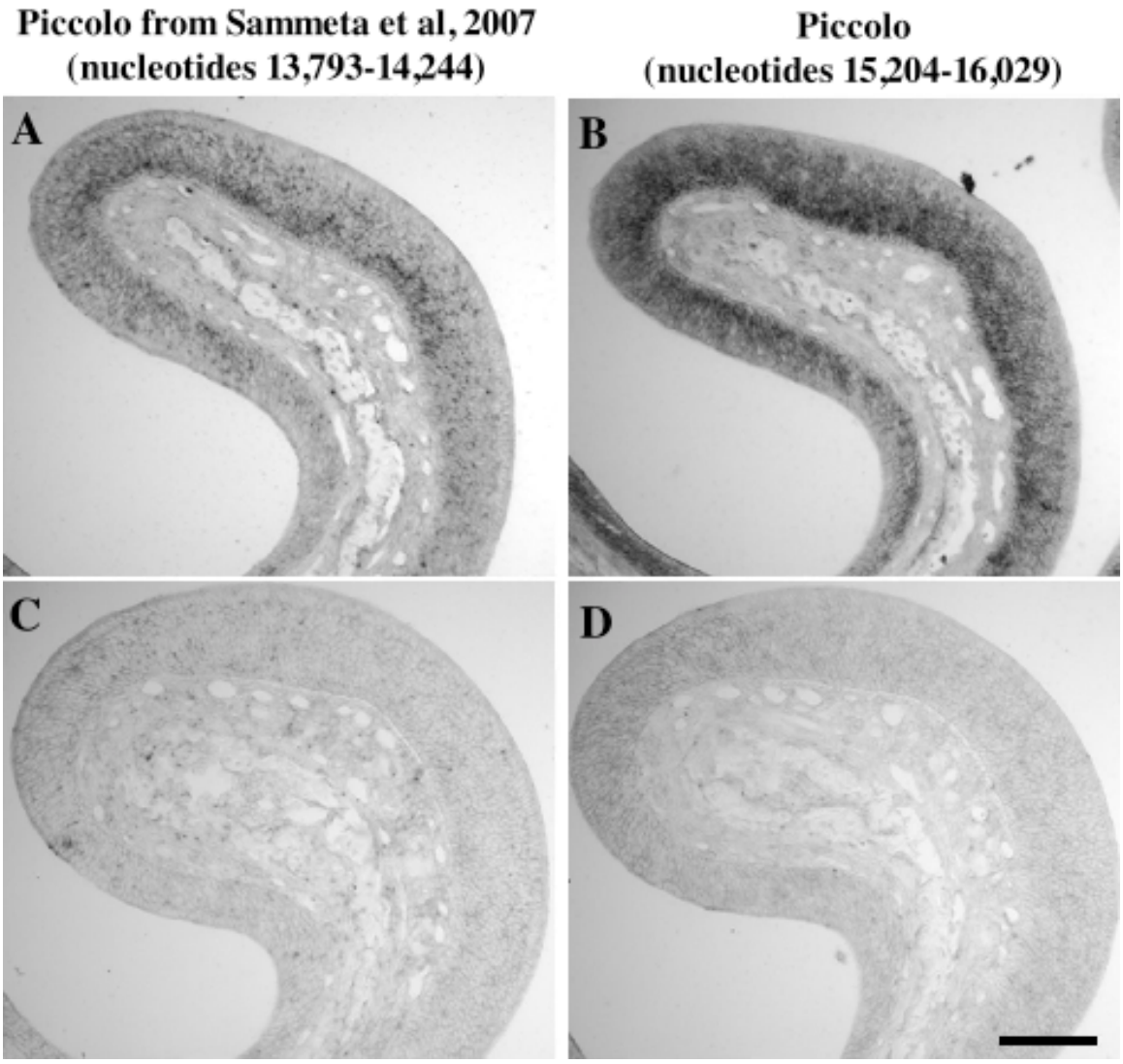

Figure II.2: Two probes targeting different regions of piccolo mRNA were tested simultaneously in chromogenic *in situ* hybridization experiments performed on 20-day old olfactory epithelium.

(A) Piccolo probe described in Sammeta et al, 2007 recognizes nucleotides 13,793-14,244 from the sequence NM_011995.

(B) Piccolo probe used in Figure 1 recognizes nucleotides 15,204-16,029 from the sequence NM_011995 (see also Table 1).

(C) and (D) are negative control sense probes for (A) and (B) respectively. Scale bar: 30 μm.

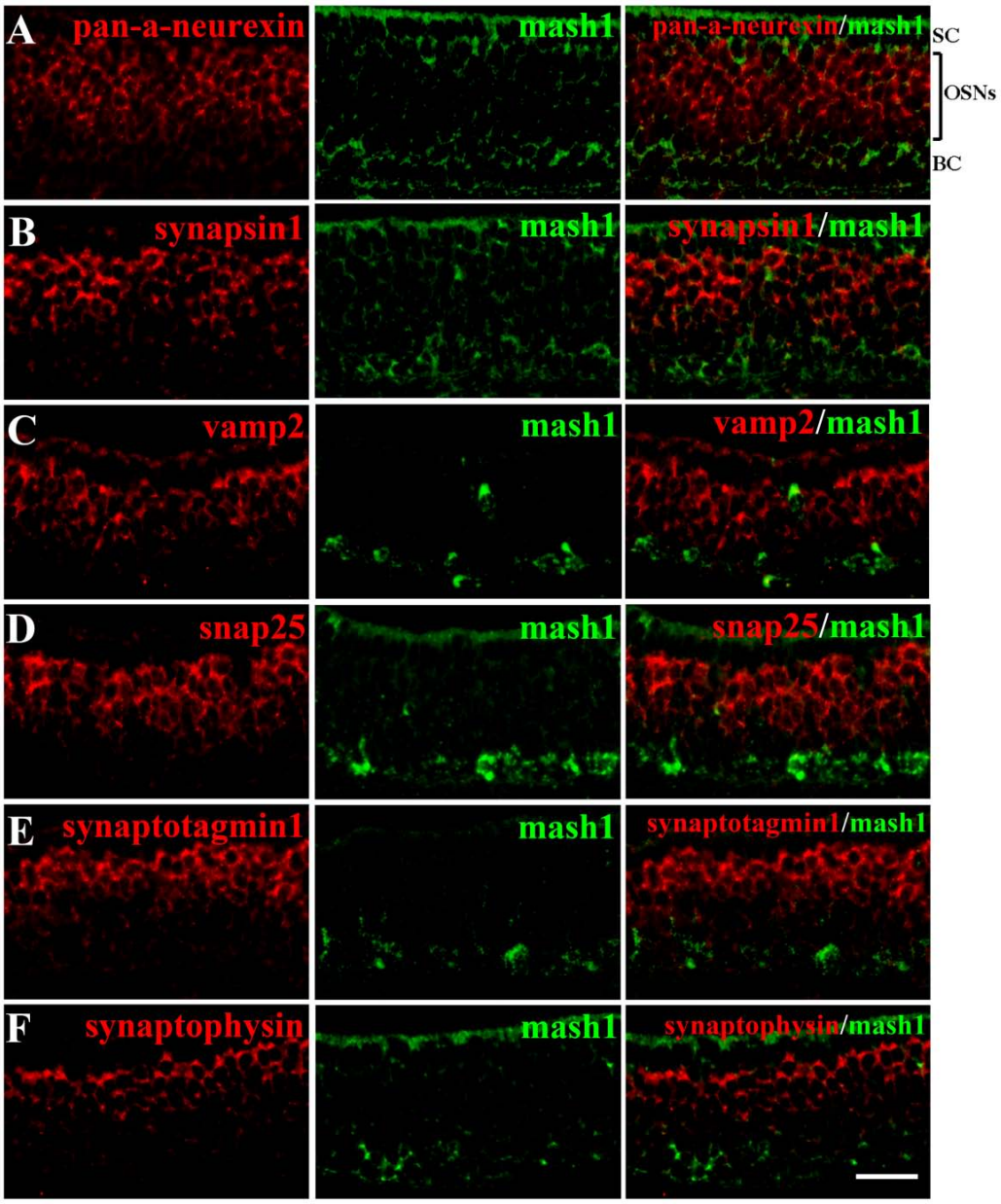

Figure II.3: Pan-α-neurexins, synapsin 1, VAMP2, SNAP25, synaptotagmin 1 and synaptophysin mRNA were expressed later in olfactory sensory neuron lineage.

Fluorescent double *in situ* hybridization was performed on post-natal day 5 mouse olfactory epithelium combining probes recognizing α-neurexins mRNA (A), synapsin 1 mRNA (B), VAMP2 mRNA (C), SNAP25 mRNA (D), synaptotagmin 1 mRNA (E) or synaptophysin mRNA (F) (in red) with a probe recognizing MASH1 mRNA (in green). The expressions of the six pre-synaptic genes tested in this set of experiments did not overlap with MASH1 expression (overlay red plus green). Pan-a-neurexin probe recognizes α-neurexin 1, 2 and 3 gene transcripts. Scale bar: 30 μm. Abbreviations: SC: Sustentacular Cells; OSNs: Olfactory Sensory Neurons; BC: Basal Cells.

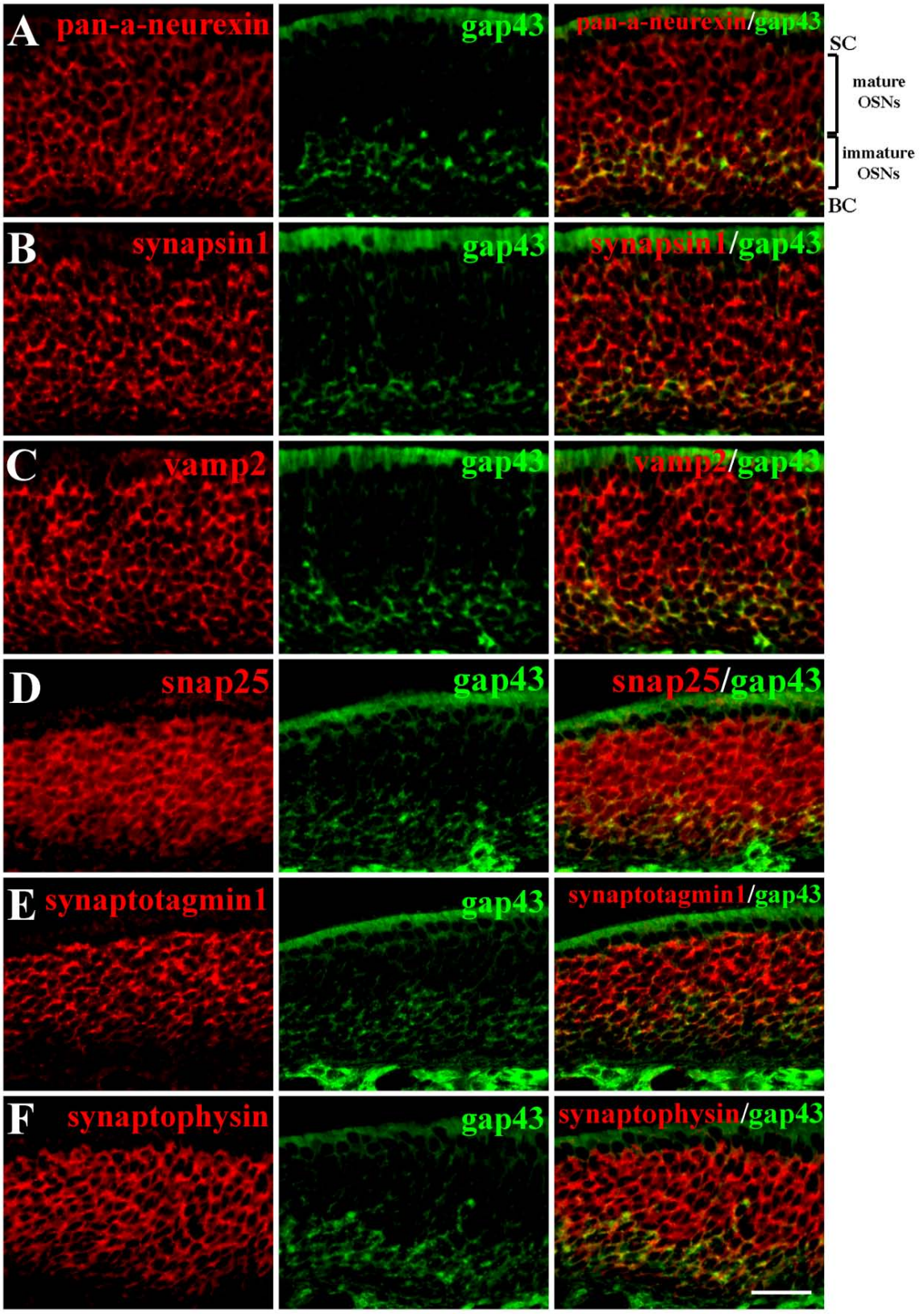
A
pan-a-neurexin
gap43
pan-a-neurexin/gap43
SC
mature OSNs
immature OSNs
BC
B
synapsin1
gap43
synapsin1/gap43
C
vamp2
gap43
vamp2/gap43
D
snap25
gap43
snap25/gap43
E
synaptotagmin1
gap43
synaptotagmin1/gap43
F
synaptophysin
gap43
synaptophysin/gap43

Figure II.4: Expression of pan-α-neurexins, synapsin 1, VAMP2, SNAP25, synaptotagmin 1 and synaptophysin mRNAs overlapped with that of GAP43 mRNA.

Fluorescent double *in situ* hybridization was performed on post-natal day 20 mouse olfactory epithelium. Probes recognizing α-neurexins mRNA (A), synapsin 1 mRNA (B), VAMP2 mRNA (C), SNAP25 mRNA (D), synaptotagmin 1 mRNA (E) or synaptophysin mRNA (F) (in red) were combined individually with a probe recognizing GAP43 mRNA (in green). Immature GAP43+ cells did express these six pre-synaptic genes, indicating that the expression of α-neurexins, synapsin 1, VAMP2, SNAP25, synaptotagmin 1 and synaptophysin begun during OSN maturation (overlay red plus green). Scale bar: 30 μm. Abbreviations: SC: Sustentacular Cells; OSNs: Olfactory Sensory Neurons; BC: Basal Cells.

Examples of genes whose expression overlapped with the immature cell marker GAP43 are α-neurexins, synapsin 1, VAMP2, SNAP25, synaptotagmin 1 and synaptophysin. The mRNA for these genes also continued to be expressed through later stages in olfactory sensory neuron lineage.

Finally, we examined the expression of the glutamate transporter VGluT2, a transporter responsible for the accumulation and storage of glutamate within synaptic vesicles and known to be restricted to glutamatergic neurons. In the olfactory epithelium, VGluT2 mRNA showed a late onset of expression. Indeed, VGluT2 mRNA was absent from immature GAP43+ cells and was restricted only to mature OMP+ cells (Figure II.5, C and F) (Farbman & Margolis 1980). Therefore, VGluT2 was exclusively expressed by fully differentiated olfactory sensory neurons, once their axons have reached the corresponding targets at the glomeruli in the bulb.

VGluT2 protein expression in the Olfactory Epithelium

The mechanisms that regulate SV protein expression appear to be complex. Indeed, previous work has shown that, for some pre-synaptic molecules, there is discordance between the patterns of mRNA expression and protein expression, suggesting that post-transcriptional mechanisms might be involved (Bergmann et al 1991; Daly & Ziff 1997; Lou & Bixby 1993).

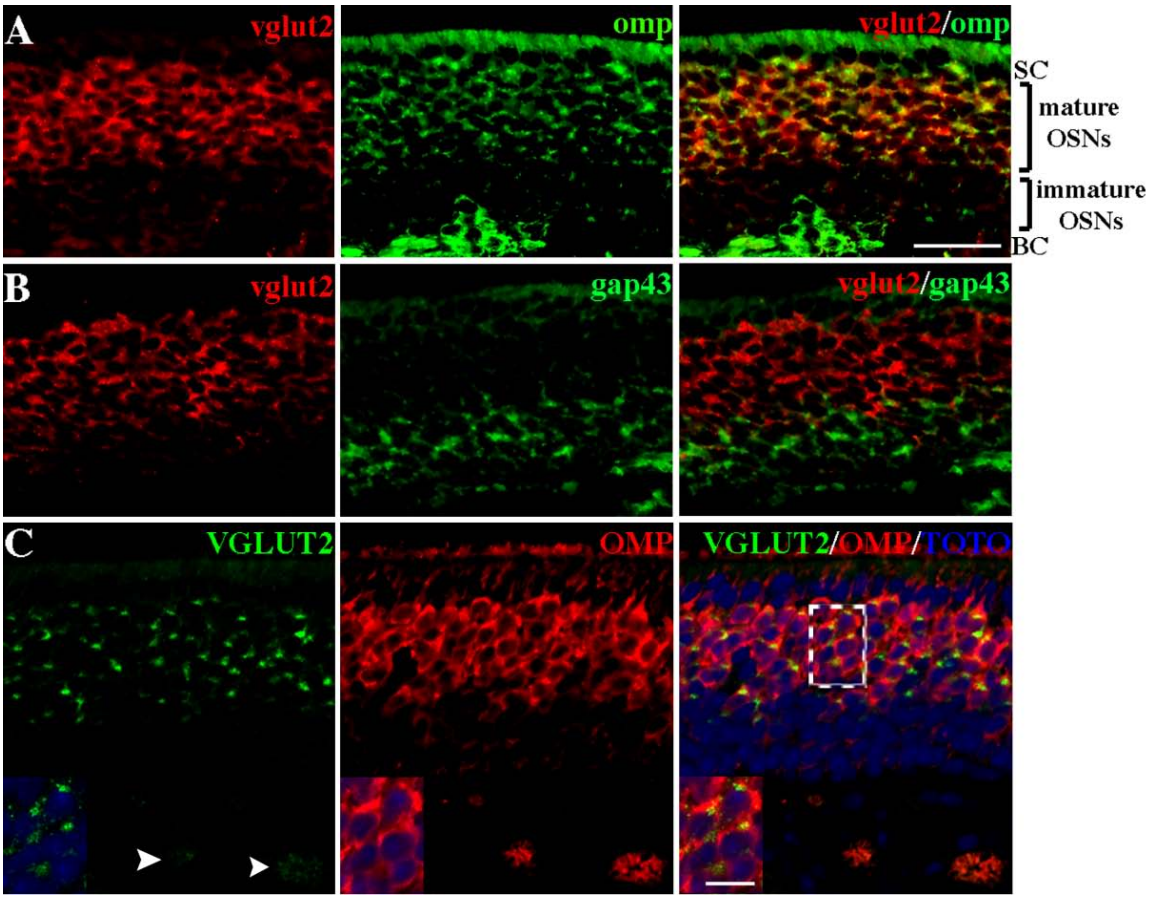

Figure II.5: VGluT2 was expressed by fully mature olfactory sensory neurons only.

A and B: Fluorescent double *in situ* hybridization in post-natal day 20 mouse olfactory epithelium showing that Vesicle Glutamate Transporter 2 (VGluT2) mRNA was expressed in cells that also expressed olfactory marker protein (OMP) (A) and that VGluT2 was absent from cells that express the immature cell marker GAP43 (B). This indicated that the initiation of VGluT2 expression coincided with that of OMP, a marker of mature olfactory sensory neurons.

(C): Immunohistochemistry in post-natal day 20 mouse olfactory epithelium showing co-localization of VGluT2 and OMP at the protein level (anti-VGLUT2 in green, anti-OMP in red, nuclear marker TOTO-3 in blue). Area inside the dashed box in is shown with higher magnification in the corresponding insets. Arrowheads indicate axon bundles stained for VGLUT2.

Scale bar: 30 µm. Scale bar inset in (I): 10 µm. Abbreviations: SC: Sustentacular Cells; OSNs: Olfactory Sensory Neurons; BC: Basal Cells.

Consequently we sought to determine whether VGluT2 protein was concomitantly expressed with its mRNA in the olfactory epithelium. Because VGluT2 is a synaptic vesicle membrane protein its main cellular localization is at the sensory neuron pre-synaptic terminals in the olfactory bulb. Nevertheless, we could detect VGluT2 protein in the cell body of olfactory sensory neurons, probably localized in the endoplasmic reticulum. VGluT2 protein overlapped with OMP protein in the olfactory epithelium (Figure II.5I), suggesting that, at least in this olfactory tissue, there is no delay between the appearance of VGluT2 mRNA and imunnocytochemically detectable VGluT2 protein. This also confirms that VGluT2 is restricted to mature OSNs, not only at the mRNA level but also at the protein level.

Expression of pre-synaptic molecules in target-deprived olfactory tissue

Because, in chick ciliary ganglion and spinal motor neurons, contact with the target regulates the expression of synaptotagmin 1 (Campagna et al 1997; Plunkett et al 1998), we investigated whether in mouse olfactory epithelium the expression of genes involved in synapse function was also dependent on contact between olfactory sensory neurons and second order neurons in the olfactory bulb. To address this question, we performed unilateral olfactory bulbectomies (OBX), a surgical technique that involves the ablation of one of the olfactory bulbs, designed to deprive the ipsilateral sensory neurons of their target. Importantly, the contralateral epithelium, for which the olfactory bulb targets remain, is used as an internal control in this kind of experiment. Shortly after bulbectomy, contact-deprived sensory neurons become apoptotic and die causing a

dramatic decrease in ipsilateral epithelial thickness that peaks at day 5 post-surgery (Carson et al 2005; Cowan et al 2001; Michel et al 1994). Degeneration of the olfactory neurons after target deprivation is followed by an increase in basal cell proliferation, which gives rise to new neurons and leads to epithelial recovery. Nevertheless in the chronic absence of the bulb the epithelium remains thinner than normal and there is a significant reduction in the number of sensory neurons expressing OMP (Schwob et al 1992; Verhaagen et al 1990). We tested our panel of *in situ* hybridization probes in olfactory epithelium tissue from animals sacrificed 30 days post-bulbectomy (OBX-30), at which time the initial acute retrograde degeneration has ceased and the epithelium has stabilized in thickness (Costanzo & Graziadei 1983). We observed that the expression of all the pre-synaptic genes was restored after the tissue recovered from bulbectomy (Figure II.6). Furthermore, 30 days after surgery, VGluT2 expression was still restricted to OMP+ cells only (Figure II.7), illustrating that the absence of the synaptic target did not alter sensory neuron pre-synaptic differentiation.

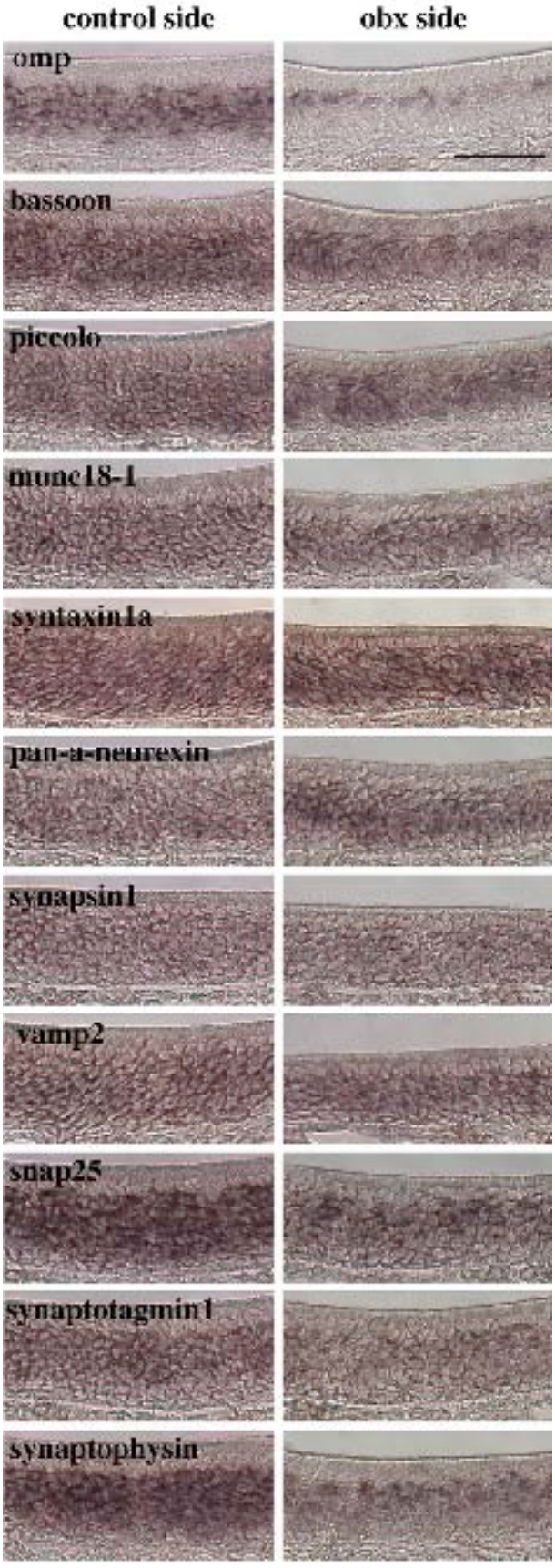
control side
obx side
omp
bassoon
piccolo
munc18-1
syntaxin1a
pan-a-neurexin
synapsin1
vamp2
snap25
synaptotagmin1
synaptophysin

Figure II.6: Expression of pre-synaptic molecules by olfactory sensory neurons was restored after recovery from unilateral bulbectomy.

Chromogenic *in situ* hybridization showing expression of OMP, bassoon, piccolo, Munc18-1, syntaxin 1A, α-neurexins, synapsin 1, VAMP2, SNAP25, synaptotagmin 1 and synaptophysin mRNAs in non-bulbectomized (control) and bulbectomized (OBX) sides of mouse olfactory epithelium 30 days post-surgery. Note the thinning of the neuroepithelium on the bulbectomized side when compared to the non-bulbectomized side. Scale bar: 50 μm. Abbreviations: control side: non-bulbectomized side of the olfactory epithelium; obx side: bulbectomized side of the olfactory epithelium.

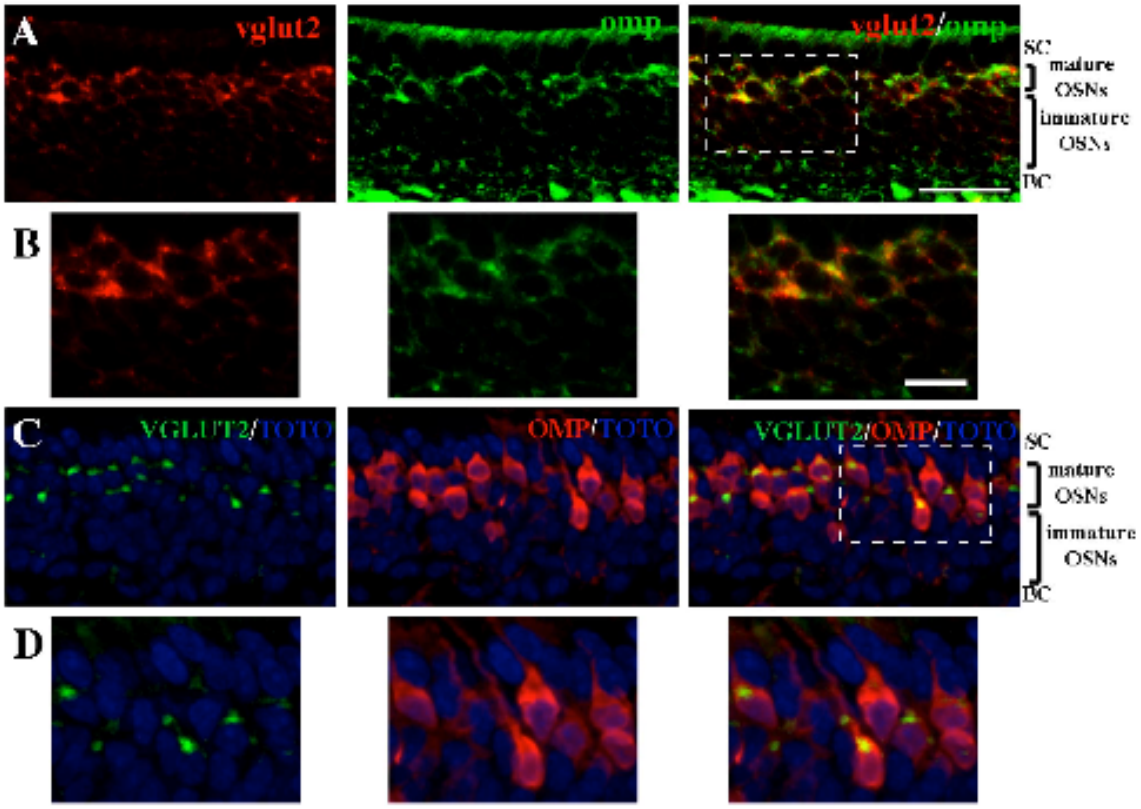

Figure II.7: Expression of VGluT2 was restored in olfactory neurons after recovery from unilateral bulbectomy.

(A and B): Fluorescent double *in situ* hybridization was performed combining probes for Vesicle Glutamate Transporter 2 (VGluT2, red) and OMP (green) in the bulbectomized side from olfactory epithelium 30 days post-bulbectomy. We observed that after recovery from bulbectomy VGluT2 mRNA was still restricted to fully mature OMP+ neurons only (overlay red plus green).

(C and D): Immunohistochemistry showed co-localization of VGLUT2 (green) and OMP (red) proteins in the bulbectomized side of mouse olfactory epithelium 30 days post-surgery (anti-VGLUT2 in green, anti-OMP in red, nuclear marker TOTO-3 in blue).

B and C are higher magnification from areas inside the dashed boxes on A and B respectively. Scale bar in A and C: 30 μm, in B and D: 10 μm. Abbreviations: SC: Sustentacular Cells; OSNs: Olfactory Sensory Neurons; BC: Basal Cells.

DISCUSSION

The present study was designed to correlate the pattern of expression of specific pre-synaptic molecules with the basic processes occurring during olfactory sensory neuron (OSN) maturation. *In situ* hybridization was used to reveal the localization of pre-synaptic mRNA molecules in the olfactory epithelium at different stages of the olfactory sensory neuron lineage. We observed that as olfactory sensory neurons mature they sequentially acquire the expression of pre-synaptic molecules (results are summarized in Figure II.8). Thus, mRNA from genes encoding pre-synaptic molecules localized at the active zone (piccolo and bassoon) together with a T-SNARE (syntaxin 1A) and its interacting partner (Munc18-1) co-localized with MASH1 mRNA, a progenitor cell marker, illustrating the initial onset of pre-synaptic genes expression in the sensory neuron lineage. During the later stage of development, as determined by the expression of the immature sensory neuron marker GAP43, we observed expression of synaptic molecules associated with the synaptic vesicle membrane (the V-SNARE VAMP2, synapsin 1, synatophysin and synaptotagmin 1) together with the T-SNARE SNAP25 and the trans-synaptic adhesion molecules α-neurexins. Finally, it is not until olfactory sensory neurons express OMP and are fully mature that Vesicle Glutamate Transporter 2 expression occurred, both at the mRNA and protein levels. We also assessed our panel of *in situ* hybridization probes in epithelial tissue from bulbectomized mice. After recovery from surgery, the expression of all pre-synaptic molecules tested was restored; in particular VGluT2 mRNA and protein expression were still restricted to OMP+ cells after bulbectomy. These results are consistent with the hypothesis that in the OE, maturation

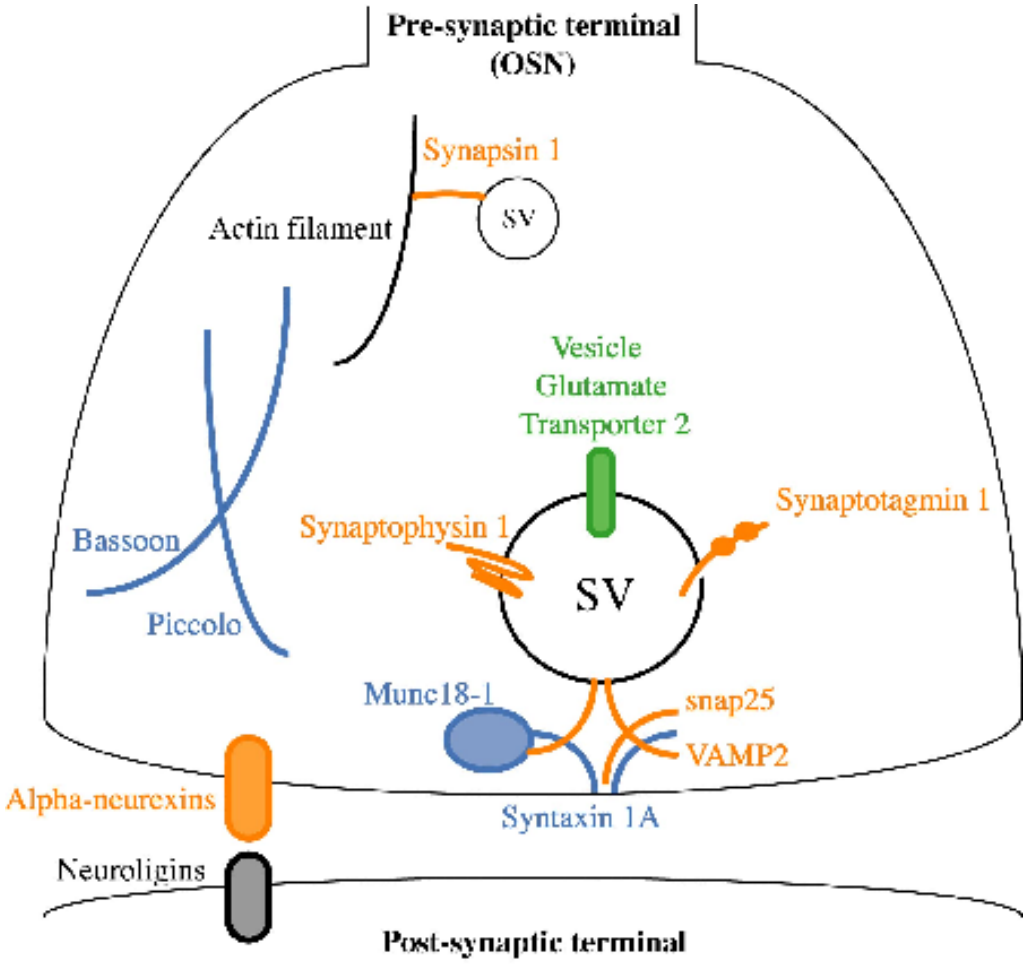

Figure II.8: Summary illustrating the function and distribution of the pre-synaptic molecules addressed in this study.

In situ hybridization was used in this study to reveal the localization of pre-synaptic mRNA molecules in the olfactory epithelium at different stages of the olfactory sensory neuron lineage. We observed that as olfactory sensory neurons mature they sequentially acquire the expression of pre-synaptic molecules. We observed that the pre-synaptic molecules bassoon, piccolo, syntaxin 1A and its interacting partner Munc18-1 (represented in blue) showed the earliest onset of expression during OSN lineage. The mRNA of these genes co-localized with MASH1 mRNA, a cellular marker for olfactory sensory neurons progenitors. The pre-synaptic molecules whose expression was initiated during OSN maturation are α-neurexins, synapsin 1, VAMP2, SNAP25, synaptotagmin 1 and synaptophysin (represented in orange). The expression of these genes overlapped with that of GAP43, a marker for immature olfactory sensory neurons. The pre-synaptic molecule with the latest onset of expression is the Vesicle Glutamate Transporter 2 (represented in green). VGluT2 expression overlapped with OMP expression, a mature cellular marker, suggesting that is not until OSNs are fully mature that they acquire the ability to release glutamate. Neurexins and Munc18-1 interact indirectly through the CASK/Mint complex (Biederer & Sudhof 2000). In turn, piccolo can interact with VAMP2 through the preanylated Rab receptor protein PRA1 (Dresbach et al 2001).

and pre-synaptic differentiation of olfactory sensory neurons can occur independently of their target.

To date little is known about how synapses between olfactory sensory neurons and second order neurons are formed, which pre-synaptic molecules are involved and how they are distributed along the olfactory receptor neuron lineage (Bergmann et al 1993). Here we described that, as they mature, OSNs sequentially acquire the expression of specific pre-synaptic molecules. Interestingly, genes with the earliest onset of expression encode proteins that provide the structural basis to organize the release and retrieval of synaptic vesicles (SV), like piccolo and bassoon, and for proteins that are necessary for SV docking and fusion, such as syntaxin 1A and Munc18-1. Genes that are expressed later, when OSNs are still immature but already committed to a receptor neuron fate, encode for proteins known to promote synapse formation and assembly of the pre-synaptic secretory apparatus (α-neurexins), for proteins involved in exocytosis of vesicles (VAMP2 and SNAP25), for SV proteins implicated in the regulation of neurotransmitter release (synaptotagmin 1 and synapsin 1) and for synaptophysin, the most abundant SV membrane protein with still unclear function (Dean & Dresbach 2006; Geppert et al 1994; Missler et al 2003; Rosahl et al 1995; Sollner et al 1993; Sudhof 2004). The onset of expression of the pre-synaptic genes described thus far precedes vesicular release of neurotransmitter. Although our experiments do not address when synaptic contact between OSNs and second order neurons is made under normal circumstances, the early expression of these genes may suggest other functions besides synapse formation. It has been proposed that exocytosis plays a fundamental role in axon outgrowth by allowing an

increase of the surface of the plasma membrane (Futerman & Banker 1996). Indeed treatments that disrupt membrane transport retard axon growth (Osen-Sand et al 1993). Since most, if not all, of the genes with an early onset of expression studied here participate in exocytosis, we suggest that their early presence is involved not only in synapse formation but also in axon elongation.

The pre-synaptic gene with the latest onset of expression coincides with that of OMP expression and encodes VGluT2, a transporter involved in loading SVs with the neurotransmitter glutamate. We were unable to detect the other two glutamate transporter family members VGluT1 and VGluT3 mRNAs in the olfactory epithelium (data not shown). Consistent with that, it has been suggested that VGluT1 and VGluT3 proteins are absent from OSNs terminals in the olfactory bulb (Gabellec et al 2007). Thus, in OSNs, vesicular release of neurotransmitter is likely dependent on VGluT2 exclusively and occurs only after cells are fully mature. Indeed vesicular uptake of glutamate is specific to glutamatergic axon terminals and is a necessary process before glutamate is released from synaptic vesicles into the synaptic cleft. Expression of VGluT2 in heterologous cells is sufficient to make gabaergic neurons glutamatergic (Takamori et al 2001). Interestingly, VGluT2 protein is still detected in *omp* knock out background by immunohistochemistry (data not shown), suggesting that VGluT2 expression is not dependent on OMP. Also, it is of interest to note that similarly to VGluT2, Dopamine Receptor 2 mRNA is also absent from immature OSNs and is also present in fully mature OSNs only (Masayo Omura, Peter Mombaerts Lab, personal communication). This would suggest that OSNs acquire the ability to release glutamate concomitantly with the capacity of being modulated by dopamine.

In order to assess whether the expression of pre-synaptic molecules is activity dependent we tested our panel of *in situ* hybridization probes in olfactory epithelium tissue from animals lacking Adenylyl Cyclase 3 (Wong et al 2000). In the knock out background all pre-synaptic molecules were expressed at the same stages in OSN lineage as in control tissue (unpublished observations). This result shows that the expression of pre-synaptic genes in the OE is not dependent on the cAMP-signaling cascade.

Regeneration of OSNs following recovery from bulbectomy has been studied extensively (Costanzo & Graziadei 1983; Konzelmann et al 1998; Shetty et al 2005). Schwob et al., 1992 proposed that the olfactory bulb does not induce or stimulate neuronal differentiation but rather provides OSNs with the necessary trophic support for their survival (Schwob et al 1992). Our results are in line with this hypothesis and show that pre-synaptic differentiation of OSNs can occur even in the absence of their post-synaptic partners. Altogether our results suggest that olfactory sensory neurons follow an intrinsic program of maturation and pre-synaptic differentiation.

SUPPLEMENTARY FIGURE

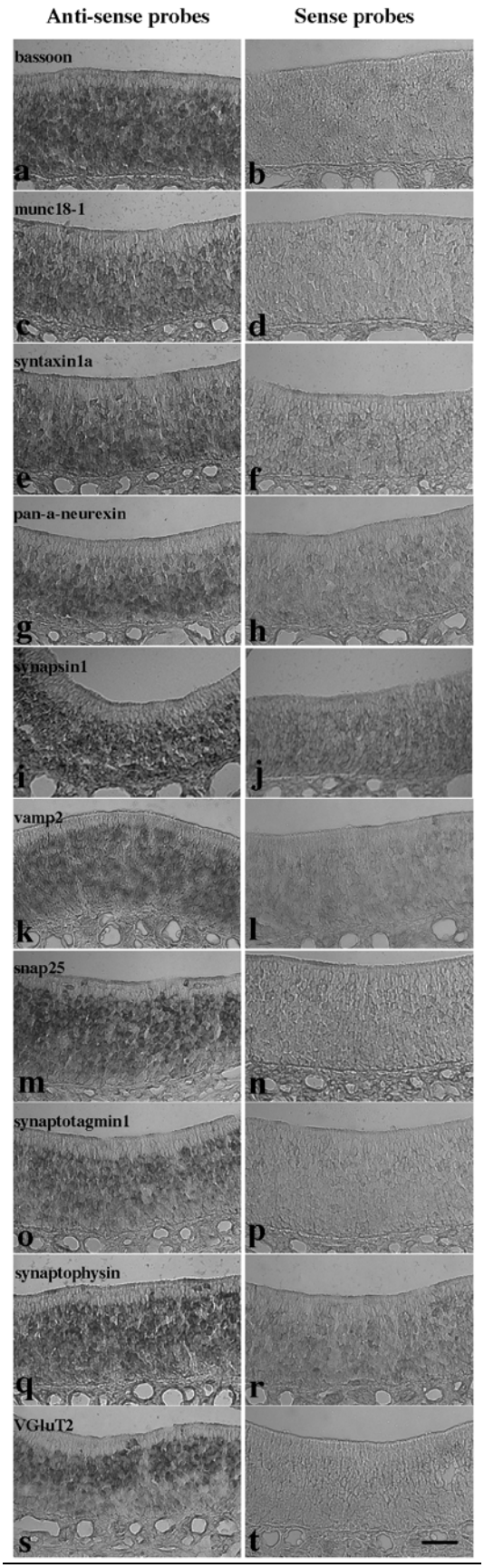
Anti-sense probes
Sense probes
bassoon
a
b
munc18-1
c
d
syntaxin1a
e
f
pan-a-neurexin
g
h
synapsin1
i
j
vamp2
k
l
snap25
m
n
synaptotagmin1
o
p
synaptophysin
q
r
VGluT2
s
t

Figure II.1: Bassoon (a and b), Munc18-1 (c and d), syntaxin 1A (e and f), α-neurexins (g and h), synapsin 1 (i and j), VAMP2 (k and l), SNAP25 (m and n), synaptotagmin 1 (o and p), synaptophysin (q and r) and VGluT2 (s and t) are expressed in olfactory sensory neurons.

Anti-sense and sense probes were tested simultaneously in chromogenic *in situ* hybridization experiments performed on 20-day old olfactory epithelium. Negative control sense probes show specificity of the signal of the anti-sense probes. Scale bar: 50 μm.

CHAPTER III

EXUBERANT GROWTH OF OLFACTORY SENSORY NEURON AXONAL ARBORIZATIONS

ABSTRACT

Neural connections in the adult nervous system are set up with a high degree of precision. Several examples throughout the nervous system indicate that precision is achieved by establishing first an initial exuberant immature pattern of connectivity that is sculpted into the adult pattern via pruning mechanisms. In most cases, this emerges as an activity-dependent process. In the olfactory system, sensory axons project to the olfactory bulb with high precision. Wiring of the olfactory bulb by sensory axons occupies a central position in olfactory processing. However, mostly due to technical impediments, there have been few studies on how individual olfactory sensory axons elaborate during development. Here we developed a novel technique of electroporation that allowed us to simultaneously label single olfactory sensory axonal arbors and their pre-synaptic specializations. Using this method we were able to incorporate plasmids into olfactory sensory neurons at an immature stage, thereby allowing a time-course study of axonal arbor development and synapse formation in the olfactory bulb. We observed that total number of branch points, total number of branch length and total number and density of pre-synaptic specializations peaked at post-injection day 7 and decreased afterwards. Our data demonstrates for the first time that olfactory sensory axons develop in an exuberant way, both in terms of branch growth and synaptic composition. Exuberant branches and synapses are eliminated to achieve the mature pattern in a process likely to be regulated by neural activity.

INTRODUCTION

The olfactory system is widely utilized as a model for studying neural plasticity and regeneration due to its unique characteristic that olfactory sensory neurons are generated continuously into adulthood. In the mouse, axonal innervation of the olfactory bulb begins between embryonic days 15-16 and continues throughout life (Blanchart et al 2006). Olfactory axons originating in the olfactory epithelium gather in bundles to cross the cribiform plate. After reaching the olfactory bulb, sensory axons enter the glomerular layer where, together with the dendritic tufts of projection neurons as well as with the neurites from the local periglomerular cells, they form structures of dense neuropil called glomeruli. The proper innervation of a glomerulus by olfactory sensory axons is considered central for functional odor processing.

The glomerulus is a complex and well-delineated neuropil that is the site of the first synapse in the olfactory pathway. Surrounding cell bodies of juxtaglomerular cells define the limits of a glomerulus. Within each glomerulus, olfactory sensory neurons elaborate complex axonal processes. Dense networks of sensory axons make excitatory synapses onto the dendritic processes of projection neurons, namely mitral and tufted cells, as well as local circuit interneurons, termed periglomerular cells. Reciprocal dendro-dendritic synapses between the dendritic processes modulate intra-glomerular processing of odor. Axo-dendritic and dendro-dendritic synapses appear to be segregated to different compartments within the glomerulus probably as the result of a strategy to minimize non-specific effects due to the diffusion of glutamate (Kasowski et al 1999).

During the development of the nervous system there is an exuberant production of axons and collaterals that regress during late pre-natal or early post-natal life until reaching the definite pattern of connectivity in adult animals (Shatz 1996). Elimination of immature connections has been demonstrated in several systems. In the visual system, individual retinal ganglion cell axons projecting to the dorsal lateral geniculate nucleus develop exuberant side branches that are selectively pruned back to the adult pattern (Sretavan & Shatz 1986). In the auditory system, significant refinement of the topographic specificity of the primary afferent axons from the spiral ganglion innervating the cochlear nucleus occurs (Leake et al 2002). In the neocortex, developmental degeneration of large portions of thalamocortical axonal arbors over the first 3 weeks of post-natal development has been reported in mice (Portera-Cailliau et al 2005). Similarly, *Drosophila* mushroom body neurons undergo specific pruning of axons during metamorphosis, so that neurons used in the larval nervous system can be reused in the adult (Watts et al 2003).

Evidence for developmental pruning in the olfactory system has been elusive. Efforts to understand how olfactory sensory axons develop have been hindered due to the limitations of the existing techniques to label receptor neurons and their developing axons at an immature stage. Published work on this topic was performed using Golgi staining of axonal arbors in olfactory bulb slices (Klenoff & Greer 1998), anterograde labeling of sensory axons with HRP or DiI (Tenne-Brown & Key 1999) and genetic labeling of sensory axons with tauLacZ (Cao et al 2007). In all three studies, authors concluded that sensory neuron axons innervate specific glomeruli without any evidence of exuberance or un-specific targeting. However, the methods used in these three studies labeled

populations of olfactory sensory neurons that were heterogeneous in terms of their age. As a result, at any given age, old and newly born OSNs will be labeled, rendering these methods not suitable to perform a time course analysis.

By using a novel technique, we revisited the question of how olfactory sensory axons elaborate during development. We developed a post-natal electroporation method that incorporates plasmids into immature olfactory sensory neurons. This technique allowed us to label individual olfactory sensory neuron axons and synapses and to follow their development throughout olfactory sensory neuron lineage. Our results suggest for the first time that olfactory sensory axons innervate specific glomeruli in an exuberant fashion. Following an initial phase of exuberant growth olfactory sensory neuron axons undergo a remodeling process by retracting branches and synaptic contacts.

MATERIALS AND METHODS

Animals

SVE129 wild-type animals were obtained from Taconic, Farms, Inc. (Germantown, NY). Homozygous Olfactory Marker Protein (OMP) – Green Fluorescent Protein (GFP) (Potter et al 2001) mice were obtained from Dr. Peter Mombaerts (Max Planck Institute, Germany). OMP-GFP mice were obtained by replacing the OMP gene sequence with the GFP sequence. All animals were housed at Columbia University in accordance with institutional requirements for animal care.

Postnatal electroporation of mouse olfactory epithelium

The procedure was performed on postnatal day 1 pups when there was noticeable milk in their bellies. Pups were anesthetized by hypothermia. Plasmid injection was done with a fine glass capillary that had been pulled and polished with a 30 degrees angle to have a 20-50 μm sharp tip opening. The anesthetized pups were placed under a dissecting microscope and a micromanipulator was used to guide the sharpened micropipette into the nasal cavity (Figure 1). 1-2 μl of plasmid at a concentration of 3-4 μg/μl was injected using a picospritzer generating a pressure of 4-8 PSI. In order to visualize the site of injection Fast Green dye (Sigma) was added to the plasmid mixture at a final concentration of 0.01%. Immediately after injection the 7 mm paddletrodes (BTX) were placed on the dorsal and ventral sides of the head, with the positive paddle placed dorsally and the negative paddle placed ventrally, (see Figure 1). 5 pulses of 150V with 50 msec duration and one second interval between pulses were given using an ECM830

Electro Square Pulser (BTX). Animals were let to recover in a warm water circulation blanket. Once fully recovered they were placed back in the cage with the dam. Pup recovery was virtually 100%. Electroporated animals were allowed to recover and were sacrificed at time points ranging from 2 to 30 days post procedure. Each animal contained variable numbers of labeled olfactory sensory neurons localized to zones 1-2-3 of the olfactory epithelium.

Plasmids

The sequences encoding for Red Fluorescent Protein (RFP) and the C-terminus fusion protein Synaptophysin-GFP (SypGFP, kind gift from Dr. Eduard Ruthazer, McGill University, Canada (Ruthazer et al 2006)) were placed under the chicken β-actin promoter (pCAG-RFP and pCAG-SypGFP). Plasmids were purified with endotoxin free Maxi or Mega kits (Qiagen, Germany) to a final concentration of 3-4 μg/μl.

Immunohistochemistry

Mice were transcardially perfused with 4% PFA in PBS. Olfactory epithelial tissue and olfactory bulbs were dissected out and postfixed for 2 hours, followed by overnight immersion in 30% sucrose-PBS, all at 4°C. Immunohistochemistry was performed on 16 μm cryosections on slides (Superfrost, Fischer, Fair Lawn, NJ). For antigen retrieval, slides were warmed to 55°C for 10 minutes followed by steaming in 0.01 M sodium citrate pH 6.0 for 10 minutes. The slides were cooled then rinsed in PBSTx (0.1% Triton

X in PBS). The sections were blocked in 10% Normal Donkey Serum (NDS) in PBSTx for 2 hours and then incubated in primary antibody mixtures in 2.5% normal donkey serum in PBSTx overnight at 4°C. Sections were washed in PBSTx (4x10 minutes) and then incubated in secondary antibody in 2.5% NDS-PBSTx at room temperature for 2 hours. The secondary antibodies were AlexaFluor-conjugated 488 or 594-donkey anti-rabbit or anti-goat diluted 1:750 in blocking buffer (Molecular Probes, Eugene, OR). Slides were washed 2x10 minutes in PBSTx and 2x10 minutes in PBS before counterstaining with TOTO-3 diluted 1:10,000 in PBS (Molecular probes, Eugene, OR). Mounting of the sections was performed using Vectashield (Vector, Burlingame, CA).

TOTO-3 counterstaining for olfactory bulb sections was performed as follows. Mice were transcardially perfused with 4% PFA in phosphate-buffered saline (PBS). Olfactory bulbs were dissected out and postfixed for 2 hours. Based on the average mouse glomerular size (Richard et al 2010), olfactory bulbs were sectioned 60 μm thick with a Leica CM1850 cryostat (Wetzlar, Germany). Immunohistochemistry was performed on 60 μm cryosections on slides (Superfrost, Fischer, Fair Lawn, NJ). Tissue was incubated for 10 minutes with TOTO-3 (Molecular probes, Eugene, OR) diluted 1:10,000 in PBS. Mounting of the sections was performed using Vectashield (Vector, Burlingame, CA).

Primary antibodies

Goat anti-OMP (Wako, Dallas, TX, #544-10001) was used in immunohistochemistry at 1:2,000. This polyclonal serum was obtained from a goat through multiple immunizations with rodent olfactory marker protein (OMP). It recognizes a protein of 19 kDa by

Western blot analysis, and its specificity in immunohistochemistry has been verified by pre-adsorption of the antiserum with high-performance liquid chromatrography (HPLC)-purified OMP, which abolishes all immunoreactivity (Baker et al 1989).

Rabbit anti-GFP (Molecular probes, Eugene, OR, #A11122) was used at 1:2,000. This IgG fraction was obtained from a rabbit upon immunization with full-length GFP isolated directly from *Aequorea victoria* and purification by ion-exchange chromatography to remove non-specific immunoglobulins.

Microscopy

Tissue sections were imaged on an Olympus confocal microscope (Olympus FluoView 600). Thin optical sections (1 μm) through the entire extent of the axonal arbors were collected at 100x magnification. GFP and RFP confocal images were obtained simultaneously, below saturation levels, with minimal gain and contrast enhancement.

Evaluation of axon arbors

TOTO-3 positive juxtaglomerular cells delineated the glomerular limits. We sampled axons from the entire bulb without any spatial bias. 90% of the axonal arbors were co-labeled with both mRFP and Syp-GFP; only co-labeled neurons were included in the study. Axonal arbors were evaluated as described previously (Klenoff & Greer 1998). Quantitative analysis was made with only those axonal arbors branching within the limits of a glomerulus and confined to a single section. Axonal arbors were reconstructed and

analyzed by using Neurolucida and Neuroexplorer softwares respectively (MBF Bioscience, Williston, VT). Reconstructions of axonal arbors were performed blind to condition and by applying the same criteria throughout samples. The axonal arbors were evaluated on the basis of number of branch points per neuron, number of synaptic clusters per neuron, total branch length (in micrometers), average branch length (in micrometers), density of SypGFP positive puncta, total volume (in micrometers^3) and average distance between SypGFP positive puncta (in micrometers). The total branch length and the total volume were measured as the summed length or volume of all branches from the first branch point to the glomerulus onward. The average branch length was calculated by dividing the total branch length by the total number of branches per neuron. To characterize the distribution of SypGFP puncta to particular axonal regions, yellow regions of complete red and green overlap were identified and counted. SypGFP labeled puncta of ~ 5 pixel intensity and ~ 1 μm in size (size of smallest puncta observed) were considered single synaptic clusters. Number of synaptic clusters was calculated counting synaptic clusters from the first branch point to the glomerulus onward.

Statistics

Variables were statistically analyzed using a one-way ANOVA and post-hoc paired comparisons (Fisher PLSD test). The dependent variables evaluated across the different age groups were as follows: number of branch points per neuron, number of synaptic clusters per neuron, total branch length, average branch length, density of synaptic clusters, total volume and average distance between synaptic clusters.

RESULTS

Post-natal electroporation of olfactory sensory neurons

To analyze the post-natal development of olfactory sensory neuron (OSN) axons we first developed a method that would reliably and robustly label sensory neuron axonal arborizations. We adapted a postnatal electroporation technique previously used in our lab to label progenitors in the subventricular zone (Chesler et al 2008). Here, we injected a high concentration plasmid encoding for a fluorescent protein into the nasal cavity of post-natal day 1 mice (Figure III.1A). Pups were electroporated and returned to their dam for recovery.

Two days after electroporation, GFP-positive olfactory sensory neurons were detected in the olfactory epithelium. The vast majority of olfactory sensory neurons (95%, data collected from four different animals) were GFP-positive but olfactory marker protein (OMP)-negative. Also, the majority of labeled olfactory neurons were located in the deep layers of the olfactory epithelium close to the progenitor cell layer (Figure III.1B). Taken together, both observations indicate that our post-natal electroporation protocol incorporates the plasmid into immature olfactory sensory neurons. Eight days after the procedure was performed, electroporated OSNs that migrated into the mature layer where Olfactory Marker Protein (OMP) is normally expressed were observed (Figure III.1C), suggesting that the electroporation procedure did not interrupt the OSN maturation program. We also observed plasmid incorporation by sustentacular cells (sustentacular cells were defined by their characteristic morphology and the superficial localization of their nucleus, Supplementary Figure III.1).

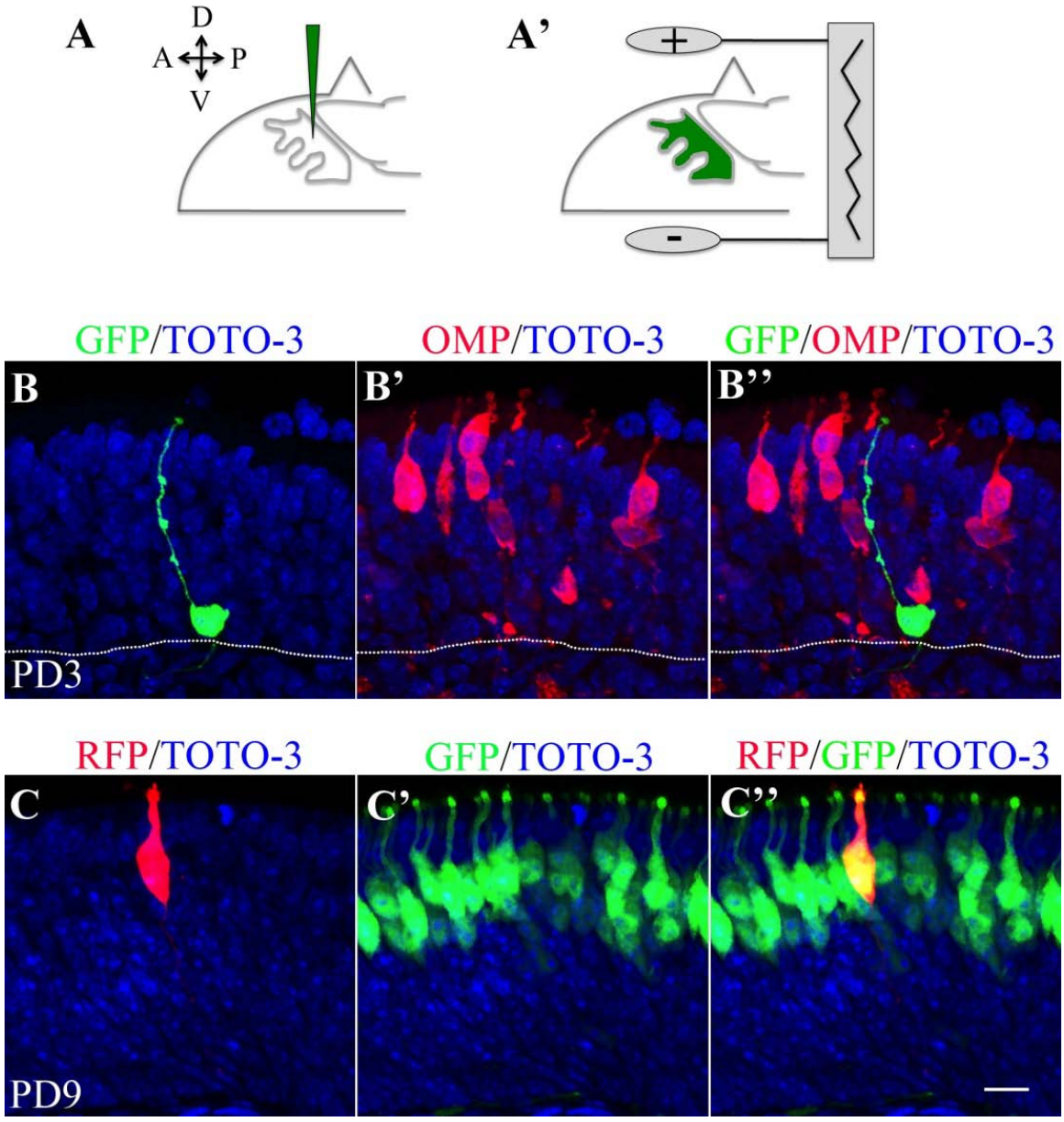

Figure III.1: *Post-natal electroporation of mouse olfactory epithelium.*

A) A high concentration plasmid preparation was injected into the nasal cavity of early post-natal mice. A') Paddletrodes were placed along the dorso-ventral axis of the pup's head; the positive electrode was placed dorsally and the negative electrode ventrally.

B, B', B'') Coronal sections of mouse Olfactory Epithelium (OE) electroporated with a plasmid encoding for GFP at post-natal Day 1 (PD1) and harvested at PD3. B) Olfactory sensory neuron labeled with GFP by electroporation. B') OMP immunoreactivity. B'') Two days after electroporation the majority of GFP-positive Olfactory Sensory Neurons

(OSNs) were not OMP positive (anti-GFP in green, anti-OMP in red and nuclear marker TOTO-3 in blue). At his age electroporated OSNs were located basally. Arrow indicates an extending axon. Dotted line delineates the lamina propia.

C. C', C'') Coronal sections of OMP-GFP mouse olfactory epithelium electroporated with RFP and harvested at PD9. In OMP-GFP mice the genetic sequence encoding for OMP has been replaced with the sequence encoding for GFP; therefore in OMP-GFP mice, the endogenous OMP promoter drives the expression of GFP. C) Representative olfactory sensory neuron labeled with RFP by electroporation. C') Mature OSNs labeled with GFP. C'') Elecroporated olfactory sensory neuron is GFP positive and has migrated to a more apical layer into the OE where mature OSNs are located.

Scale bar for B, B', B'', C, C' and C'' 20 µm.

Since sustentacular cells are non-neuronal and therefore do not project axons to the olfactory bulb, labeled sustentacular cells did not interfere with our study.

Labeling of olfactory sensory neuron axonal arbors and SypGFP positive puncta in vivo

Golgi-like effective labeling of individual olfactory sensory neuron axons and their axonal arborizations was accomplished by electroporating a plasmid encoding for RFP into the nasal cavity of post-natal day 1 mice (Figure III.2). Labeling was sparse, which allowed a detailed analysis of morphological features and patterns of arborization of individual axons.

Some fundamental characteristics of olfactory sensory neuron axonal arborizations emerged in a first analysis. Across all ages analyzed, an individual axon innervated a single glomerulus, with no evidence of inter-glomerular axon collaterals (For examples of representative axons see Figure III.2). We never observed axons growing beyond the glomerular layer. Also, axonal branching in the nerve layer was rare. Axonal branching typically occurred only after axons have entered into the glomerular neuropil. Some axons made abrupt turns upon innervating a glomerulus but most axons presented a fairly straight and non-tortuous trajectory before beginning to arborize. Axonal branching patterns tended to be morphologically heterogeneous. Moreover, as reported previously for rat and hedgehog (Halasz & Greer 1993; Lopez-Mascaraque et al 1990) the distribution of olfactory neuron fibers within the glomeruli was not homogeneous.

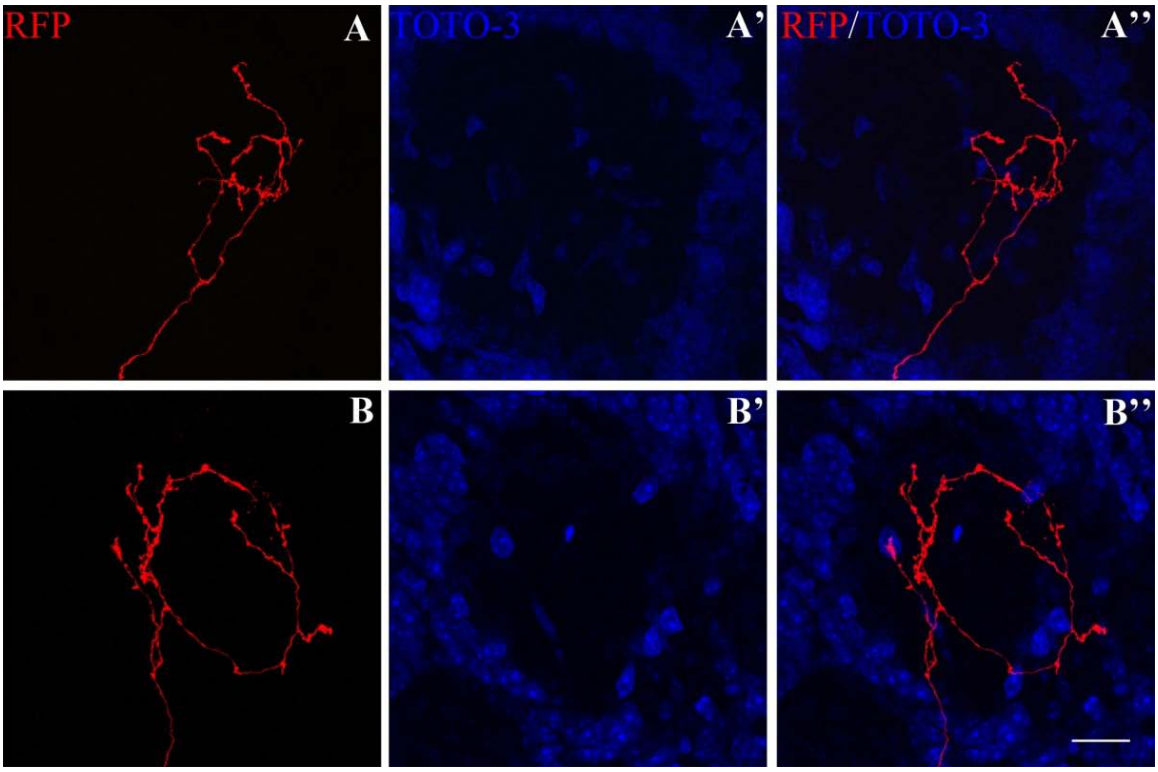

Figure II.2: *Labeling of olfactory sensory neuron axonal arbors*

Coronal sections of mouse olfactory bulbs harboring representative olfactory sensory neuron axonal arbors labeled with RFP by electroporation. Mice were electroporated at PD1 with an RFP-expressing plasmid and tissue was harvested at PD15. Patterns of axonal morphology are very diverse. Axonal arborizations innervate an area restricted to the periphery of the gomerulus (A, A', A'') or borders of the glomerulus (B, B', B'').

Scale bar: 10 µm.

Within the glomerulus, axons generally arborized in a localized compartment either restricted to the core or to the periphery of the glomerulus (Figure III.2A) or delineating the limits of the glomerulus (Figure III.2B). Only in rare instances the axonal arbor occupied the total volume of a glomerulus (Data not shown). As previously reported, the specific segregation of olfactory axonal arborizations suggested a sub-compartmentalization of the terminal fields within the glomerulus (Kasowski et al 1999).

In order to simultaneously visualize axon arbor morphology and synaptic localization, we co-electroporated two plasmids into the nasal cavity of post-natal day 1 mice (Figure III.3). One plasmid encoded for Red Fluorescent Protein (RFP) to label the entire axonal arbor and the other encoded for the fusion protein Synaptophysin-GFP (SypGFP) to localize pre-synaptic specializations.

We have chosen SypGFP to visualize synaptic sites based on several characteristics of the synaptophysin protein. First, synaptophysin is a major synaptic membrane protein and currently the most widely used marker for nerve terminals. Second, SypGFP consistently produced a clear punctuate pattern of labeling in axon terminals with little or no labeling in non-synaptic structures, such as axon fascicles (Figure III.3). Moreover, the exact same SypGFP construct has been used in a previous study by Ruthazer et al., 2006 conducted in tadpole and shown by electron microscopy to localize to pre-synaptic sites (Ruthazer et al 2006). We observed that the discrete and punctuate pattern of SypGFP in olfactory sensory neuron axonal arbors was mainly co-localized with varicosities that are normally

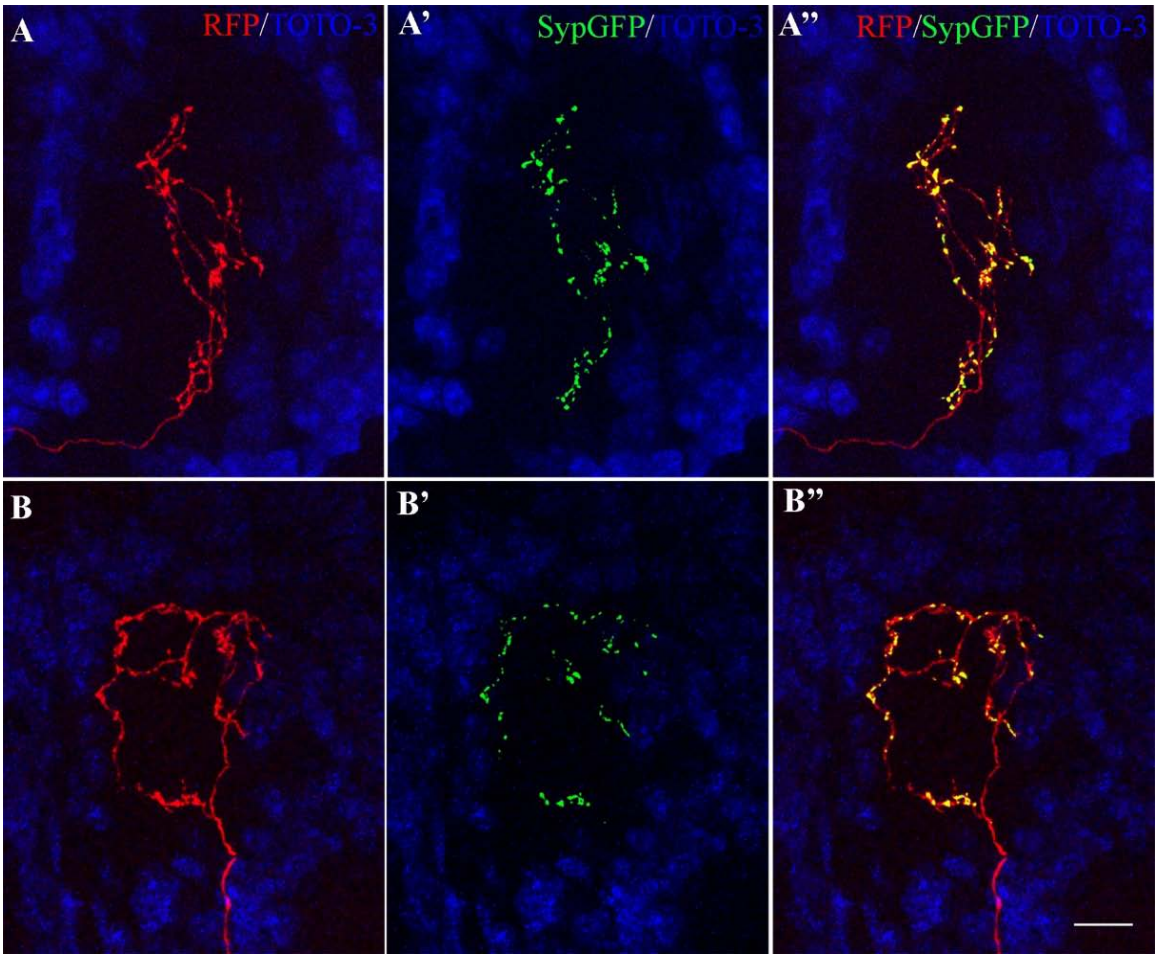

Figure III.3: *Labeling of olfactory sensory neuron axonal arbors and pre-synaptic specializations*

Coronal sections of olfactory bulbs with representative olfactory sensory neuron axonal arbors labeled with RFP and their pre-synaptic specializations labeled with the fusion protein Synaptophysin-GFP. Mice were electroporated at PD1 and tissue was harvested at PD10 (A) or PD20 (B). Note that the accumulation of SypGFP occurs within the limits of the glomerulus and only after the first branch point. There is no accumulation of Syp-GFP in the incoming axon before it has entered the glomerulus. RFP in red and TOTO-3 in blue.

Scale bar: 10 µm

observed at regular intervals in the axon arbor. The punctuate distribution of GFP-tagged synaptophysin suggested accumulation of synaptic vesicles at pre-synaptic nerve terminals and therefore, we used SypGFP to localize pre-synaptic specializations in mice *in vivo*.

Accumulation of SypGFP occurred typically within the glomerular boundary and after the first branch point (Figure III.3). SypGFP clusters mainly localized to thin portions of the arbor, branch tips and branch points. However, not all branch points contained SypGFP clusters. These characteristics of sensory neuron axons did not change across development. Importantly, the expression of exogenous synaptophysin did not alter axonal terminal morphology. As seen in Figure III.4, number of branch points, total arbor length and volume do not differ significantly in SypGFP-negative versus SypGFP-positive axons.

Time course of olfactory sensory neuron axonal elaboration

Since our post-natal electroporation method labeled olfactory sensory neurons at an immature stage, it allowed us to follow the emergence of axonal arbors and the formation of synapses of these sensory neurons throughout development. Olfactory sensory neurons and pre-synaptic specializations were labeled by electroporation at post-natal day 1 and mice were sacrificed for analysis at PD5, 7, 8, 10, 15, 20 and 30 (For representative axons of PD5, 7, 8, 15 and 20 see Figure III.5). At post-natal day 5 olfactory sensory neurons that were leaving the nerve layer of the olfactory bulb and penetrating into the glomerular layer were detected (Figure III.5A).

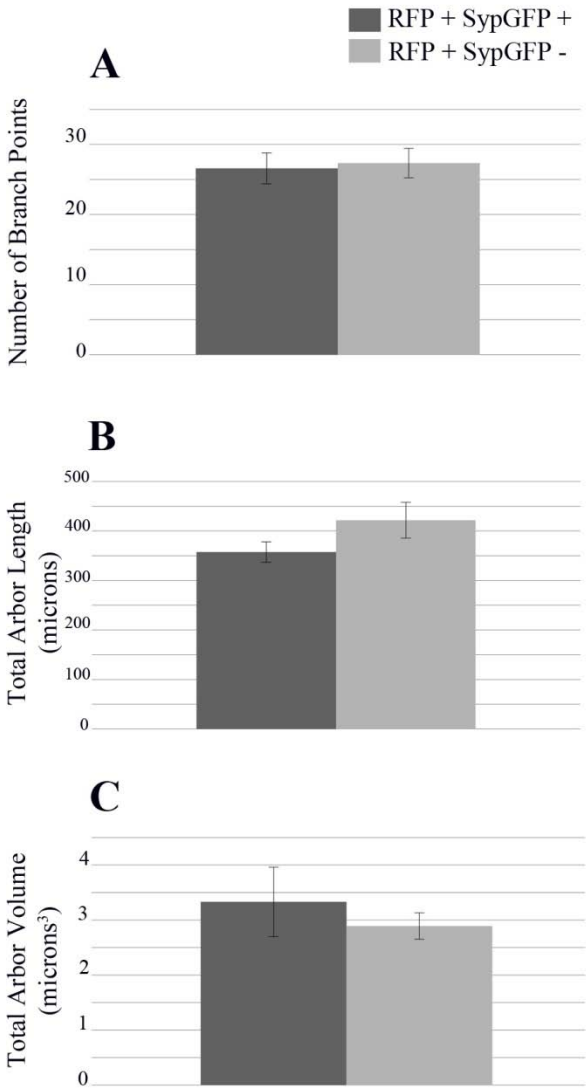

Figure III.4: *Ectopic expression of Synaptophysin-GFP did not affect axonal morphology.*

Olfactory sensory neuron axonal arbors labeled with RFP and SypGFP or with RFP alone were traced. Mice were electroporated at PD1 and olfactory bulbs were harvested at PD15. Terminal arborizations were compared in terms of number of branch points (A), total arbor length (B) and total arbor volume (C). No significant differences between double and single labeled arbors were identified. RFP+SypGFP+ N = 14 axons; RFP+SypGFP- N = 9 axons. RFP in red, SypGFP in green and TOTO-3 in blue.

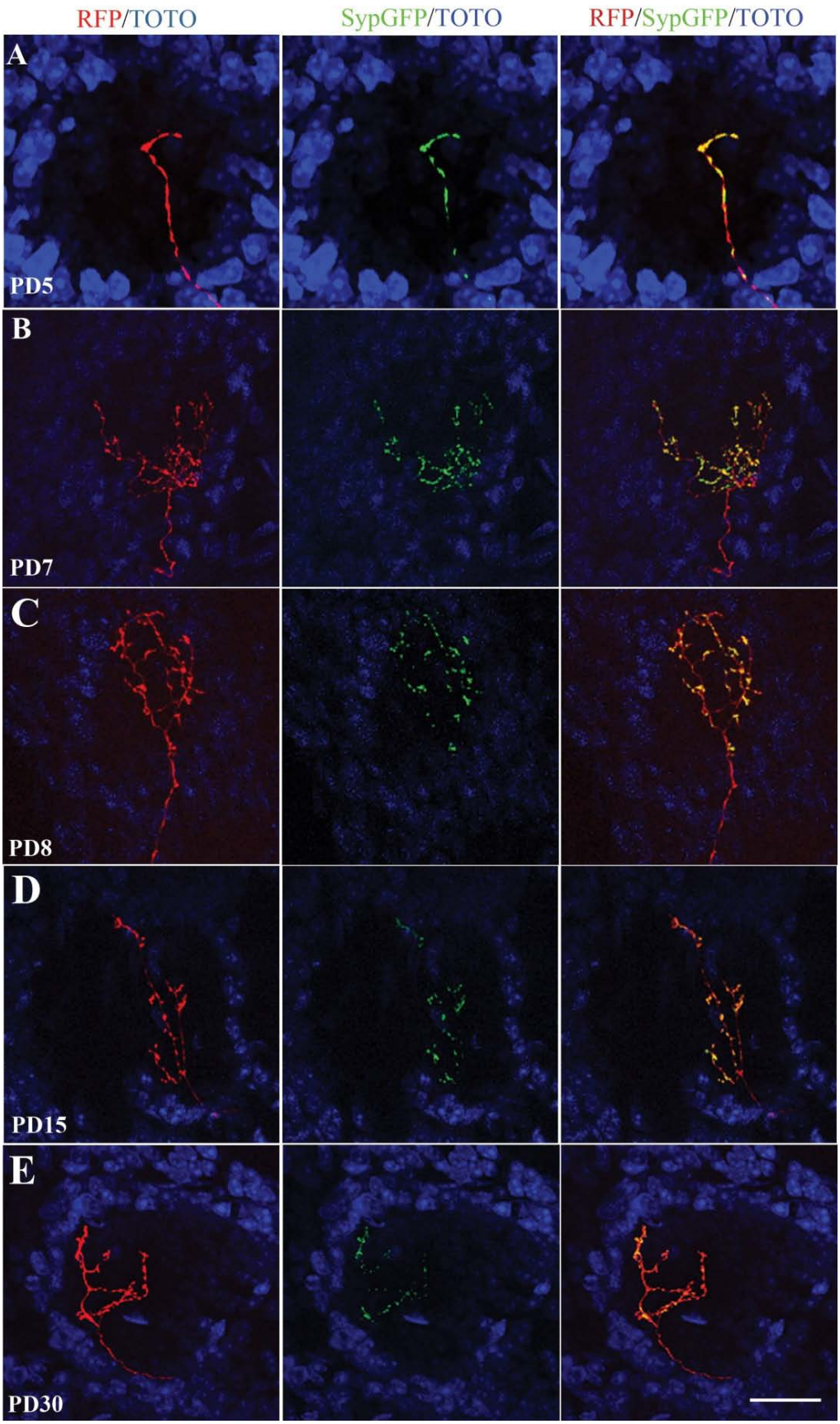
RFP/TOTO
SypGFP/TOTO
RFP/SypGFP/TOTO
A
PD5
B
PD7
C
PD8
D
PD15
E
PD30

Figure III.5: *Time course of olfactory sensory neuron axon development*.

Representative examples of olfactory neuron axonal arbors labeled with RFP and Synaptophysin-GFP at post-natal day 1 and sacrificed at post-natal days 5 (A), 7 (B), 8 (C), 15 (D) and 20 (E). Throughout the different ages axons innervates single glomerulus. Also, once axonal branching is established, it occurs only within the limits of the glomeruli. Accumulation of Syp-GFP is observed as early as olfactory neuron axons penetrate into the glomerular layer of the olfactory bulb. RFP in red, SypGFP in green and TOTO-3 in blue.

Scale bar: 20 μm.

A punctuate patter of SypGFP within the glomerular boundaries was already visible at this stage. Occasionally, four days after electroporation branching axon terminals were observed (Data not shown). At post-natal day 7, axons penetrated fully into the glomeruli and started to arborize by elaborating complex processes (Figure III.5B). As previously observed, axonal arborizations presented diverse and complexes morphologies throughout the different ages post-electroporation analyzed (Figure III.5C, D and E).

Olfactory sensory neuron axonal arbors co-labeled with RFP and SypGFP were reconstructed with Neurolucida and analyzed with Neuroexplorer software. In order to study axonal morphology, the axonal arbors were evaluated on the basis of number of branch points (as a way to evaluate axonal complexity), average branch length, total arbor length and volume (Figure III.6). By performing one-way ANOVA, statistically significant age-dependent changes were observed in all variables analyzed (average number of branch points: $p = 0.0008$, average branch length: $p = 0.0002$, total arbor length: $p = 0.0224$ and total arbor volume: $p = 0.0039$).

Consistent with previous results (Cao et al 2007; Klenoff & Greer 1998), olfactory sensory neuron axon complexity increased during the early post-natal period. In the present study, the average number of branch points increased up to approximately post-natal day 8 and decreased at subsequent ages resulting in a relatively simple arborization pattern by post-natal day 30 (Figure III.6A). Post-hoc paired comparisons further confirmed the peak of axonal complexity at PD8 (Supplementary Table III.1). As an alternative way to evaluate axonal complexity we scored the total number of branch tips

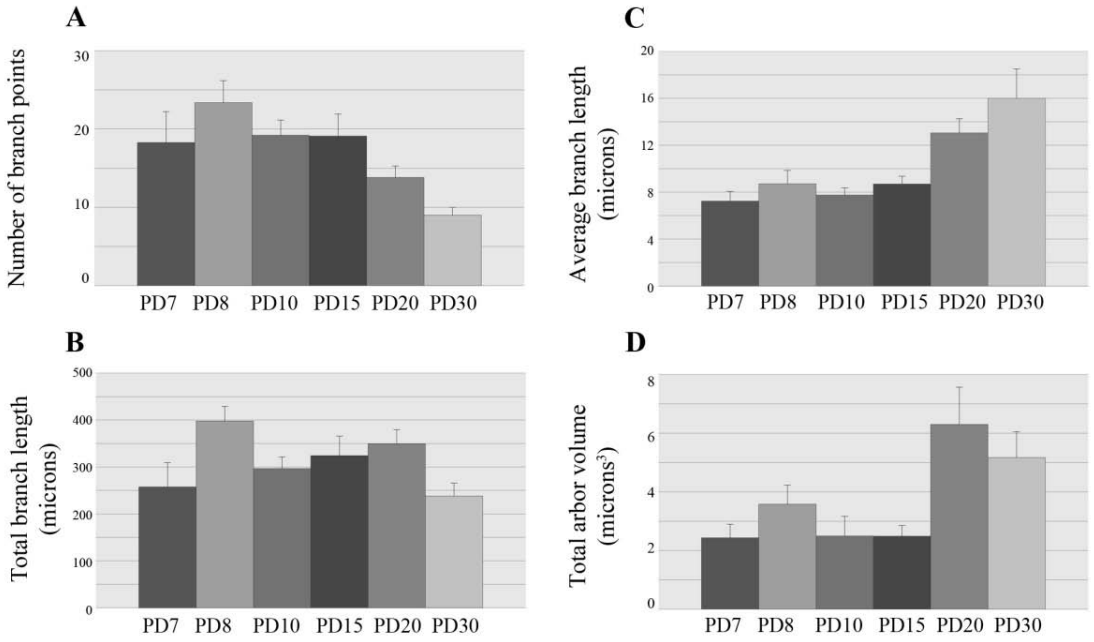

Figure III.6: *Time course analysis of axonal growth*

Olfactory sensory neurons were electroporated at PD1 with RFP and SypGFP and olfactory bulbs were collected at PD7, 8, 10, 15, 20 and 30. Double labeled axonal arbors were evaluated in terms of number of branch points (A), total branch length (B), average branch length (C) and total arbor volume (D). By performing one-way ANOVA, statistically significant age-dependent changes were observed in all variables analyzed (average number of branch points: $p = 0.0008$, average branch length: $p = 0.0002$, total arbor length: $p = 0.0224$ and total arbor volume: $p = 0.0039$). PD7 N = 7 axons; PD8 N = 8 axons; PD10 N = 10 axons; PD15 N = 10 axons; PD20 N = 11 axons, PD30 N = 11 axons.

and observed a similar pattern (data now shown). Total arbor length, as measured by the summed length of all branches after the first branch point, also increased until post-natal day 8 and decreased at later times (Figure III.6B). Post-hoc paired comparisons further confirmed the peak of total arbor length at PD8 (Supplementary Table III.2). Contrarily to previously published results, our data shows for the first time that olfactory sensory neuron axons grow in an exuberant fashion and that branches are pruned out to reach a mature pattern.

Average branch length showed a sharp increase at post-natal day 20 (Figure III.6C), indicating that as some branches were pruned away the remaining branches increased in length (See also post-hoc paired comparisons in Supplementary Table III.3). Taken together these results suggest that as olfactory sensory neuron axons develop the branching pattern becomes less elaborated and with longer branches.

The total volume occupied by the axonal arbor showed also a sharp increase at post-natal day 20. This increase in volume is consistent with a developmental increase in glomerular size (Figure III.6D and see also post-hoc paired comparisons in Supplementary Table III.4).

Time course of synapse formation

In order to study the pre-synaptic composition of olfactory axonal arbors, olfactory sensory neurons were labeled with both RFP and SypGFP by electroporation at post-natal day 1. Olfactory bulbs were collected at PD7, 8, 10, 15, 20 and 30 and SypGFP-positive puncta were identified as regions of complete RFP and GFP overlap.

SypGFP labeled puncta of at least ~ 5 pixel intensity and ~ 1 μm in size (size of smallest puncta observed) were scored. The data gathered was evaluated on the basis of average number (Figure III.7A) and density (Figure III.7B) of pre-synaptic specializations and average distance between SypGFP-positive puncta (Figure III.7C). We detected a statistically significant variation across development in the three variables analyzed (average number of SypGFP-positive puncta: $p \leq 0.0001$, density of SypGFP -positive puncta: $p = 0.0003$ and average distance between SypGFP-positive puncta: $p = 0.0061$).

We observed that the average number of SypGFP-positive puncta per neuron peaked sharply 8 days post-natally (Figure III.7A and Supplementary Table III.5). To normalize for changes in total branch length, we calculated the density of SypGFP-positive puncta as the number of SypGFP-positive puncta divided by the total branch length for each labeled neuronal arbor. We observed a decline in the density of SypGFP clusters 10 days post-natally, providing further evidence for exuberant synapse formation throughout post-natal development (Figure III.7B and Supplementary Table III.6).

In order to evaluate the distribution of the pre-synaptic clusters, we analyzed the average distance of SypGFP-positive puncta over time. We observed that the average distance between pre-synaptic clusters increased with age, suggesting that as the axonal arbor develops the spacing between pre-synaptic specializations on individual axons increases (Figure III.7C and Supplementary Table III.7).

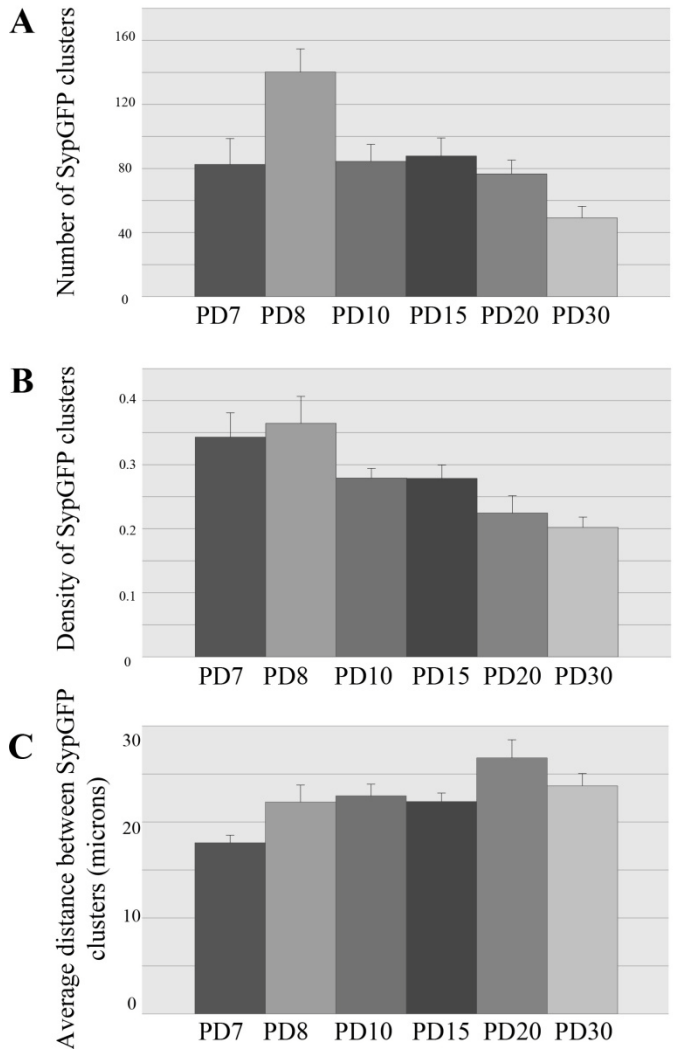

Figure III.7: *Time course analysis of synapse formation*

Olfactory sensory neurons were electroporated at PD1 with RFP and SypGFP and olfactory bulbs were collected at PD7, 8, 10, 15, 20 and 30. Double-labeled axonal arbors were evaluated in terms of number of SypGFP clusters (A), density of SypGFP clusters (B) and average distance between SypGFP clusters (C). By performing one-way ANOVA, statistically significant age-dependent changes were observed in all variables analyzed (average number of pre-synaptic specializations: $p \leq 0.0001$, density of pre-synaptic specializations: $p = 0.0003$ and average distance between SypGFP-positive puncta: $p = 0.0061$). PD7 N = 7 axons; PD8 N = 8 axons; PD10 N = 10 axons; PD15 N = 10 axons; PD20 N = 11 axons, PD30 N = 11 axons

DISCUSSION

In this study, we developed a method to label individual olfactory sensory neuron axonal arbors and their pre-synaptic specializations *in vivo*. This technique was used to establish the time course of axonal elaboration and synapse formation by sacrificing mice at specific ages post-electroporation. Our results show for the first time that olfactory sensory neuron axonal arbors develop with exuberant growth and synapse formation that peak at post-natal day 8. Pruning of the initial exuberant arborizations and pre-synaptic sites is observed at subsequent ages until reaching an adult pattern that plateaus after 20 days post-natal.

Previous studies on rat and mouse single olfactory sensory neuron axons reported that neurons innervate glomeruli without evidence of exuberant growth or pre-synaptic specialization (Cao et al 2007; Klenoff & Greer 1998) (Tenne-Brown & Key 1999). These studies were performed based on reconstructions from olfactory sensory neuronal arbors labeled with Golgi (Klenoff & Greer 1998), Dil and HRP injections in the olfactory bulb nerve layer (Tenne-Brown & Key 1999) or genetically encoded tauLacZ (Cao et al 2007) at different post-natal ages. Since axonal innervation of the olfactory bulb begins at around embryonic days 15-16 in the mouse and rat and continues throughout the post-natal period, in all three studies, mature and immature axons were present, and therefore analyzed, at any given age. Therefore, the lack of an age effect in the morphometric parameters analyzed in these previous studies is likely a reflection of the heterogeneous age composition of axons. In contrast, our post-natal electroporation method labels selectively immature olfactory sensory neurons before they have reached and branched into glomeruli thereby unmasking an age effect and allowing a temporal

analysis of axonal arbor development.

Many studies in both vertebrates and invertebrates suggest that axon growth cones can select correct pathways and targets by responding to a variety of specific molecular cues provided by the cell surfaces, the extracellular matrix or diffusion from distant sources. Once axons invade their targets, the initial connections they make with individual target neurons are frequently inaccurate and the process of error correction almost always requires neural activity. A well described example of this phenomenon takes place in the visual system where activity dependent mechanisms determine the elimination of synaptic contacts and side branches to achieve the segregation of retinal ganglion cell axons into the layered pattern observed in the adult (reviewed in (Shatz 1996)). In the olfactory system, by utilizing a strategy that abolished neurotransmitter release in a subset of olfactory sensory neurons, Cao et al provided evidence for a specific effect of BDNF signaling on axonal arbor pruning under competition in vivo (Cao et al 2007). Therefore, it is plausible to propose that similar mechanisms come into play for the pruning of early axonal exuberance to achieve the mature pattern described here.

Many of the morphometric parameters evaluated in the present study peaked at post-natal day 8 (total number of branches, total branch length, number and density of pre-synaptic clusters) and decreased afterwards. This suggests the intriguing possibility of a critical period for the formation and maintenance of specific synaptic contacts between sensory axons and projection and juxta-glomerular neurons. Coincidently, double-labeled cells for the deoxy-uridine analog BrdU and OMP appeared at 7 days after injecting into mice (Kondo et al 2010; Miragall & Monti Graziadei 1982), suggesting that the exuberant axonal arbors that we observed 7 days post-electroporation may well correspond to the

onset of OMP expression in sensory neurons. Also, the onset of expression of VGLUT2 occurs concomitantly with the onset of expression of OMP, suggesting that is not until olfactory sensory neurons fully mature that vesicular release of glutamate occurs (Marcucci et al 2009). Therefore, we speculate that the growth peak of olfactory sensory arbors coincides with the time when they start to release glutamate. Once vesicular release of glutamate is established, only functioning synaptic connections with post-synaptic targets will be maintained. Weak or inactive synaptic contacts will be eliminated together with their branches. Branches harboring functional synaptic connections will continue to grow. We propose that exuberant growth emerged as a strategy to sample a larger glomerular space to increase the probabilities of encountering post-synaptic partners and establishing functional synaptic connections.

In summary, our results suggest that olfactory sensory neuron axons innervate specific glomeruli with evidence of exuberant growth where the adult pattern of connections is sculpted from an immature pattern. We further speculate that activity-driven competition between branches from a single axonal arbor may play an essential role in wiring the olfactory system. The requirement for neuronal activity in producing the adult pattern of connectivity is a genetically conservative way to achieve a high degree of precision in the wiring.

SUPPLEMENTARY INFORMATION

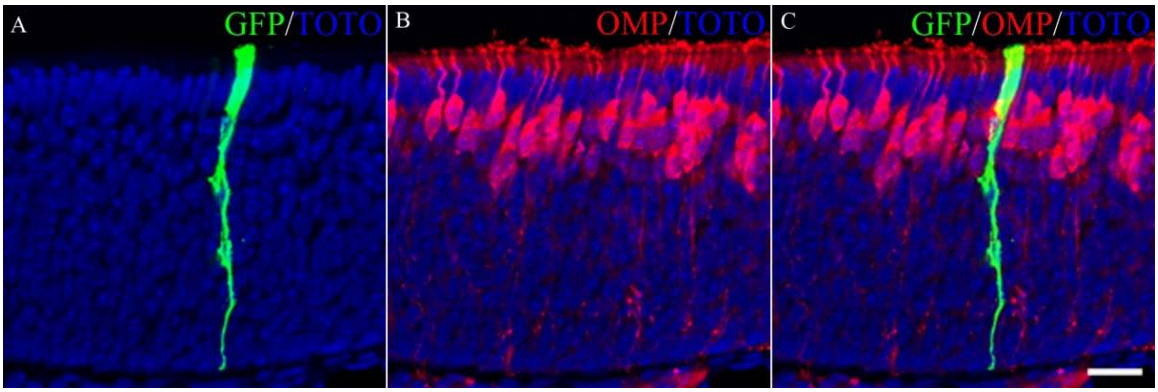

Supplementary Figure III.1: *Post-natal electroporation of sustentacular cells*

(A, B, C) Mouse olfactory cavity was electroporated at Post-natal Day 1 (PD1) with a plasmid encoding for GFP, olfactory epithelium was harvested at PD9 and prepared for immunohistochemistry. GFP-positive sustentacular cells were detected. Anti-GFP in green, anti-OMP in red and TOTO-3 in blue.

Scale bar = 10 µm.

A

	Count	Mean	Std. Dev.
PD7	7	18.286	10.420
PD8	8	23.375	7.891
PD10	10	19.200	6.161
PD15	10	19.100	8.888
PD20	11	13.818	4.895
PD30	11	9.000	3.317

B

	P-value	
PD7, PD8	0.1654	
PD7, PD10	0.7917	
PD7, PD15	0.8140	
PD7, PD20	0.1919	
PD7, PD30	0.0082	S
PD8, PD10	0.2135	
PD8, PD15	0.2029	
PD8, PD20	0.0049	S
PD8, PD30	<0.0001	S
PD10, PD15	0.9746	
PD10, PD20	0.0839	
PD10, PD30	0.0016	S
PD15, PD20	0.0896	
PD15, PD30	0.0017	S
PD20, PD30	0.1120	

Supplementary Table III.1: *Number of branch points*

A) Means table for number of branch points.

B) Fisher's PLSD for number of branch points, effect: age, significance level: 5%.

A

	Count	Mean	Std. Dev.
PD7	7	257.543	136.569
PD8	8	397.725	89.169
PD10	10	296.520	78.414
PD15	10	324.190	131.392
PD20	11	349.418	98.780
PD30	11	238.145	90.945

B

	P-value	
PD7, PD8	0.0125	S
PD7, PD10	0.4533	
PD7, PD15	0.2021	
PD7, PD20	0.0753	
PD7, PD30	0.7030	
PD8, PD10	0.0467	S
PD8, PD15	0.1447	
PD8, PD20	0.3252	
PD8, PD30	0.0019	S
PD10, PD15	0.5570	
PD10, PD20	0.2527	
PD10, PD30	0.2075	
PD15, PD20	0.5835	
PD15, PD30	0.0656	
PD20, PD30	0.0159	S

Supplementary Table III.2: *Total branch length*

A) Means table for total branch length.

B) Fisher's PLSD for total branch length, effect: age, significance level: 5%.

A

	Count	Mean	Std. Dev.
PD7	7	7.239	2.177
PD8	8	8.913	3.231
PD10	10	7.755	1.975
PD15	10	8.695	2.096
PD20	11	13.056	3.968
PD30	11	16.006	8.247

B

	P-value	
PD7, PD8	0.5259	
PD7, PD10	0.8154	
PD7, PD15	0.5107	
PD7, PD20	0.0094	S
PD7, PD30	0.0002	S
PD8, PD10	0.6524	
PD8, PD15	0.9931	
PD8, PD20	0.0411	S
PD8, PD30	0.0009	S
PD10, PD15	0.6394	
PD10, PD20	0.0089	S
PD10, PD30	<0.0001	S
PD15, PD20	0.0296	S
PD15, PD30	0.0004	S
PD20, PD30	0.1269	

Supplementary Table III.3: *Average branch length*

A) Means table for average branch length.

B) Fisher's PLSD for average branch length, effect: age, significance level: 5%.

A

	Count	Mean	Std. Dev.
PD7	7	7.239	2.177
PD8	8	8.913	3.231
PD10	10	7.755	1.975
PD15	10	8.695	2.096
PD20	11	13.056	3.968
PD30	11	16.006	8.247

B

	P-value	
PD7, PD8	0.5259	
PD7, PD10	0.8154	
PD7, PD15	0.5107	
PD7, PD20	0.0094	S
PD7, PD30	0.0002	S
PD8, PD10	0.6524	
PD8, PD15	0.9931	
PD8, PD20	0.0411	S
PD8, PD30	0.0009	S
PD10, PD15	0.6394	
PD10, PD20	0.0089	S
PD10, PD30	<0.0001	S
PD15, PD20	0.0296	S
PD15, PD30	0.0004	S
PD20, PD30	0.1269	

Supplementary Table III.4: *Total arbor volume*

A) Means table for total arbor volume.

B) Fisher's PLSD for total arbor volume, effect: age, significance level: 5%.

A

	Count	Mean	Std. Dev.
PD7	7	82.571	42.766
PD8	8	140.250	40.784
PD10	10	84.500	33.444
PD15	10	87.800	35.636
PD20	11	76.636	28.433
PD30	11	49.182	23.978

B

	P-value	
PD7, PD8	0.0017	S
PD7, PD10	0.9080	
PD7, PD15	0.7542	
PD7, PD20	0.7172	
PD7, PD30	0.0456	S
PD8, PD10	0.0010	S
PD8, PD15	0.0019	S
PD8, PD20	0.0002	S
PD8, PD30	<0.0001	S
PD10, PD15	0.8276	
PD10, PD20	0.5957	
PD10, PD30	0.0202	S
PD15, PD20	0.4519	
PD15, PD30	0.0115	S
PD20, PD30	0.0617	

Supplementary Table III.5: *Number of SypGFP clusters*

A) Means table for number of SypGFP clusters.

B) Fisher's PLSD for number of SypGFP clusters, effect: age, significance level: 5%.

A

	Count	Mean	Std. Dev.
PD7	7	0.343	0.101
PD8	8	0.365	0.118
PD10	10	0.279	0.047
PD15	10	0.279	0.066
PD20	11	0.225	0.088
PD30	11	0.202	0.052

B

	P-value	
PD7, PD8	0.6053	
PD7, PD10	0.1096	
PD7, PD15	0.1065	
PD7, PD20	0.0034	S
PD7, PD30	0.0006	S
PD8, PD10	0.0282	S
PD8, PD15	0.0272	S
PD8, PD20	0.0004	S
PD8, PD30	<0.0001	S
PD10, PD15	0.9870	
PD10, PD20	0.1228	
PD10, PD30	0.0315	S
PD15, PD20	0.1267	
PD15, PD30	0.0327	S
PD20, PD30	0.5131	

Supplementary Table III.6: *Density of SypGFP clusters*

A) Means table for density of SypGFP clsuters.

B) Fisher's PLSD for density of SypGFP clusters, effect: age, significance level: 5%.

A

	Count	Mean	Std. Dev.
PD7	7	17.829	2.104
PD8	8	22.075	4.996
PD10	10	22.720	3.871
PD15	10	22.130	2.792
PD20	11	26.673	6.279
PD30	11	23.764	4.240

B

	P-value	
PD7, PD8	0.0670	
PD7, PD10	0.0279	S
PD7, PD15	0.0519	
PD7, PD20	0.0001	S
PD7, PD30	0.0072	S
PD8, PD10	0.7577	
PD8, PD15	0.9790	
PD8, PD20	0.0283	S
PD8, PD30	0.4110	
PD10, PD15	0.7647	
PD10, PD20	0.0442	S
PD10, PD30	0.5883	
PD15, PD20	0.0215	S
PD15, PD30	0.3978	
PD20, PD30	0.1259	

Supplementary Table III.7: *Average distance between SypGFP clusters*

A) Means table for average distance between SypGFP clusters.

B) Fisher's PLSD for average distance between SypGFP clusters, effect: age, significance level: 5%.

CHAPTER IV

AXONAL MORPHOLOGY AND SYNAPTIC COMPOSITION OF OLFACTORY SENSORY NEURONS IN THE ABSENCE OF ODOR ACTIVITY

ABSTRACT

Throughout the nervous system, neural activity is critical for establishing a precise pattern of connectivity. For example in the visual system, blocking cell activity or synaptic transmission severely alters the morphology of retinal ganglion cells. To study how sensory activity modulates axonal morphology and synaptic composition in olfactory sensory neurons OSNs), we combined our previously described post-natal electroporation method (See Chapter 3) with two different anosmic mouse models, Cyclic Nucleotide Gated Channel (CNG) and Adenylyl Cyclase 3 (AC3) knock-out (KO) mice. We observed that the morphology of OSN axonal arborizations and the number and distribution of pre-synaptic clusters are normal in CNG KO mice when compared to wild type littermates. This suggests that odor-induced depolarization is not required for axonal arbor development and synapse formation. In contrast, AC3 KO mice show dramatic reductions in axonal terminal complexity and number of pre-synaptic clusters. We therefore propose that in olfactory sensory neurons odor-induced cAMP signaling events rather than odor-induced depolarization mediate axonal arbor development and synapse formation.

INTRODUCTION

Binding of odorant molecules to odorant receptors located in the cilia of olfactory sensory neurons initiates a transduction cascade that involves a G protein and the activation of Adenylyl Cyclase 3 (AC3). AC3 produces the second messenger cyclic adenosine monophosphate (cAMP). When cAMP binds to a Cyclic Nucleotide Gated (CNG) ion channel its opening time is increased leading to an influx of Na^+ and Ca^{2+}, which in turn depolarizes the cell membrane. Influx of Ca^{2+} through the CNG channel can also activate Ca^{2+}-dependent Cl^- channels. Since olfactory sensory neurons, unlike many other types of neurons, maintain a high level of intracellular Cl^-, opening of these channels produces an efflux of Cl^-, further depolarizing the cell membrane and generating action potentials. These electrical signals propagate down the axons to the synapses in the glomeruli of the olfactory bulb where the signals are relayed to mitral and tufted cells that project to higher olfactory centers (Figure IV.1).

The influence of input activity on olfactory bulb innervation by sensory neuron processes has been extensively investigated by surgical and genetic manipulations. Using naris occlusion to block environmental odorant stimulation post-natally, major changes were observed in the olfactory bulb, including delayed glomerular maturation and increased survival of OSNs in the closed side (Zou et al 2004). Expression of the Kir2.1 inward rectifying potassium channel in order to inhibit both odor-evoked and spontaneous action potentials in all mature olfactory sensory neurons delays the innervation of the olfactory bulb and perturbs axonal targeting (Yu et al 2004).

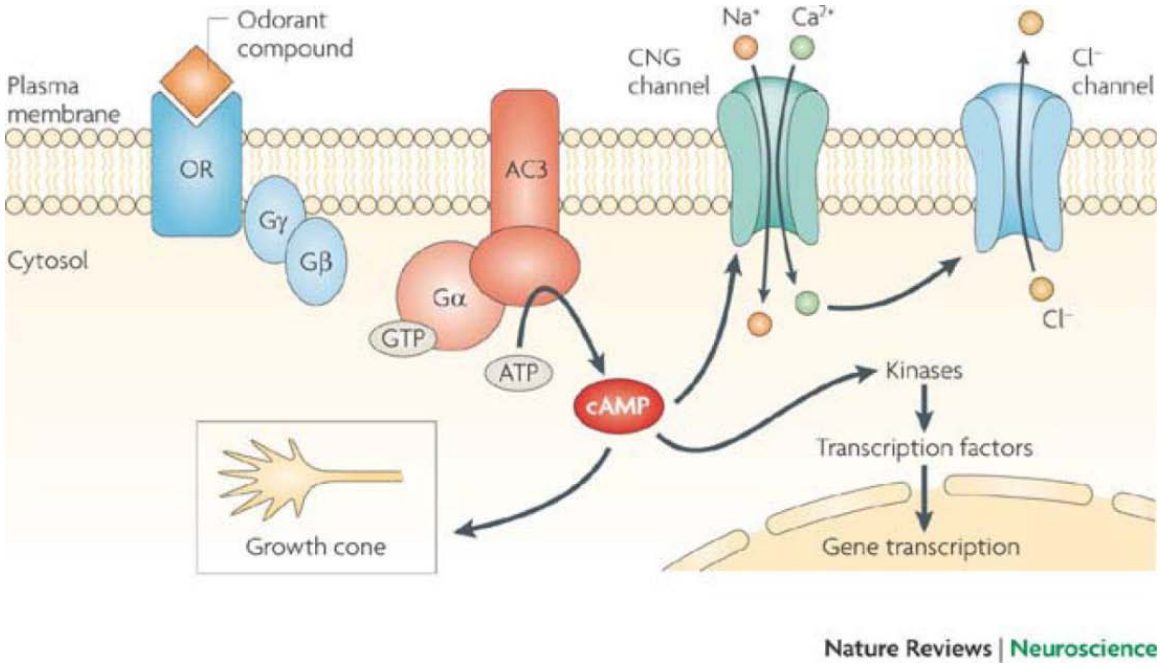

Figure IV.1: *The odorant transduction pathway*.

Binding of odorant compounds to an olfactory receptor (OR) initiates a transduction cascade that involves a G protein and the activation of adenylate cyclase 3 (AC3). AC3 produces the second messenger cyclic AMP, which in turn binds to a cyclic nucleotide-gated (CNG) channel and results in the influx of Na^+ and Ca^{2+}. The influx of cations depolarizes the cell membrane and Ca^{2+} activates a Ca^{2+}-dependent Cl^- channel resulting in a further depolarization of the cell membrane. Notably, the elevated levels of cAMP in the soma have a crucial role in regulating the phosphorylation of proteins and the transcription of genes important for growth and survival of the axons of OSNs (adapted from (Zou et al 2009)).

In Chapter 2 we presented the results from an extensive study addressing the morphology and synaptic composition of olfactory sensory neuron axons in wild type conditions. Our work has established for the first time that axons and synapses from olfactory sensory neurons develop in an exuberant way that, via pruning, is sculpted into the adult pattern. We now seek to investigate whether neuronal activity modifies axonal structure and synaptic composition. To this end, we used our previously described post-natal electroporation method with two genetically modified mouse models where olfactory sensory neurons lack odor evoked activity, Cyclic Nucleotide Gated Channel (CNG) alpha 2 and Adenylyl Cyclase 3 (AC3) knock-out mice.

Reed lab genetared CNG knock-out mice by replacing the alpha subunit of the CNG channel with tau-GFP (Zhao & Reed 2001). As a result, odorant-evoked activity was almost completely eliminated in the olfactory epithelium as tested by electro-olfactograms, and therefore CNG knock-out mice are anosmic. In the case of the AC3 knock-out mice, Storm lab disrupted the promoter and the first 310 amino acids of the protein with a neomycin cassette (Wong et al 2000). Evoked field potentials for cAMP and IP3 dependent odorants are disrupted in AC3 knock-out mice and, as previously established by our lab and others, they show defects in olfactory sensory projections convergence (Zou et al 2007). The combined use of both anosmic mouse models allowed us to dissect the electrical component (mediated by CNG-induced membrane depolarization) from the biochemical component (mediated by AC3 production of cAMP) of the odor-evoked response.

Our results showed that olfactory sensory neuron axons from CNG knock-out and wild type mice were undistinguishable in terms of both morphology and synaptic composition. In contrast, axonal projections from AC3 knock-out mice showed severe morphological defects and reduced numbers of pre-synaptic specializations. These results suggest that odor-evoked electrical activity does not play a major role in the elaboration of sensory neuron terminal fields and synaptic composition. In contrast, cAMP related signaling events might be more important for the growth and elaboration of axonal terminals and synapse formation.

MATERIALS AND METHODS

Animals

SVE129 wild-type animals were obtained from Taconic, Farms, Inc. (Germantown, NY). AC3 heterozygous (AC3 +/-) were provided by Dr. Daniel Storm of the University of Washington (Seattle, USA) (Wong et al 2000). Male CNG -/0 and females heterozygous +/- were provided by Dr. Haiqing Zhao of the Johns Hopkins University (Baltimore, USA) (Zhao & Reed 2001). All animals were housed at Columbia University in accordance with institutional requirements for animal care.

Postnatal electroporation of mouse olfactory epithelium

The procedure was performed on postnatal day 1(PD1) CNG pups after there was noticeable milk in their bellies. For AC3 pups, the procedure was carried out on PD2 pups. Since AC3 -/- pups are at a disadvantage for milk competition, survival is impaired beyond PD2 unless litter size is reduced to about 5 pups within 24 h of birth. Pups were anesthetized by hypothermia. Plasmid injection was done with a fine glass capillary that had been pulled and polished with a 30 degrees angle to have a 20-50 μm sharp tip opening. The anesthetized pups were placed under a dissecting microscope and a micromanipulator was used to guide the sharpened micropipette into the nasal cavity (Figure 1). 1-2 μl of plasmid at a concentration of 3-4 μg/μl was injected using a

picospritzer generating 4-8 PSI. In order to visualize the site of injection Fast Green dye (Sigma) was used in the plasmid mixture at a final concentration of 0.01%. Immediately after injection the 7 mm paddletrodes (BTX) were placed on the dorsal and ventral sides of the head (positive paddle was placed dorsally and negative paddle was placed ventrally, see Figure 1) and 5 pulses of 150V with 50 msec duration and one second interval between pulses were given using an ECM830 Electro Square Pulser (BTX). Animals were gently warmed in a warm water circulation blanket. Once fully recovered they were placed back in the cage with the dam. Injected animals were allowed to recover and were sacrificed at 14 days post procedure. Each animal contained variable numbers of labeled olfactory sensory neurons localized to zones 1-2-3 of the olfactory epithelium.

Plasmids

The sequences encoding for Green Fluorescent Protein (GFP), Red Fluorescent Protein (RFP), the C-terminus fusion protein Synaptophysin- *Dicosoma sp*. reef coral (SypdsRED) and the C-terminus fusion protein Synaptophysin-GFP (SypGFP, kind gift from Dr. Edward Ruthazer, McGill University, Canada) (Ruthazer et al 2006) were placed under the chicken β-actin promoter (pCAG-GFP, pCAG-RFP, pCAG-SypdsRED and pCAG-SypGFP). Plasmids were purified with endotoxin free Maxi or Mega kits (Qiagen, Germany) to a final concentration of 3-4 μg/μl.

TOTO counterstaining

Mice were transcardially perfused with 4% PFA in PBS. Olfactory bulbs were dissected out and postfixed for 2 hours. Based on the average mouse glomerular size (Richard et al 2010), olfactory bulbs were sectioned 60 μm thick with a Leica CM1850 cryostat (Wetzlar, Germany). Immunohistochemistry was performed on 60 μm cryosections on slides (Superfrost, Fischer, Fair Lawn, NJ). Slides were warmed to 55°C for 10 minutes followed by 3 x 10 minutes washes in phosphate-buffered saline (PBS) and 1 x 10 minutes wash in PBSTx (0.1% Triton X in PBS). Tissue was incubated for 10 minutes with TOTO-3 diluted 1:10,000 in PBS (Molecular probes, Eugene, OR). Mounting of the sections was performed using Vectashield (Vector, Burlingame, CA).

Evaluation of axon arbors

Pairs of plasmids pCAG-SypdsRED and pCAG-GFP or pCAG-SypGFP and pCAG-RFP were injected into the nasal cavity. Only co-labeled neurons were included in the study. Axonal arbors were evaluated as described previously (Klenoff & Greer 1998). Only those axonal arbors branching within the limits of a glomerulus and confined to a single section were considered for this study. Glomerular limit was delineated by TOTO-positive juxtaglomerular cells. We sampled axons from the entire bulb without any

spatial bias. Axonal arbors were reconstructed and analyzed by using Neurolucida and Neuroexplorer softwares respectively (MBF Bioscience, Williston, VT). Reconstructions of axonal arbors were done applying the same criteria throughout samples. The axonal arbors were evaluated on the basis of number of branch points per neuron, total branch length (in micrometers), total volume (in micrometers^3), number of synaptic clusters per neuron, density of synaptic clusters and average distance between synaptic clusters (in micrometers). The total branch length and the total volume were measured as the summed length or volume of all branches from the first branch point to the glomerulus onward. To characterize the distribution of Syp-dsRED or SypGFP puncta to particular axonal regions, yellow regions of complete red and green overlap were identified and counted. Syp-dsRED or SypGFP labeled puncta of ~ 5 pixel intensity and ~ 1 μm in size (size of smallest puncta observed) were considered single synaptic clusters. Number of synaptic clusters was calculated counting synaptic clusters from the first branch point to the glomerulus onward.

Statistics

Variables were statistically analyzed using Student's t test. The dependent variables evaluated across the different groups were as follows: number of branch points per neuron, total branch length, total arbor volume, number of synaptic clusters per neuron, density of synaptic clusters and average distance between synaptic clusters.

RESULTS

Olfactory sensory neurons axonal arborizations and synaptic composition in Cyclic Nucleotide Gated Channel (CNG) knock-out mice

A combination of pCAG-GFP and pCAG-SypdsRED plasmids was injected into the nasal cavity of post-natal day one CNG wild type and knock out littermates. After electroporation, mice were returned to the dam for recovery and sacrificed at post-natal day 15. Olfactory bulbs were dissected out and prepared for immunohistochemistry. Axonal arborizations were visualized with GFP and pre-synaptic specializations by the accumulation of SypdsRED (Figure IV.2). Only double-labeled sensory neuron axonal arbors were considered in this study.

Axonal arbors were traced and analyzed with Neurolucida and Neuroexplorer softwares respectively. The morphology of axonal arborizations was evaluated in terms of the number of branch points, total arbor length, total arbor volume, total number of SypdsRED puncta, density of SypdsRED puncta and average distance between SypdsRED puncta. Upon quantification and statistic analysis, we observed that knock-out axons did not show any significant difference from wild type axons in terms of the morphometric parameters addressing axonal complexity and morphology (Figure IV.3, number of branch points $p = 1$; total arbor length $p = 0.9$; total arbor volume $p = 0.26$). Similarly, we observed that olfactory sensory neuron arbors from CNG KO mice did not show any differences in synaptic composition when compared to wild type axons (Figure IV.4, total number of SypdsRED puncta $p = 0.87$; density of SypdsRED puncta $p = 0.99$;

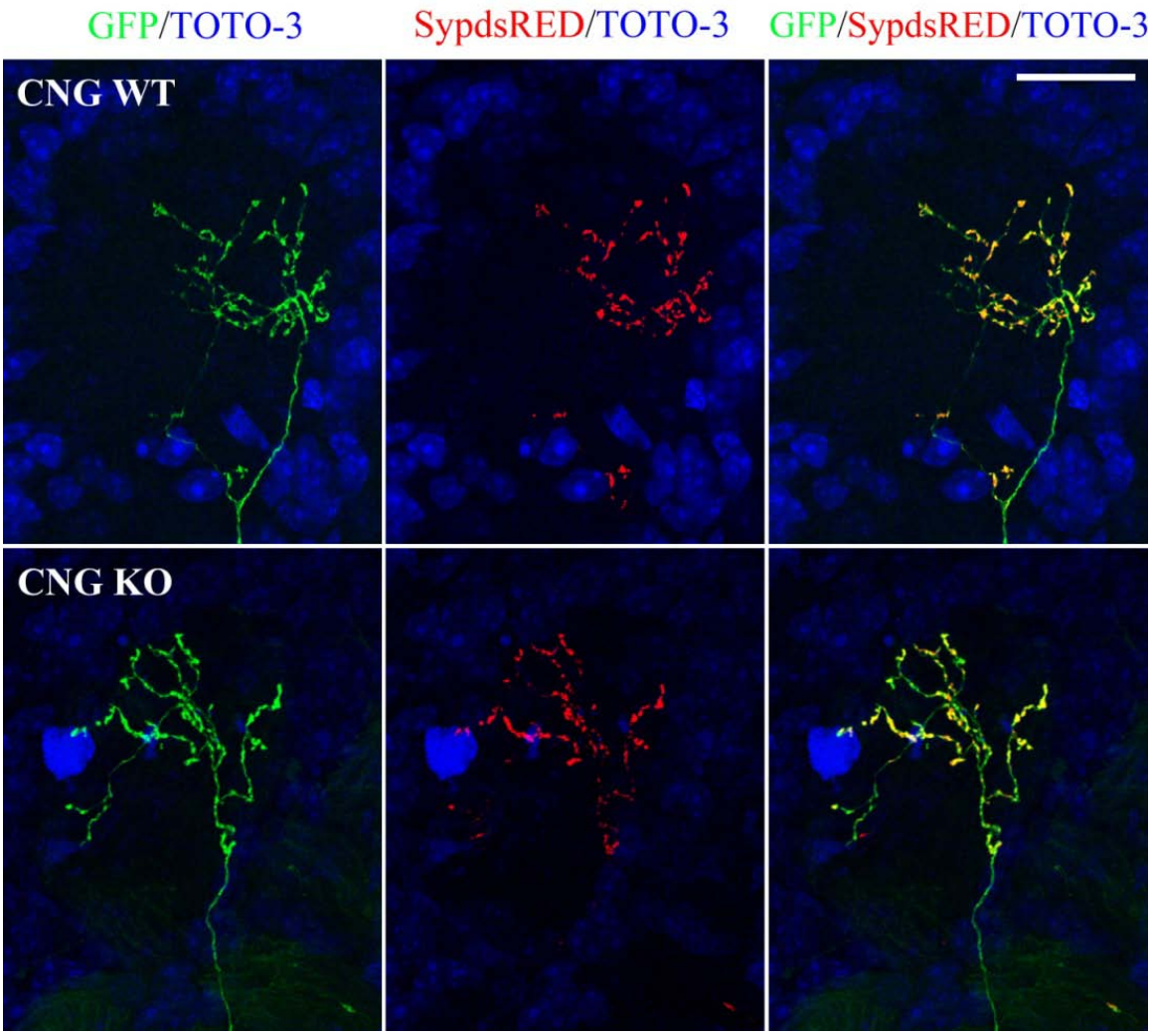

Figure IV.2: *Labeling of olfactory sensory neuron axonal arbors and pre-synaptic specializations in CNG mice*

Coronal sections of olfactory bulbs from CNG WT (top) and CNG KO (bottom) mice with representative olfactory sensory neuron axonal arbors labeled with GFP and their pre-synaptic specializations labeled with the fusion protein Synaptophysin-dsRED. Mice were electroporated at PD1 and tissue was harvested at PD15. Note that the accumulation of Syp-dsRED occurs within the limits of the glomerulus and only after the first branch point. There is no accumulation of Syp-dsRED in the incoming axon before it has entered the glomerulus. Scale bar: 20 µm.

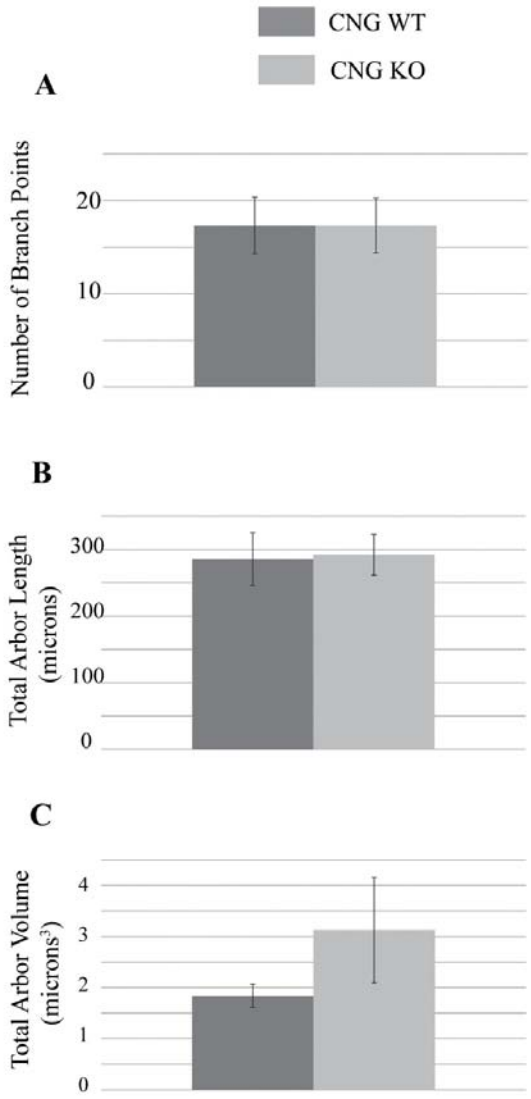

Figure IV.3: *Analysis of axonal morphology CNG WT vs KO mice*
Olfactory sensory neurons were electroporated with GFP and SypdsRED at PD1 and mice were sacrificed at PD15. Double labeled axonal arbors were evaluated on the basis of number of branch points (A), total branch length (B) and total arbor volume (C). No significant differences were found. Number of branch points $p = 1$; total arbor length $p = 0.9$; total arbor volume $p = 0.26$. $N = 9$ for CNG WT and KO.

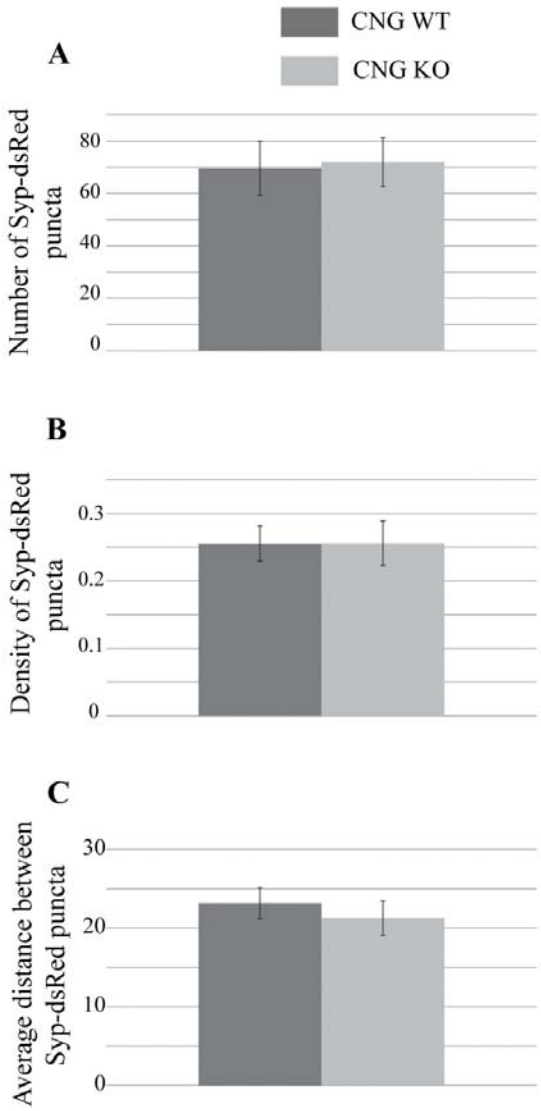

Figure IV.4: *Analysis of synaptic composition CNG WT vs KO mice*
Olfactory sensory neurons were electroporated with GFP and SypdsRED at PD1 and mice were sacrificed at PD15. Double-labeled axonal arbors were evaluated on the basis of number of Syp-dsRED puncta (A), density of Syp-dsRED puncta (B) and average distance between Syp-dsRED puncta (C). No significant differences were found. Total number of SypdsRED puncta $p = 0.87$; density of SypdsRED puncta $p = 0.99$; average distance between SypdsRED puncta $p = 0.53$. $N = 9$ for CNG WT and KO.

average distance between SypdsRED puncta p = 0.53). These results suggest that odor-induced membrane depolarization and the resulting action potentials are not critical for axonal arbor development and synapse formation.

Olfactory sensory neurons axonal arborizations and synaptic composition in Adenylyl Cyclase 3 (AC3) knock-out mice

A combination of pCAG-RFP and pCAG-SypGFP plasmids was injected into the nasal cavity of post-natal day two AC3 wild type and knock-out littermates. We should note that in this set of experiments, electroporations were performed at post-natal day two in order to increase the chances of survival of AC3 -/- pups. After electroporation, mice were returned to the dam for recovery and sacrificed at post-natal day 15. Olfactory bulbs were dissected out and prepared for immunohistochemistry. Axonal arborizations were visualized with RPF and pre-synaptic specializations by the accumulation of SypGFP (Figure IV.5). Only double labeled sensory neurons terminal fields were considered in this study.

Consistent with previous results from our lab (Zou et al 2007), in a first analysis we observed a dramatic disruption of the glomerular structure in AC3 KO mice. Also, consistent with previous observations that olfactory sensory neuron turnover is increased in AC3 KO mice (DongJing Zou, unpublished results), labeled axonal arbors in knock-out mice were fewer in number than in wild type littermates.

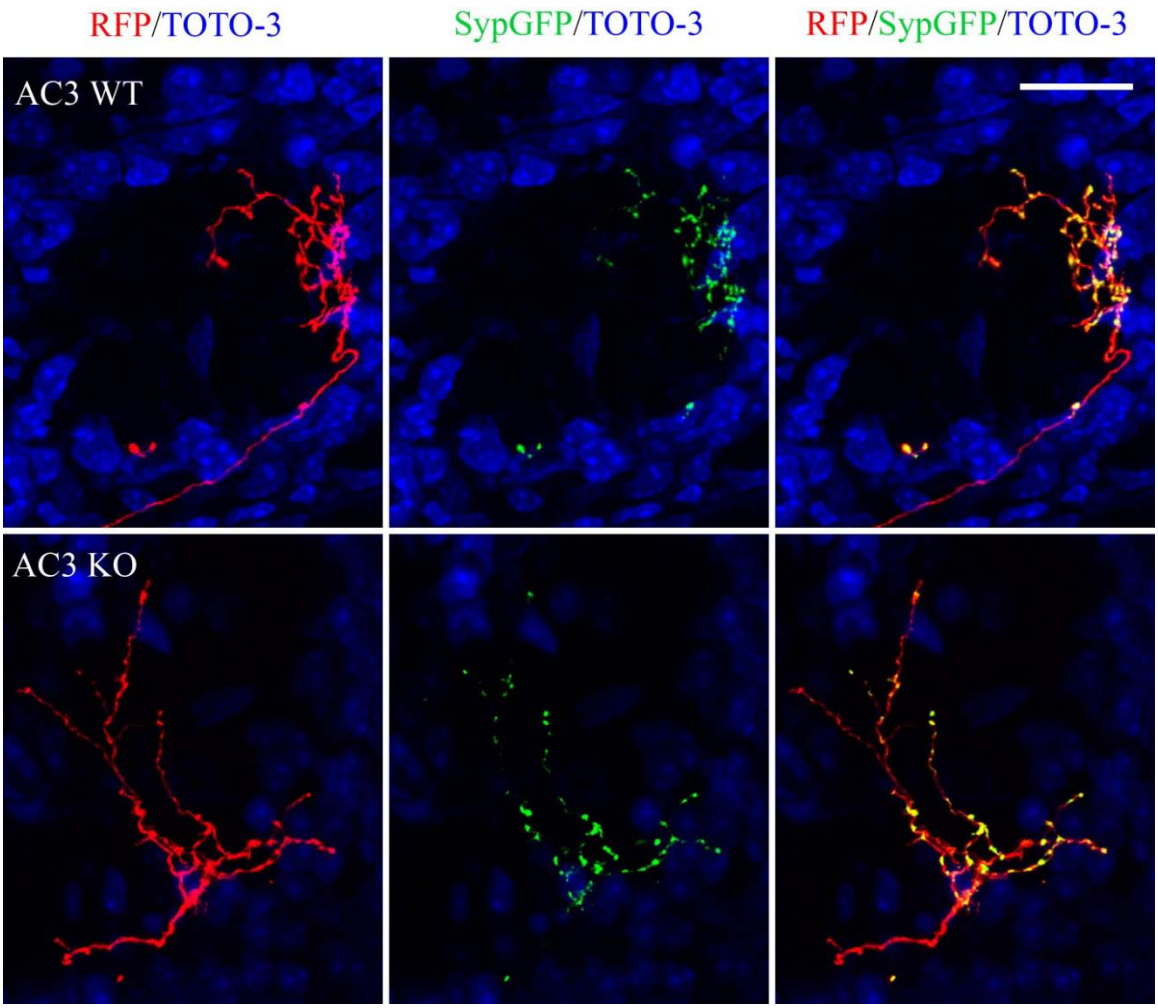

Figure IV.5: *Labeling of olfactory sensory neuron axonal arbors and pre-synaptic specializations in AC3 mice*

Coronal sections of olfactory bulbs from AC3 WT (top) and AC3 KO (bottom) mice with representative olfactory sensory neuron axonal arbors labeled with RFP and their pre-synaptic specializations labeled with the fusion protein Synaptophysin-GFP. Mice were electroporated at PD2 and tissue was harvested at PD15. Note that the accumulation of SypGFP occurs within the limits of the glomerulus and only after the first branch point. There is no accumulation of SypGFP in the incoming axon before it has entered the glomerulus. Scale bar: 20 µm.

Axonal arbors were traced and analyzed with Neurolucida and Neuroexplorer softwares respectively. The OSNs axonal arbors were evaluated in terms of their number of branch points, total arbor length, total arbor volume, total number of SypGFP puncta, density of SypGFP puncta and average distance between SypGFP puncta. We observed that axonal complexity, as evaluated by the number of branch points, was significantly reduced in mice that lack AC3 whereas total arbor length and volume were unchanged (Figure IV.6; number of branch points $p < 0.0001$, total arbor length $p = 0.998$ and total arbor volume $p = 0.218$). Regarding synaptic composition, both the number and density of SypGFP-positive puncta were dramatically reduced in AC3 KO mice (Figure IV.7, number of SypGFP puncta $p < 0.0001$, density of SypGFP puncta $p < 0.0001$). Also, the distribution of pre-synaptic specializations was altered in the absence of AC3 as observed by the increased value of nearest neighbor average distance (Figure IV.7, $p = 0.003$). Moreover, AC3 knock-out mice showed dramatic reductions in axonal terminal complexity and synaptic composition. We therefore propose that in OSNs, odor-induced cAMP signaling events are critical for axonal arbor development and synapse formation.

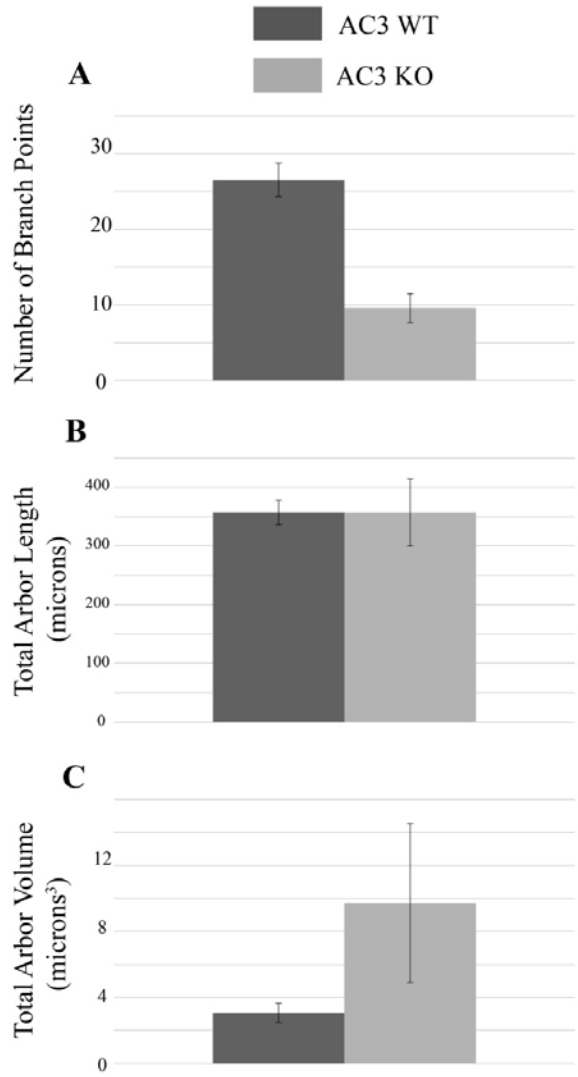

Figure IV.6: *Analysis of axonal morphology AC3 WT vs KO mice*
Olfactory sensory neurons were electroporated with RFP and SypGFP at PD2 and mice were sacrificed at PD15. Double labeled axonal arbors were evaluated on the basis of number of branch points (A), total branch length (B) and total arbor volume (C). Number of branch points $p < 0.0001$, total arbor length $p = 0.998$ and total arbor volume $p = 0.218$. N = 14 for AC3 WT and N = 7 for AC3 KO.

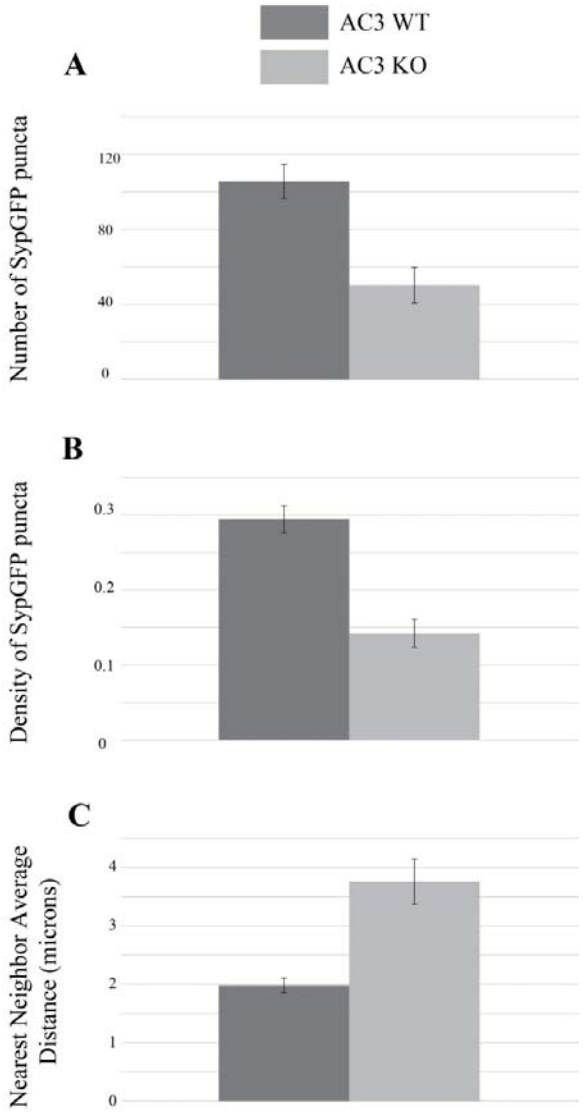

Figure IV.7: *Analysis of synaptic distribution AC3 WT vs KO mice*
Olfactory sensory neurons were electroporated with RFP and SypGFP at PD2 and mice were sacrificed at PD15. Double-labeled axonal arbors were evaluated on the basis of number of Syp-GFP positive puncta (A), density of Syp-GFP puncta (B) and average distance between Syp-GFP puncta (C). Number of SypGFP puncta $p < 0.0001$, density of SypGFP puncta $p < 0.0001$, nearest neighbor average distance $p = 0.003$. N =14 for AC3 WT and N = 7 for AC3 KO.

DISCUSSION

Several examples across the nervous system have implicated neural activity in the establishment of a precise pattern of connectivity. To examine whether lack of neural activity is modulating axonal morphology and synaptic composition of olfactory sensory neurons, in the present study we combined *in vivo* post-natal electroporation of the nasal cavity with two anosmic mouse models. We observed that CNG knock-out mice, which lack generation of action potentials upon odorant binding, did not present any defect in axonal morphology and synaptic composition when compared to wild type littermates. In contrast AC3 knock-out mice, which lack the enzyme responsible for an increase of intracellular cAMP after odorant binding, had severe defects in axonal morphology and synaptic composition. Taken these two results together, we propose that odor-evoked cAMP related signaling events, rather than odor-evoked membrane depolarization, are modulating the morphology and synaptic composition of olfactory sensory neuron axons.

Previous manipulations of the olfactory signal transduction cascade have already indicated the involvement of cAMP production in olfactory sensory neuron axonal growth and sorting. Ectopic expression of constitutively active G proteins is sufficient to induce the coalescence of axons (Chesler et al 2007). Genetic manipulation of cAMP-protein dependent kinase (PKA) and cAMP response element binding protein (CREB) shifted the axonal projection sites along the anterior-posterior axis in the olfactory bulb (Imai et al 2006). In AC3 knock-out animals, axons from neurons expressing specific olfactory receptors are found in numerous and atypical loci of convergence (Chesler et al 2007; Zou et al 2007) and the refinement process of glomerular innervation is disrupted at every age analyzed (Zou et al 2007). In contrast, glomeruli form normally in CNG and G_{olf} knock-out backgrounds (Belluscio et al 1998; Lin et al 2000; Zheng et

al 2000). Also, robust expression of AC3 is detected in axons during the critical period of glomerular formation in neonatal mice (Zou et al 2007). Together, these results suggest that proper development of OSN projections requires the activation of cAMP dependent signaling pathways. Such a model would explain why CNG KO mice, which retain cAMP production despite odor-evoked electrical silence, achieve largely normal axonal development and synapse formation, but AC3 KO mice do not.

What is then the role of cAMP in olfactory sensory neurons beyond activating CNG ion channels? Intracellular levels of cAMP at the growth cone might be affecting axon turning and guidance (Lohof et al 1992; Ming et al 1997; Song & Poo 1999). Also, cAMP is a potent regulator of gene expression and, thus, may regulate genes important for axonal growth, glomerular and synapse formations. Indeed, modulation of cAMP has been shown to alter the transcription profile of neuropilin-1 (Imai et al 2006), which is a molecule implicated in guidance of OSNs axons. Other gene targets for cAMP and the processes it influences in the regulation of olfactory projections to the bulb remain to be identified.

In summary, our results provide evidence that in the olfactory system, as in many other neural systems, activity is shaping the formation of the proper pattern of connectivity. In the olfactory system, the innervation of the olfactory bulb by sensory axons seems to be dependent on a mechanism involving cAMP. We also provide evidence that cAMP is not only important for axonal growth and branching but also for synapse formation.

CHAPTER V

DISCUSSION, FUTURE DIRECTIONS AND PERSPECTIVES

The mammalian olfactory epithelium (OE) possesses the rare capacity of continuous neurogenesis even into adulthood. As a result, newborn olfactory sensory neurons (OSNs) continuously project their axons into the olfactory bulb (OB) to establish synapses with mitral and tufted cells. The processes of OSN synaptic maturation and axonal growth are central to establish functional connections within the system. My doctoral work focused on different aspects of synapse formation and axonal development of olfactory sensory neurons (OSNs).

First, I conducted a study aimed to understand the regulation of expression of pre-synaptic molecules in the olfactory epithelium. By utilizing *in situ* hybridization, my findings show that, as they mature, mouse olfactory sensory neurons sequentially express specific pre-synaptic genes. Furthermore, the different patterns of expression of these pre-synaptic genes suggest the existence of discrete steps in pre-synaptic development: genes encoding proteins involved in scaffolding show an early onset of expression whereas expression of genes encoding proteins involved in the regulation of vesicle release starts later. In particular, Vesicle Glutamate Transporter 2, the signature molecule for glutamatergic neurons and necessary for neurotransmitter release, exhibits the latest onset of expression. In addition, contact with the targets in the olfactory bulb does not control pre-synaptic protein gene expression, suggesting that olfactory sensory neurons follow an intrinsic program of development.

Second, I performed a time course study where I followed the development of axonal arborizations and pre-synaptic specializations of olfactory sensory neurons *in vivo* at different post-natal ages. To this end, I adapted an electroporation technique that allowed me to visualize with great detail the complex processes of OSN axonal arborizations and their pre-synaptic specializations in the glomeruli of the olfactory bulb. My data demonstrates for the first time that olfactory sensory axons develop in an exuberant way, both in terms of branch growth and

synaptic composition. The elaboration of OSN axonal arbors and formation of synapses displayed a peak at post-natal day eight. Exuberant branches and synapses are eliminated to achieve the mature pattern of connectivity in a process likely to be regulated by neural activity.

Third and last, I investigated the consequences of abolishing neuronal activity in the axonal morphology and synaptic composition of olfactory sensory neurons by combining the post-natal electroporation method with two anosmic mouse models, cyclic nucleotide gated channel (CNG) and adenylyl cyclase 3 (AC3) knockout mice. I observed that the morphology of terminal arborizations as well as pre-synaptic cluster number and distribution are normal in CNG KO mice when compared to wild type littermates. This suggests that odor-induced depolarization is not critically involved in axonal arbor development and synapse formation. In contrast, AC3 KO mice show dramatic reductions in axonal growth and number of pre-synaptic composition. I therefore propose that in olfactory sensory neurons odor-induced cAMP signaling events are more important for axonal arbor development and synapse formation than odor-induced depolarization. I envision that cAMP is involved in axonal growth and changes in gene expression.

A. Regulation of pre-synaptic genes

Little is known about the regulation of genes encoding for components of the synaptic machinery. Here I presented evidence showing that different groups of genes encoding for pre-synaptic molecules with related function are expressed in a sequential manner as olfactory sensory neurons mature. Genes encoding for proteins that play a structural role at the active zone showed an early onset of expression, whereas genes encoding for proteins associated with

synaptic vesicles showed a later onset of expression. This result raises the intriguing idea that within each group, the expression of genes would occur in a concerted way, perhaps under the regulation of the same set of transcription factors. To test this hypothesis, in collaboration with XiaoHong Zhang, we used the computational tool AliBaba2 (http://gene-regulation.com/pub/programs.html) to attempt to identify known transcription factor binding motifs that would be present in all of the gene members from each group (the groups were as follows: omp and vglut2; gap43, synapsin 1, synaptophysin, synaptotagmin 1, VAMP2 and snap25). However, we were unable to identify transcription factors that would co-regulate pre-synaptic genes within each group (Data not shown). One difficulty that might have hindered our efforts is the limited knowledge we have about promoter regions of pre-synaptic genes and the limited number of known transcription factor binding motifs.

Since I presented evidence that the expression of pre-synaptic genes seemed to follow a specific order or hierarchy, I also hypothesize that the expression of late genes is dependent on the expression of early genes. To further explore this possibility, I propose to eliminate, or at least attenuate, the expression of an early gene by electroporating constructs harboring small hairpins RNAs (shRNAs) for early pre-synaptic markers and to determine whether later markers are still expressed in electroporated OSNs. If the expression of late pre-synaptic genes, for example VGLUT2, depends on the expression of early pre-synaptic genes, for example Munc18-1, I would predict that OSNs electroporated with shMunc18-1will not express VGLUT2.

B. Is pruning activity dependent?

In chapter 3, I presented evidence showing that in the olfactory system, as in many other neural systems of the mammalian brain, olfactory sensory neurons develop with exuberant growth and synapse formation. I demonstrated that in the mouse, pruning of the immature exuberant pattern of axonal arborizations into the mature pattern occurs early in post-natal life. It has been shown that in other places of the nervous system pruning during development requires neuronal activity. In particular, in the visual system, it is well established that the spontaneous and synchronous firing of retinal ganglion cells occurring *in utero* and before vision is established, is responsible for the non-overlapping organization of axonal inputs from the two eyes (Shatz 1996).

Whether the developmental refinement of olfactory sensory neuron projections is also activity dependent is unknown. I hypothesized that sensory stimulus may be important for developmental pruning of OSN axonal arbors. In contrast to this hypothesis, my electroporation experiments using CNG knock-out mice show no defects on axonal morphology and synaptic composition at post-natal day 15. Because CNG knock-out mice lack odor-evoked activity, I conclude that in the olfactory system, developmental pruning still occurs in the absence of odor-evoked activity. To determine if the temporal course of developmental pruning is perturbed in the absence of odor-evoked activity, I propose to compare CNG WT vs CNG KO axonal morphology and synaptic composition at additional time points including post-natal day eight, when exuberant projections are most pronounced in wild type animals. If developmental pruning is not perturbed by the absence of odor-evoked activity, I predict that axonal morphology and synaptic composition of CNG WT vs CNG KO will not differ significantly at post-natal day eight. I also predict that the values for axonal morphology and synaptic distribution will be significantly higher at post-natal day eight than at post-natal day 15.

Olfactory sensory neurons exhibit spontaneous firing of action potentials (Reisert 2010; Rospars et al 1994) raising the possibility that spontaneous activity and/or neurosecretion could be responsible for the developmental pruning observed here rather than odor-evoked activity. Since CNG KO mice exhibit spontaneous action potential generation (Brunet et al 1996), other strategies should be considered to study the role of spontaneous activity and neurotransmitter release in shaping the adult pattern of connectivity. One alternative I pursued was to express a small hairpin RNA targeted against Munc1-1 (shMunc18-1) to suppress neurosecretory activity in individual olfactory sensory neurons *in vivo*. shMunc18-1 did not induce any changes in axonal morphology or synaptic composition *in vivo* although shMunc18-1 was proven to decrease mRNA levels by 80% and protein levels of Munc18-1in HEK293 cells (Data not shown). One possible explanation for this negative result is that our shRNA was not effective enough to abolish Munc18-1 function *in vivo*. Also, we cannot rule out the possibility that genetic redundancy would have hindered our efforts to abolish neurosecretion with shMunc18-1. In a second attempt to suppress neurosecretion, I designed shRNAs against the late expressing pre-synaptic molecule VGLUT2. We are currently in the process of analyzing the axonal arborizations of electroporated OSNs harboring shVGLUT2.

In order to study the role of spontaneous activity in the generation of a sensory map in the olfactory bulb, Yu et al 2004 expressed the inward potassium rectifier ion channel Kir2.1 to reduce both odor-evoked and spontaneous activity, thereby silencing olfactory sensory neurons (Yu et al 2004). I propose to use this mouse in combination with the post-natal electroporation method to follow the development of individual axons and their synapses at specific post-natal ages in the absence of spontaneous activity. If developmental pruning in OSNs depends on the generation of spontaneous activity, I predict that olfactory sensory neuron axonal arbor

complexity and synapse numbers will not decrease after post-natal day eight in mice expressing Kir2.1.

C. The role of cAMP in axonal growth and guidance

Several recent lines of evidence point to cAMP as an instrumental factor for axon sorting, convergence and growth. By using elegant mouse genetic manipulations, Imai et al. showed that the OR-derived cAMP levels, and not the action of the OR molecules *per se*, determine the loci of convergence of ONS axons in the olfactory bulb (Imai et al 2006). By manipulating G_{α}, our lab provided further evidence that activation of the olfactory signal transduction cascade is sufficient to cause axonal convergence into glomeruli and that the generation of cAMP through AC3 is necessary to establish proper axonal identity and growth (Chesler et al 2007; Zou et al 2009; Zou et al 2007). The results presented in chapter 4 further complete the above mentioned studies by performing an analysis of AC3-deficient OSNs at a single axon level. Here we provide evidence showing that the generation of cAMP by AC3, and not just odor stimulation, is necessary for establishing the proper morphology and synaptic composition of OSN axonal arbors.

Since AC3 has already been implicated in axon growth (Zou et al 2007), I hypothesize that the differences observed between AC3 WT vs. AC3 KO axons are the result of a profound impairment on axonal growth and synapse formation and not the mere result of accelerated pruning. My experimental results therefore confirm the importance of cAMP signaling in the development of axonal complexity. They further suggest that cAMP-related signaling is implicated in synapse formation. I should note that I tested the panel of pre-synaptic *in situ*

hybridization probes in olfactory epithelium tissue from animals lacking Adenylyl Cyclase 3. In the AC3 knock out background all pre-synaptic molecules were expressed at the same stages in OSN lineage as in control tissue (unpublished observations). This result shows that the expression of pre-synaptic genes in the OE is not dependent on the cAMP-signaling cascade. Because axon growth and synapse formation are not affected in CNG knock-out mice, axon growth and synapse formation are regulated via mechanisms that do not involve odor-evoked membrane depolarization.

In order to investigate whether downstream cAMP-related signaling events are responsible for the phenotype observed in the AC3 KO mice, I propose to ectopically express constitutively active forms of PKA (Imai et al 2006) and CREB (Barco et al 2002) in AC3 KO background in an attempt to rescue the phenotype. Complementary studies would include electroporations with dominant negative forms of PKA (Imai et al 2006) and CREB (ACREB, (Jancic et al 2009)) in AC3 wild-type background in order to induce an aberrant phenotype in axonal morphology and synaptic composition (work in progress).

In conclusion, the classical view of axons that fire together wire together does not seem to apply to the olfactory system, where mounting evidence shows that the role of cAMP signaling is more important than electrical activity for sensory neuron convergence and glomeruli development. The recent publication of a novel tool that can be used to manipulate cAMP levels *in vivo* could help to further extend the existing work on the topic. Ryu et al 2010 recently characterized a photoactivated nucleotidyl cyclase (Ryu et al 2010) that when expressed under the OMP promoter in a mouse transgenic system could become a useful tool to study axonal convergence. It would also be interesting to express this photoactivated nucleotidyl cyclase under the regulation of promoter regions from two different olfactory receptors that normally converge to

distinct but close glomeruli within the bulb (for instance, M71 and M72). According to our model, once the exogenous nucleotidyl cyclase is activated, it will induce the convergence of M71 and M71 axons into a single glomerulus.

D. Perspectives

In summary, my results provide new insights into olfactory sensory neuron axonal development and synapse formation. I provided evidence indicating that in olfactory sensory neurons synaptic differentiation occurs in a sequential fashion and that axons elaborate with exuberant growth and synapse formation. Moreover, cAMP-related signals are critical for OSN axonal growth. These findings may be instrumental for understanding axonal development and synapse formation in other systems of the mammalian brain.

Although disorders such as autism and schizophrenia are considered multifactorial syndromes, recent evidence has pointed to a neurodevelopmental origin specifically involving axonal growth and synaptogenesis. Mutations in many genes have been associated with familial autism spectrum disorders (ASDs). A consistent observation emerging from recent studies is the discovery of mutations in the genes encoding Neurexin1, Neuroligin3 and Neurologin4. Neurexins and neurologins are synaptic cell-adhesion molecules expressed by the pre-synaptic and post-synaptic neurons respectively and they are required for synapse formation and function. They function by binding to each other and by interacting with intracellular proteins. Their dysfunction impairs the properties of synapses and disrupts neuronal networks without completely abolishing synaptic transmission (Missler et al 2003; Varoqueaux et al 2006). Consistently, mice carrying one of the Neuroligin3 mutations recapitulated some of the cognitive

symptoms observed in humans and showed an increase in inhibitory synaptic transmission (Tabuchi et al 2007).

Disrupted-in-schizophrenia 1 (DISC1) was identified as a novel gene disrupted by a translocation that segregated with schizophrenia in a Scottish family. DISC1, through interactions with FEZ1, has been implicated in growth of neurite and axons (Miyoshi et al 2003) and provides support the neurodevelopmental hypothesis of schizophrenia (Mackie et al 2007). However, how these cellular changes explain the complex symptomatology observed in this debilitating disorder is not fully understood. Therefore, understanding the molecular mechanisms of synapse formation, axonal elongation and pruning in the normal brain might enlighten future strategies to treat mental disorders.

REFERENCES

Alsina B, Vu T, Cohen-Cory S. 2001. Visualizing synapse formation in arborizing optic axons in vivo: dynamics and modulation by BDNF. *Nat Neurosci* 4:1093-101

Baker H, Grillo M, Margolis FL. 1989. Biochemical and immunocytochemical characterization of olfactory marker protein in the rodent central nervous system. *J Comp Neurol* 285:246-61

Barco A, Alarcon JM, Kandel ER. 2002. Expression of constitutively active CREB protein facilitates the late phase of long-term potentiation by enhancing synaptic capture. *Cell* 108:689-703

Belluscio L, Gold GH, Nemes A, Axel R. 1998. Mice deficient in G(olf) are anosmic. *Neuron* 20:69-81

Bennett MK, Calakos N, Scheller RH. 1992. Syntaxin: a synaptic protein implicated in docking of synaptic vesicles at presynaptic active zones. *Science* 257:255-9

Bergmann M, Lahr G, Mayerhofer A, Gratzl M. 1991. Expression of synaptophysin during the prenatal development of the rat spinal cord: correlation with basic differentiation processes of neurons. *Neuroscience* 42:569-82

Bergmann M, Schuster T, Grabs D, Marqueze-Pouey B, Betz H, et al. 1993. Synaptophysin and synaptoporin expression in the developing rat olfactory system. *Brain Res Dev Brain Res* 74:235-44

Biederer T, Sudhof TC. 2000. Mints as adaptors. Direct binding to neurexins and recruitment of munc18. *J Biol Chem* 275:39803-6

Blanchart A, De Carlos JA, Lopez-Mascaraque L. 2006. Time frame of mitral cell development in the mice olfactory bulb. *J Comp Neurol* 496:529-43

Blanchart A, Romaguera M, Garcia-Verdugo JM, de Carlos JA, Lopez-Mascaraque L. 2008. Synaptogenesis in the mouse olfactory bulb during glomerulus development. *Eur J Neurosci* 27:2838-46

Brunet LJ, Gold GH, Ngai J. 1996. General anosmia caused by a targeted disruption of the mouse olfactory cyclic nucleotide-gated cation channel. *Neuron* 17:681-93

Calof AL, Bonnin A, Crocker C, Kawauchi S, Murray RC, et al. 2002. Progenitor cells of the olfactory receptor neuron lineage. *Microsc Res Tech* 58:176-88

Campagna JA, Prevette D, Oppenheim RW, Bixby JL. 1997. Target contact regulates expression of synaptotagmin genes in spinal motor neurons in vivo. *Mol Cell Neurosci* 8:377-88

Cao L, Dhilla A, Mukai J, Blazeski R, Lodovichi C, et al. 2007. Genetic modulation of BDNF signaling affects the outcome of axonal competition in vivo. *Curr Biol* 17:911-21

Carson C, Saleh M, Fung FW, Nicholson DW, Roskams AJ. 2005. Axonal dynactin p150Glued transports caspase-8 to drive retrograde olfactory receptor neuron apoptosis. *J Neurosci* 25:6092-104

Cases-Langhoff C, Voss B, Garner AM, Appeltauer U, Takei K, et al. 1996. Piccolo, a novel 420 kDa protein associated with the presynaptic cytomatrix. *Eur J Cell Biol* 69:214-23

Chesler AT, Le Pichon CE, Brann JH, Araneda RC, Zou DJ, Firestein S. 2008. Selective gene expression by postnatal electroporation during olfactory interneuron nurogenesis. *PLoS One* 3:e1517

Chesler AT, Zou DJ, Le Pichon CE, Peterlin ZA, Matthews GA, et al. 2007. A G protein/cAMP signal cascade is required for axonal convergence into olfactory glomeruli. *Proc Natl Acad Sci U S A* 104:1039-44

Chess A, Simon I, Cedar H, Axel R. 1994. Allelic inactivation regulates olfactory receptor gene expression. *Cell* 78:823-34

Chin LS, Li L, Ferreira A, Kosik KS, Greengard P. 1995. Impairment of axonal development and of synaptogenesis in hippocampal neurons of synapsin I-deficient mice. *Proc Natl Acad Sci U S A* 92:9230-4

Costanzo RM, Graziadei PP. 1983. A quantitative analysis of changes in the olfactory epithelium following bulbectomy in hamster. *J Comp Neurol* 215:370-81

Cowan CM, Thai J, Krajewski S, Reed JC, Nicholson DW, et al. 2001. Caspases 3 and 9 send a pro-apoptotic signal from synapse to cell body in olfactory receptor neurons. *J Neurosci* 21:7099-109

Daly C, Ziff EB. 1997. Post-transcriptional regulation of synaptic vesicle protein expression and the developmental control of synaptic vesicle formation. *J Neurosci* 17:2365-75

Deak F, Xu Y, Chang WP, Dulubova I, Khvotchev M, et al. 2009. Munc18-1 binding to the neuronal SNARE complex controls synaptic vesicle priming. *J Cell Biol* 184:751-64

Dean C, Dresbach T. 2006. Neuroligins and neurexins: linking cell adhesion, synapse formation and cognitive function. *Trends Neurosci* 29:21-9

Dresbach T, Qualmann B, Kessels MM, Garner CC, Gundelfinger ED. 2001. The presynaptic cytomatrix of brain synapses. *Cell Mol Life Sci* 58:94-116

Edelmann L, Hanson PI, Chapman ER, Jahn R. 1995. Synaptobrevin binding to synaptophysin: a potential mechanism for controlling the exocytotic fusion machine. *Embo J* 14:224-31

Farbman AI, Margolis FL. 1980. Olfactory marker protein during ontogeny: immunohistochemical localization. *Dev Biol* 74:205-15

Fenster SD, Kessels MM, Qualmann B, Chung WJ, Nash J, et al. 2003. Interactions between Piccolo and the actin/dynamin-binding protein Abp1 link vesicle endocytosis to presynaptic active zones. *J Biol Chem* 278:20268-77

Fujimoto K, Shibasaki T, Yokoi N, Kashima Y, Matsumoto M, et al. 2002. Piccolo, a Ca2+ sensor in pancreatic beta-cells. Involvement of cAMP-GEFII.Rim2.Piccolo complex in cAMP-dependent exocytosis. *J Biol Chem* 277:50497-502

Futerman AH, Banker GA. 1996. The economics of neurite outgrowth--the addition of new membrane to growing axons. *Trends Neurosci* 19:144-9

Gabellec MM, Panzanelli P, Sassoe-Pognetto M, Lledo PM. 2007. Synapse-specific localization of vesicular glutamate transporters in the rat olfactory bulb. *Eur J Neurosci* 25:1373-83

Geppert M, Goda Y, Hammer RE, Li C, Rosahl TW, et al. 1994. Synaptotagmin I: a major Ca2+ sensor for transmitter release at a central synapse. *Cell* 79:717-27

Halasz N, Greer CA. 1993. Terminal arborizations of olfactory nerve fibers in the glomeruli of the olfactory bulb. *J Comp Neurol* 337:307-16

Hinds JW. 1968. Autoradiographic study of histogenesis in the mouse olfactory bulb. I. Time of origin of neurons and neuroglia. *J Comp Neurol* 134:287-304

Hinds JW, Hinds PL. 1976. Synapse formation in the mouse olfactory bulb. I. Quantitative studies. *J Comp Neurol* 169:15-40

Hua JY, Smear MC, Baier H, Smith SJ. 2005. Regulation of axon growth in vivo by activity-based competition. *Nature* 434:1022-6

Huard JM, Schwob JE. 1995. Cell cycle of globose basal cells in rat olfactory epithelium. *Dev Dyn* 203:17-26

Imai T, Suzuki M, Sakano H. 2006. Odorant receptor-derived cAMP signals direct axonal targeting. *Science* 314:657-61

Ishii T, Omura M, Mombaerts P. 2004. Protocols for two- and three-color fluorescent RNA in situ hybridization of the main and accessory olfactory epithelia in mouse. *J Neurocytol* 33:657-69

Jancic D, Lopez de Armentia M, Valor LM, Olivares R, Barco A. 2009. Inhibition of cAMP response element-binding protein reduces neuronal excitability and plasticity, and triggers neurodegeneration. *Cereb Cortex* 19:2535-47

Kaeser PS, Sudhof TC. 2005. RIM function in short- and long-term synaptic plasticity. *Biochem Soc Trans* 33:1345-9

Kasowski HJ, Kim H, Greer CA. 1999. Compartmental organization of the olfactory bulb glomerulus. *J Comp Neurol* 407:261-74

Klenoff JR, Greer CA. 1998. Postnatal development of olfactory receptor cell axonal arbors. *J Comp Neurol* 390:256-67

Kondo K, Suzukawa K, Sakamoto T, Watanabe K, Kanaya K, et al. 2010. Age-related changes in cell dynamics of the postnatal mouse olfactory neuroepithelium: cell proliferation, neuronal differentiation, and cell death. *J Comp Neurol* 518:1962-75

Konzelmann S, Saucier D, Strotmann J, Breer H, Astic L. 1998. Decline and recovery of olfactory receptor expression following unilateral bulbectomy. *Cell Tissue Res* 294:421-30

Leake PA, Snyder RL, Hradek GT. 2002. Postnatal refinement of auditory nerve projections to the cochlear nucleus in cats. *J Comp Neurol* 448:6-27

Leal-Ortiz S, Waites CL, Terry-Lorenzo R, Zamorano P, Gundelfinger ED, Garner CC. 2008. Piccolo modulation of Synapsin1a dynamics regulates synaptic vesicle exocytosis. *J Cell Biol* 181:831-46

Li L, Chin LS. 2003. The molecular machinery of synaptic vesicle exocytosis. *Cell Mol Life Sci* 60:942-60

Lin DM, Wang F, Lowe G, Gold GH, Axel R, et al. 2000. Formation of precise connections in the olfactory bulb occurs in the absence of odorant-evoked neuronal activity. *Neuron* 26:69-80

Lise MF, El-Husseini A. 2006. The neuroligin and neurexin families: from structure to function at the synapse. *Cell Mol Life Sci* 63:1833-49

Lohof AM, Quillan M, Dan Y, Poo MM. 1992. Asymmetric modulation of cytosolic cAMP activity induces growth cone turning. *J Neurosci* 12:1253-61

Lopez-Mascaraque L, De Carlos JA, Valverde F. 1990. Structure of the olfactory bulb of the hedgehog (Erinaceus europaeus): a Golgi study of the intrinsic organization of the superficial layers. *J Comp Neurol* 301:243-61

Lou X, Bixby JL. 1993. Coordinate and noncoordinate regulation of synaptic vesicle protein genes during embryonic development. *Dev Biol* 159:327-37

Mackie S, Millar JK, Porteous DJ. 2007. Role of DISC1 in neural development and schizophrenia. *Curr Opin Neurobiol* 17:95-102

Malnic B, Hirono J, Sato T, Buck LB. 1999. Combinatorial receptor codes for odors. *Cell* 96:713-23

Marcucci F, Zou DJ, Firestein S. 2009. Sequential onset of presynaptic molecules during olfactory sensory neuron maturation. *J Comp Neurol* 516:187-98

Marler KJ, Becker-Barroso E, Martinez A, Llovera M, Wentzel C, et al. 2008. A TrkB/EphrinA interaction controls retinal axon branching and synaptogenesis. *J Neurosci* 28:12700-12

McAllister AK. 2007. Dynamic aspects of CNS synapse formation. *Annu Rev Neurosci* 30:425-50

Michel D, Moyse E, Brun G, Jourdan F. 1994. Induction of apoptosis in mouse [correction of rat] olfactory neuroepithelium by synaptic target ablation. *Neuroreport* 5:1329-32

Ming GL, Song HJ, Berninger B, Holt CE, Tessier-Lavigne M, Poo MM. 1997. cAMP-dependent growth cone guidance by netrin-1. *Neuron* 19:1225-35

Miragall F, Monti Graziadei GA. 1982. Experimental studies on the olfactory marker protein. II. Appearance of the olfactory marker protein during differentiation of the olfactory sensory neurons of mouse: an immunohistochemical and autoradiographic study. *Brain Res* 239:245-50

Missler M, Zhang W, Rohlmann A, Kattenstroth G, Hammer RE, et al. 2003. Alpha-neurexins couple Ca2+ channels to synaptic vesicle exocytosis. *Nature* 423:939-48

Miyoshi K, Honda A, Baba K, Taniguchi M, Oono K, et al. 2003. Disrupted-In-Schizophrenia 1, a candidate gene for schizophrenia, participates in neurite outgrowth. *Mol Psychiatry* 8:685-94

Mombaerts P. 1996. Targeting olfaction. *Curr Opin Neurobiol* 6:481-6

Moon YW, Baker H. 2002. Lectin-induced apoptosis of mature olfactory receptor cells. *J Neurosci Res* 68:398-405

Osen-Sand A, Catsicas M, Staple JK, Jones KA, Ayala G, et al. 1993. Inhibition of axonal growth by SNAP-25 antisense oligonucleotides in vitro and in vivo. *Nature* 364:445-8

Plunkett JA, Baccus SA, Bixby JL. 1998. Differential regulation of synaptic vesicle protein genes by target and synaptic activity. *J Neurosci* 18:5832-8

Portera-Cailliau C, Weimer RM, De Paola V, Caroni P, Svoboda K. 2005. Diverse modes of axon elaboration in the developing neocortex. *PLoS Biol* 3:e272

Potter SM, Zheng C, Koos DS, Feinstein P, Fraser SE, Mombaerts P. 2001. Structure and emergence of specific olfactory glomeruli in the mouse. *J Neurosci* 21:9713-23

Rashid T, Upton AL, Blentic A, Ciossek T, Knoll B, et al. 2005. Opposing gradients of ephrin-As and EphA7 in the superior colliculus are essential for topographic mapping in the mammalian visual system. *Neuron* 47:57-69

Reisert J. 2010. Origin of basal activity in mammalian olfactory receptor neurons. *J Gen Physiol* 136:529-40

Richard MB, Taylor SR, Greer CA. 2010. Age-induced disruption of selective olfactory bulb synaptic circuits. *Proc Natl Acad Sci U S A* 107:15613-8

Rodriguez-Castaneda F, Maestre-Martinez M, Coudevylle N, Dimova K, Junge H, et al. 2010. Modular architecture of Munc13/calmodulin complexes: dual regulation by Ca2+ and possible function in short-term synaptic plasticity. *EMBO J* 29:680-91

Rosahl TW, Spillane D, Missler M, Herz J, Selig DK, et al. 1995. Essential functions of synapsins I and II in synaptic vesicle regulation. *Nature* 375:488-93

Rospars JP, Lansky P, Vaillant J, Duchamp-Viret P, Duchamp A. 1994. Spontaneous activity of first- and second-order neurons in the frog olfactory system. *Brain Res* 662:31-44

Ruthazer ES, Akerman CJ, Cline HT. 2003. Control of axon branch dynamics by correlated activity in vivo. *Science* 301:66-70

Ruthazer ES, Li J, Cline HT. 2006. Stabilization of axon branch dynamics by synaptic maturation. *J Neurosci* 26:3594-603

Ryu MH, Moskvin OV, Siltberg-Liberles J, Gomelsky M. 2010. Natural and engineered photoactivated nucleotidyl cyclases for optogenetic applications. *J Biol Chem*

Sakano H. 2010. Neural map formation in the mouse olfactory system. *Neuron* 67:530-42

Sammeta N, Yu TT, Bose SC, McClintock TS. 2007. Mouse olfactory sensory neurons express 10,000 genes. *J Comp Neurol* 502:1138-56

Schmidt H, Rathjen FG. 2010. Signalling mechanisms regulating axonal branching in vivo. *Bioessays* 32:977-85

Schoch S, Castillo PE, Jo T, Mukherjee K, Geppert M, et al. 2002. RIM1alpha forms a protein scaffold for regulating neurotransmitter release at the active zone. *Nature* 415:321-6

Schoch S, Gundelfinger ED. 2006. Molecular organization of the presynaptic active zone. *Cell Tissue Res* 326:379-91

Schwob JE, Szumowski KE, Stasky AA. 1992. Olfactory sensory neurons are trophically dependent on the olfactory bulb for their prolonged survival. *J Neurosci* 12:3896-919

Shatz CJ. 1996. Emergence of order in visual system development. *Proc Natl Acad Sci U S A* 93:602-8

Shetty RS, Bose SC, Nickell MD, McIntyre JC, Hardin DH, et al. 2005. Transcriptional changes during neuronal death and replacement in the olfactory epithelium. *Mol Cell Neurosci* 30:583-600

Sollner T, Whiteheart SW, Brunner M, Erdjument-Bromage H, Geromanos S, et al. 1993. SNAP receptors implicated in vesicle targeting and fusion. *Nature* 362:318-24

Song HJ, Poo MM. 1999. Signal transduction underlying growth cone guidance by diffusible factors. *Curr Opin Neurobiol* 9:355-63

Sretavan DW, Shatz CJ. 1986. Prenatal development of retinal ganglion cell axons: segregation into eye-specific layers within the cat's lateral geniculate nucleus. *J Neurosci* 6:234-51

Sudhof TC. 2004. The synaptic vesicle cycle. *Annu Rev Neurosci* 27:509-47

Tabuchi K, Blundell J, Etherton MR, Hammer RE, Liu X, et al. 2007. A neuroligin-3 mutation implicated in autism increases inhibitory synaptic transmission in mice. *Science* 318:71-6

Takamori S, Rhee JS, Rosenmund C, Jahn R. 2001. Identification of differentiation-associated brain-specific phosphate transporter as a second vesicular glutamate transporter (VGLUT2). *J Neurosci* 21:RC182

Tenne-Brown J, Key B. 1999. Errors in lamina growth of primary olfactory axons in the rat and mouse olfactory bulb. *J Comp Neurol* 410:20-30

tom Dieck S, Sanmarti-Vila L, Langnaese K, Richter K, Kindler S, et al. 1998. Bassoon, a novel zinc-finger CAG/glutamine-repeat protein selectively localized at the active zone of presynaptic nerve terminals. *J Cell Biol* 142:499-509

Toonen RF, Verhage M. 2007. Munc18-1 in secretion: lonely Munc joins SNARE team and takes control. *Trends Neurosci* 30:564-72

Varoqueaux F, Aramuni G, Rawson RL, Mohrmann R, Missler M, et al. 2006. Neuroligins determine synapse maturation and function. *Neuron* 51:741-54

Varoqueaux F, Sigler A, Rhee JS, Brose N, Enk C, et al. 2002. Total arrest of spontaneous and evoked synaptic transmission but normal synaptogenesis in the absence of Munc13-mediated vesicle priming. *Proc Natl Acad Sci U S A* 99:9037-42

Verhaagen J, Oestreicher AB, Gispen WH, Margolis FL. 1989. The expression of the growth associated protein B50/GAP43 in the olfactory system of neonatal and adult rats. *J Neurosci* 9:683-91

Verhaagen J, Oestreicher AB, Grillo M, Khew-Goodall YS, Gispen WH, Margolis FL. 1990. Neuroplasticity in the olfactory system: differential effects of central and peripheral lesions of the primary olfactory pathway on the expression of B-50/GAP43 and the olfactory marker protein. *J Neurosci Res* 26:31-44

Verhage M, Maia AS, Plomp JJ, Brussaard AB, Heeroma JH, et al. 2000. Synaptic assembly of the brain in the absence of neurotransmitter secretion. *Science* 287:864-9

Watts RJ, Hoopfer ED, Luo L. 2003. Axon pruning during Drosophila metamorphosis: evidence for local degeneration and requirement of the ubiquitin-proteasome system. *Neuron* 38:871-85

Wong ST, Trinh K, Hacker B, Chan GC, Lowe G, et al. 2000. Disruption of the type III adenylyl cyclase gene leads to peripheral and behavioral anosmia in transgenic mice. *Neuron* 27:487-97

Yu CR, Power J, Barnea G, O'Donnell S, Brown HE, et al. 2004. Spontaneous neural activity is required for the establishment and maintenance of the olfactory sensory map. *Neuron* 42:553-66

Yu W, Ahmad FJ, Baas PW. 1994. Microtubule fragmentation and partitioning in the axon during collateral branch formation. *J Neurosci* 14:5872-84

Zhao H, Reed RR. 2001. X inactivation of the OCNC1 channel gene reveals a role for activity-dependent competition in the olfactory system. *Cell* 104:651-60

Zheng C, Feinstein P, Bozza T, Rodriguez I, Mombaerts P. 2000. Peripheral olfactory projections are differentially affected in mice deficient in a cyclic nucleotide-gated channel subunit. *Neuron* 26:81-91

Ziv NE. 2001. Recruitment of synaptic molecules during synaptogenesis. *Neuroscientist* 7:365-70

Zou DJ, Chesler A, Firestein S. 2009. How the olfactory bulb got its glomeruli: a just so story? *Nat Rev Neurosci* 10:611-8

Zou DJ, Chesler AT, Le Pichon CE, Kuznetsov A, Pei X, et al. 2007. Absence of adenylyl cyclase 3 perturbs peripheral olfactory projections in mice. *J Neurosci* 27:6675-83

Zou DJ, Feinstein P, Rivers AL, Mathews GA, Kim A, et al. 2004. Postnatal refinement of peripheral olfactory projections. *Science* 304:1976-9

APPENDIX

High throughput microarray detection of vomeronasal receptor gene expression in rodents by XiaoHong Zhang, **Florencia Marcucci** and Stuart Firestein. (2010) *Frontiers in Neuroscience*.